Determining the Role of Discoidin Domain Receptors in the Pathogenesis of Pancreatic Ductal Adenocarcinoma

by

Jeanine Marie Ruggeri

A dissertation submitted in partial fulfillment
of the requirements for the degree of
Doctor of Philosophy
(Molecular and Integrative Physiology)
in the University of Michigan
2020

Doctoral Committee:

Professor Howard C. Crawford, chair
Assistant Professor Costas Lyssiotis
Professor Bethany Moore
Professor Yatrik Shah

Jeanine Marie Ruggeri

ruggerij@umich.edu

ORCID iD: 0000-0002-6698-5303

Dedication

To Jean Filippo,

thanks for all the help from above.

Acknowledgements

Graduate school and obtaining my degree have always been my dream, but it would not have transitioned into a reality without the support and encouragement from numerous individuals. First and foremost, I would like to acknowledge my mentor, Dr. Howard Crawford, whose training methods are unparalleled. Under your mentorship, I have received a challenging, thorough, and productive training experience that has helped shape my scientific and professional development. I think it goes without saying in moving from the sunny beaches of Florida to the snowy cold subzero winters of Michigan, that I would not have traded this graduate experience under your guidance for anything. Thank you for your support and belief in me during my training.

It is a pleasure to acknowledge my graduate committee that includes Dr. Bethany Moore, Dr. Yatrik Shah, and Dr. Costas Lyssiotis. Thank you for sharing your time, knowledge and guidance in developing my scientific abilities. Additionally, thank you for your outside perspectives and expertise in keeping my projects on track for an effective training experience.

Next I would like to acknowledge the current members of the Crawford lab that have provided their expertise and advice on a daily basis. Dr. Hui-Ju Wen, thank you for your patience, help and guidance. I especially appreciate your help and training with

the animal work, which is not a trivial task when dealing with the pancreas. Dr. Simone Benitz, thank you for your emotional and scientific support during this last year. Your kind words of encouragement and help with scientific techniques has helped keep my projects and training on track and moving. Meggie Hoffman, this grad school experience would have been a very lonely journey without you. Thank you for being my colleague, roommate, lab-mate, and sometimes therapist when venting about science. Daniel Salas-Esabillas, thank you for your positive energy and help these past few months and good luck as the next generation of Crawford lab students. To the past members that were part of my informative scientific training, Dr. Ken Takeuchi and Dr. Christopher Halbrook, thank you for helping me to recognize the difference between "bad" and "good" science as well as your constructive criticisms of my data. To the adopted past member, Dr. Ethan Abel, thank you for not only keeping me sane, but for always being willing to help with experiments by sharing your expertise and materials. Special thanks to Dan Long for his help with the histopathology of my research.

It would be remiss not to acknowledge the talented, bright, and motivated group of pancreatic cancer researchers that make up the PanTERA group at the University of Michigan. Although at first, I viewed PanTERA as yet another meeting to attend, I am thankful for the opportunity to be a part of this group. It was a privilege to learn from other experts in the field with different perspectives to improve my science and I thank you for your time and support. In addition to the PanTERA group, I would like to thank our collaborators at Wayne State, Dr. Rafael Fridman and Dr, Anjum Sohail for the contributions to the DDR1 and DDR2 projects and Dr. Edna Cukierman and Dr. Janusz

Franco-Barraza at the Fox Chase Cancer Center in Philadelphia, PA for their extensive work in analyzing and interpreting the Second Harmonic Generation (SHG) polarized light microscopy.

Last, but certainly not least, I would like to acknowledge my family and friends. I am forever grateful to my parents, John and Linda Ruggeri, that had no idea what a career in science meant (and to be fair, neither did I), but somehow trusted and supported me since high school to pursue this dream. Thank you for allowing me the freedom to question my curiosities and follow my passion. My older siblings, John, Mark, and Marissa Ruggeri as well as Christopher Hollister, Carmela Ruggeri and Dana Ruggeri, thank you for setting an example for me and being a part of my inspiration to keep going. Thank you to my nieces and nephews for always putting a smile on my face when it was most needed, To my friends, thank you for the texts, phone calls, social media posts, thoughts, smoke signals, and any other form of communication you have sent to make sure I was doing ok these past years.

I am fortunate to have had such a collaborative, encouraging group of colleagues, peers, mentors, family, and friends that have helped shape my career. As I had said when I left New York to start this journey at Mayo Clinic in Rochester, Minnesota and now closing this part of the chapter in Ann Arbor, Michigan, I can never repay you for the all the support and help you have provided, but I promise to make you proud.

Table of Contents

List of Figures

Chapter 1

Chapter 2

Chapter 3

Chapter 4

List of Tables

Abstract

Pancreatic ductal adenocarcinoma (PDA) is an aggressive and devastating malignancy characterized by a collagen-rich, fibroinflammatory stroma. In the presence of a persistent injury as seen in chronic pancreatitis, a risk factor for the development of PDA, or oncogenic *KRAS*, the pancreas undergoes an initial morphological event where healthy acinar cells transdifferentiate into a ductal-like phenotype in a process called acinar-ductal metaplasia (ADM). ADM can advance into pre-cancerous lesions with a concomitant increase in collagen deposition. Due to the lack of clinical symptoms, limitations in early diagnosis and the excess collagen production that creates a barrier for treatment options, most patients are diagnosed with metastatic PDA leaving them with a 10% 5-year survival rate. Therefore, understanding the initiating molecular events of PDA and the crosstalk between the collagen-dense ECM and tumor cells is essential in providing early diagnostic methods with the potential for treatment options of this deadly disease.

To understand the molecular interactions between tumor-derived epithelial cells and the collagen dense stroma, this project focuses on a set of receptor tyrosine kinases called Discoidin Domain Receptors, DDR1 and DDR2, that bind to fibrillar collagens. This facilitates cell proliferation, migration, adhesion, and extracellular matrix remodeling. DDR1 has been shown to be expressed in epithelial cells, while DDR2 is

found in the mesenchymal compartment such as fibroblasts and connective tissue. The aim of this project was to define the roles of DDRs, independently of each other, in the pathogenesis of pancreatic disease where overproduction of collagen can serve as a natural reservoir for DDR activation.

To determine the significance of DDR1 in a model of experimental pancreatitis, I utilized a DDR1-ablated mouse *(DDR1$^{-/-}$). DDR1$^{-/-}$* mice were subjected to cerulein, a cholecystokinin ortholog that induces acinar cell stress to mimic the events of ADM and increased fibrosis seen in human pancreatitis. *DDR1$^{-/-}$* mice were also crossed into the established *Kras$^{G12D/+}$; Ptf1a$^{Cre/+}$ (KC)* model of tumorigenesis and the *Kras$^{LSL\text{-}G12D/+}$; Trp53$^{LSL\text{-}R172H/+}$; Ptf1a$^{Cre/+}$ (KPC)* of metastasis. A common phenotype observed among all models in the absence of DDR1 was significant tissue atrophy, acinar cell dropout, and perturbation in proliferation, suggesting DDR1 is necessary for pancreatic tissue homeostasis and recovery following extended injury.

To study the role of DDR2 in PDA development, we used a conditional DDR2 knockout mouse (*DDR2$^{fl/fl}$*) and bred them into the *KC* and *KPC* model. However, this only allows for DDR2 depletion within the pancreatic epithelium. To address the role of DDR2 in both the epithelial and mesenchymal compartments, we crossed *DDR2$^{fl/fl}$* into the dual recombinase system using global *B-actin^{CreERT2}* to knockout DDR2 and the *Kras$^{FSF\text{-}G12D/+}$; Ptf1a$^{Flpo/+}$ (KF)* to induce tumorigenesis and *Kras$^{FSF\text{-}G12D/+}$; Trp53$^{+/-}$ Ptf1a$^{Flpo/+}$ (KPF)* for studies in stages, including metastases. The preliminary data gathered from these models show that depletion of DDR2 promotes tumorigenesis and decreases survival in the metastatic models, suggesting DDR2 is necessary in the

tumor-stroma response during the progression of PDA.

Collectively, the role of DDRs in the context of fibrosis and cancer are complex. Further analysis is necessary to determine the role of the DDRs in an organ and cell specific manner. However, the results from these studies and my observations have helped define a prospective point of regulation between the tumor cells and the overactive collagen-dense microenvironment surrounding the pancreas throughout disease development.

Chapter 1: Physiology and Pathophysiology of The Pancreas

1.1) Anatomy and Physiology of the Pancreas

i. Anatomy of the Pancreas

The pancreas is a glandular organ located in the upper abdominal area within the gastrointestinal tract[1]. It is divided into three sections; head, body, and tail. It is strategically placed within the abdomen, anterior to the kidneys and posterior to the stomach and liver, limiting physical and environmental trauma to the pancreas that can result in long-term, irreversible effects, such as pancreatitis and pancreatic cancer (Fig.1.1)[1]. The pancreas weighs approximately 100 grams (~3.5 ounces) and reaches 5-7 inches in length within the human adult[3].

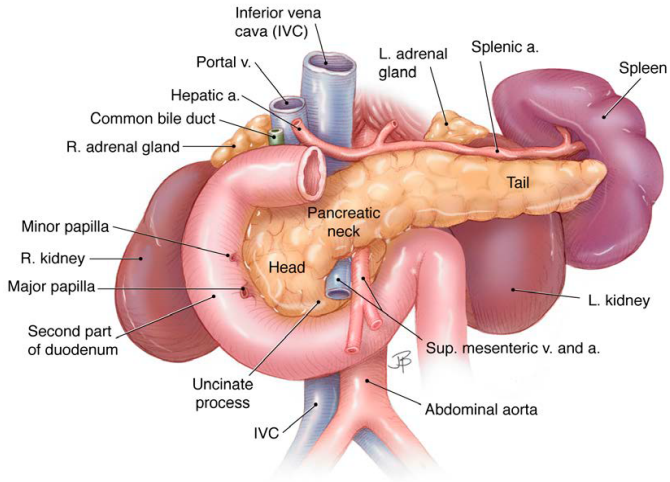

Figure 1.1 Anatomy of the Pancreas. Illustration of the orientation of the pancreas within the human abdominal cavity and surrounding organs.

Adapted from Jennifer Parsons Brumbaugh pancreapedia.org

ii. Physiology of the Pancreas

a.) Endocrine Function

The pancreas has both an endocrine and exocrine function[1]. The endocrine portion of the pancreas is comprised of the Islets of Langerhans that make ~5-10% of the pancreas[4]. Within the structure of the Islets, several cell types exist to assist in regulating blood glucose levels: 1.) Alpha cells, which secrete glucagon to raise blood glucose levels 2.) Beta cells, which secrete insulin to lower blood glucose levels 3.) Delta cells, which secrete somatostatin, to inhibit the release of both glucagon and insulin during homeostasis. 4.) Pancreatic polypeptide cells, which assist in exocrine function (Figure 1.1 B, C)[4].

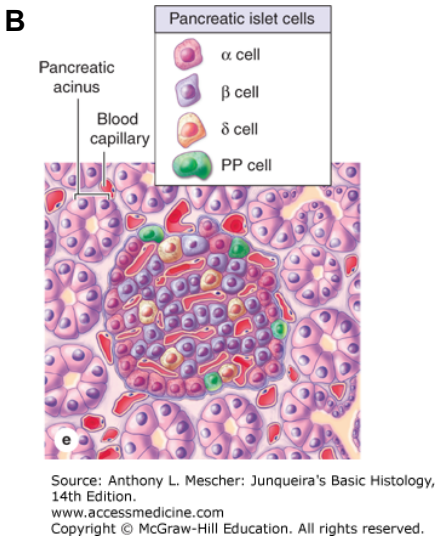

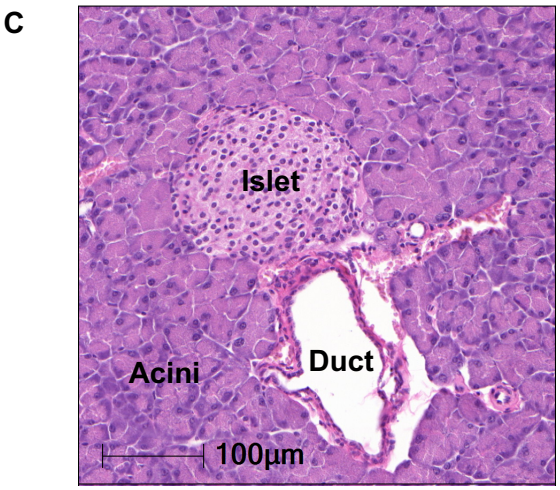

Figure 1.2.) Islet of Langerhans structure B.) Diagram of the Islet of Langerhans and cell types that exist within the structure and histology of Islets. Islets are a combination of 4 different cell types: α, β, δ and PP cells. C.) H&E histology of healthy mouse pancreas exhibiting the histology of the Islet of Langerhans.

b. Exocrine Function

The exocrine portion of the pancreas is responsible for the secretion of digestive enzymes and makes up a majority of the pancreas[1, 5]. There are two main cell types in the exocrine pancreas, the acinar and ductal cells that secrete and deliver digestive enzymes, respectively [1, 5]. Acinar cells are organized into a larger unit referred to as the acinus which collaborate with the ductal system for the efficient secretion of enzymes into the duodenum for digestion (Figure 1.3)[1, 5]. Another cell that is part of the exocrine pancreas is the centroacinar cell, which is located at the base of the acinar clusters before transitioning into the ductal system[1]. The function of centroacinar cells has been hypothesized to act as a facultative stem cell[1, 6]. Although not part of the exocrine pancreas, pancreatic stellate cells (PSC) are stromal cells found sparingly throughout the organ[1]. PSCs are inactive during normal physiology, but are activated upon tissue stress in conditions such as pancreatitis or pancreatic cancer to secrete extracellular matrix(ECM) proteins for the support, repair and recovery of the pancreas[1].

Acinar cells make up almost 90% of pancreatic tissue mass and serve as the primary functional unit of the exocrine pancreas[1, 5]. The physiological role of the acinar cell is to produce, store, and secrete digestive enzymes[1, 5]. The repertoire of enzymes the acinar cell produces include amylase, trypsinogen, carboxypeptidase A, and elastase[6]. These enzymes and other proteins are produced in high, inactive forms or stored as zymogen granules. Secretion of these enzymes are dependent on neuronal or hormonal signals directed from the basolateral membrane of the acinus and released through exocytosis into the lumen at the apical side[5]. The high

levels of protein synthesis puts acinar cells under a constant level of endoplasmic reticular (ER) stress[5]. The cell's ability to regulate ER stress must be balanced with dietary needs, appropriately[5]. Continuous, unchecked stress creates an imbalance in the acinar cells physiological function to secrete enzymes, which promotes the adaptation of acinar cells to undergo morphological changes or die at an accelerated rate that can lead to necrosis. PSCs respond to injured acinar cells and necrosis by activating and secreting ECM products, especially collagen, as a mechanism of tissue repair[5]. However, when the injury-repair cycle persists without resolution, homeostasis of the tissue is disrupted with further damage to the pancreas. The unchecked damage to the tissue results in scarring accompanied by consistent activation of PSCs to secret collagen resulting in a collagen-dense fibrotic response commonly seen in the pathophysiological conditions of pancreatitis and pancreatic cancer[5].

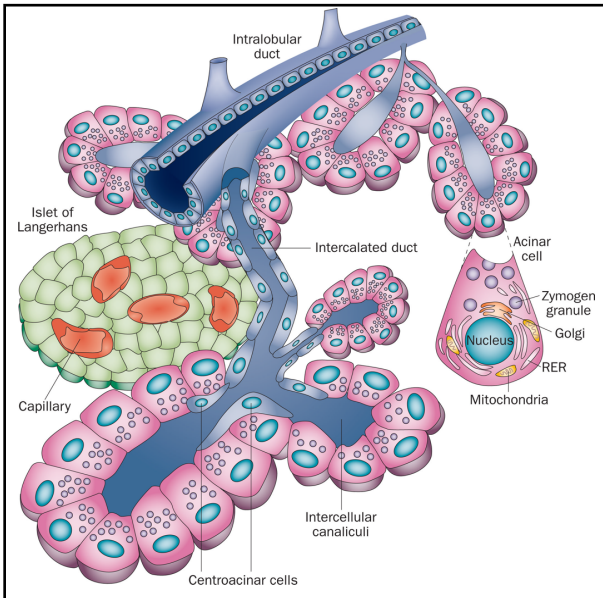

Adopted from Logsdon, Nature Rev. 2013

Figure 1.3.) Cell composition of the pancreas. The pancreas has 2 functions and is composed of: Islets of Langerhans responsible for endocrine function to deliver hormones in regulating blood sugar levels. Acinar cells form clusters that are met with centroacinar cells before entering the ductal system for the exocrine delivery of digestive enzymes produced by acinar cells.

1.2) Pathophysiology of the Pancreas: Pancreatitis and Pancreatic Ductal Adenocarcinoma

i. Pancreatitis

Pancreatitis is defined as inflammation of the pancreas and causes abdominal discomfort and severe pain[7]. Pancreatitis is generally not fatal, but does impinge on the daily activities of a patient, decreasing their quality of life[7, 8]. There are two categories of pancreatitis: acute and chronic[8]. Acute and chronic disease present with different etiologies, however, it is thought that acute pancreatitis is the precursor to the development of chronic pancreatitis[7, 8]. Despite their clinical similarities, each is distinctly diagnosed and treated respectively.

a.) Acute Pancreatitis

Acute pancreatitis (AP) is one of the most common gastrointestinal causes of hospitalization affecting over 275,000 people each year in the USA[7]. AP is defined by the occurrence of at least two isolated episodes of pancreatitis with a latent period between each episode[7]. The incidence of AP has risen in the past two decades likely due to better diagnostic testing and the rising obesity epidemic[7, 8]. Obesity increases the risk of the formation of gallstones which are a common cause of AP[7, 8]. Gallstones are usually innocuous, but in some cases can get dislodged in the common bile duct[7]. Obstruction to the bile duct blocks the secretion of digestive enzymes produced by the exocrine pancreas resulting in pancreatic inflammation followed by necrosis and the potential for infections that can be a painful situation for the patient[7]. Cholecystectomy (removal of the gall bladder) reduces the pain and risk of AP, however, this is not the only factor that contributes to the onset of AP[7]. Other non-gallstone related issues that

can result in an episode of AP include excessive alcohol consumption, cigarette smoking, and diet [7]. Although AP can usually resolve itself and does not increase the risk of further pancreatic damage, there are cases of recurrent AP[7]. Recurrent bouts of AP cause unresolved acinar damage and necrosis followed by disproportionate impairment to the pancreas[7]. Acinar cell injury by recurrent AP leads to an extended necrosis-fibrosis cycle with an increase in ECM proteins and collagen production from PSCs that further obstructs the architecture of the pancreatic epithelium and puts a patient at risk for developing chronic pancreatitis[7, 8].

b.) <u>Chronic Pancreatitis</u>

Chronic Pancreatitis (CP) has a lower incidence rate than AP and is defined as a permanent inflammatory condition and can be a risk for the development of pancreatic cancer[8]. CP is characterized by a significant loss in acinar cells from excessive cell death by necrosis accompanied by a strong collagen-dense fibrotic response that results in unresolved, perpetual damage[9]. Another characteristic feature of CP distinct from AP is the presence of acinar-ductal metaplasia (ADM), a transdifferentiating event hypothesized to protect acinar cells from injury[10, 11]. The pancreatic damage ensued during CP presents as severe abdominal pain that greatly impairs the quality of life for patients[7-9]. Based on patient data, the constant physical pain exerted by complications of CP reduces the ability to continue work which is further exacerbated by financial burden and impacts emotional well-being[7, 8]. Therefore, identifying potential risks to prevent CP would be instrumental in reducing incidences while increase our knowledge of this disease.

A majority of CP cases are considered idiopathic, but there are several risk factors associated with its occurrence. Similar to AP, the most common risk factors include chronic alcohol abuse, cigarette smoking and diet [7, 8]. Other risks are based on pancreatic susceptibility genes that in combination with environmental and/or lifestyle choices can greatly increase the risk of developing CP[7, 8]. Gain-of-function mutations in *PRSS1*, the gene for trypsinogen, are common among rare, autosomal dominant hereditary pancreatitis[8]. Mutations in the peptidase inhibitor gene, *SPINK1*, accounts for a small percentage of CP patients , whereas mutations in the cystic fibrosis transmembrane conductance regulator (*CFTR*) is responsible for a majority of CP patients [8]. Collectively, mutations in pancreatic susceptibility genes disrupts pancreatic function by inducing acinar cell stress and ductal obstructions that can promote a persistent fibrotic response and the eventual fate of CP[12].

ii. <u>Pancreatic Ductal Adenocarcinoma (PDA)</u>

Pancreatic ductal adenocarcinoma (PDA) is the most common and deadly form of pancreatic cancer[13]. Currently, PDA stands as the third leading cause of cancer deaths in the USA and is projected to be the second leading cause of cancer deaths by 2030[14]. Over 55,000 adults are diagnosed each year in the USA in which only 9% will reach the 5-year survival mark, leaving a majority of patients to succumb to this disease within a year of the initial diagnosis[14]. Several challenges remain in improving patient outcome including the absence of clinically specific presenting symptoms, lack of early detection methods, and limited therapeutic options that would considerably extend the life span and quality of life for patients. Placing consideration on these obstacles with the dire need to improve patient outcome, it is

essential to understand the risk factors and biology of PDA in order to effectively combat this disease.

1.3) Risk Factors of PDA

A large proportion of PDA patients develop the disease spontaneously after acquiring a somatic mutation in the *KRAS* oncogene[15]. However, a small percentage, almost 10%, are at risk of developing PDA due to inheritance of germline variants[15, 16]. Identifying patients that have a genetic predisposition or engage in lifestyle activities that increase the risk of PDA will not only help to understand the development of PDA, but also how to prevent it.[7]

i.) Genetic Risk Factors:

Germline incidences of PDA are low, however, studying hereditary risk factors are crucial in our understanding and prevention of this disease[15, 16]. Inheritance of a susceptibility gene places a patient at a higher risk of developing PDA, therefore, a more complete understanding of the full complement of genes that predispose patients to PDA is imperative to detect and prevent disease occurrence in these patients[17, 18]. Advances in genome-wide association studies (GWAS) have helped expand and identify panels of PDA susceptibility genes. The following is a list of several established susceptibility gene panels typically screened for in familial cases of PDA.

a.) Hereditary Breast and Ovarian Cancer Syndrome Associated Genes:

BRCA1 and *BRCA2* genes are involved in DNA repair of double-strand breaks. Mutations in either gene results in faulty DNA repair that can lead to the genomic instability that is commonly associated with Hereditary Breast and Ovarian Cancer

(HBOC)[17, 18]. It has been reported that mutations in *BRCA1* can lead to a 2-fold increased risk of PDA[17, 18]. However, *BRCA1* mutations are loosely associated with PDA and are rarely detected in familial cases[17, 18]. On the other hand, *BRCA2* mutations are well-defined and have a higher prevalence with a 3.5-fold increased risk for developing PDA[17]. *PALB2* is another HBOC susceptibility gene that is associated with familial PDA leading to a 6-fold increased risk[17]. *PALB2* encodes a protein that stabilizes *BRCA2* in the nucleus for efficient DNA repair[17, 18]. Mutations in *PALB2* can therefore disrupt *BRCA2* localization to the nucleus that is necessary to maintain genomic stability. Patients with germline mutations in *BRCA1* or the *BRCA2/PALB2* complex are at an increased risk of developing PDA[17, 18]. However, there is substantial evidence that shows therapeutic promise using targeted therapies with 1.) platinum-based therapy, which is used to inhibit DNA repair and DNA synthesis by crosslinking DNA and 2.) poly-ADP-ribose polymerase inhibitors (PARPi), which act to inhibit the PARP1 protein in highly proliferative cells that results in an overwhelming amount of double-stranded breaks in BRCA-associated PDA[19]. PDA patients with a *BRCA1* or *BRCA2/PALB2* mutation are more sensitive to these drugs, creating a more personalized therapeutic approach and improved outcome[19].

b.) <u>Lynch Syndrome Associated Genes:</u>

Lynch syndrome, or Hereditary Nonpolyposis Colorectal Cancer (HNPCC), is an inherited autosomal dominant syndrome associated with early onset colorectal cancer and endometrial cancer in women[17, 18]. Genes associated with Lynch Syndrome include *MLH1, MSH2, PMS1, PMS2,* and *MSH6*, which are responsible for DNA mismatch repair machinery[17, 18]. Patients with Lynch Syndrome are not only at an

increased risk of colorectal cancer, but also have an approximately 8-fold increased risk for PDA[17].

c.) Peutz-Jeghers Syndrome Associated Genes

Peutz-Jeghers Syndrome (PJS) is an autosomal dominant disorder that forms polyps in the gastrointestinal tract, mouth, lips, and extremities[17, 18]. Mutations in the serine-threonine kinase tumor suppressor, *STK11*, is most commonly seen in PJS patients[18]. PJS is shown to increase the risk of several cancers including PDA at 132-fold increased risk compared to the general population[17].

d.) Familial Atypical Multiple Mole Melanoma Syndrome Associated Genes:

Familial Atypical Multiple Mole Melanoma Syndrome Associated Genes (FAMMM) is usually associated with melanoma, however, the characteristic mutation in the tumor suppressor gene, *p16INK4A/CDKNA2*, is also seen in hereditary cases of PDA[17, 18]. Although the relative risk of developing PDA for those with germline mutations in FAMMM varies among populations, it is still considered an increased genetic risk and patients should be heavily monitored and screened[17].

ii.) Lifestyle Risk Factors

PDA is considered a rare cancer with low incidence, but is one of the most fatal cancers after diagnosis[17]. Knowledge of the genetic risk factors of PDA are important for understanding how the disease may develop. However, only a small percentage of patients account for familial or germline inheritance of susceptibility genes, leaving a

majority of patients to develop PDA spontaneously or through non-hereditary risk factors[17, 18]. Identifying non-hereditary, modifiable risks may help improve the numbers of PDA mortality.

a.) <u>Tobacco Smoking</u>

Tobacco in any form (cigarette, pipe, cigar, chew) is a common risk factor for several cancers, including pancreatic[7, 17]. The carcinogens in tobacco are thought to induce somatic mutations in the *KRAS* oncogene and tumor suppressor gene p53, which are commonly associated with PDA progression[17]. Long-term tobacco users have a 2-fold increased risk for developing PDA and contributes to 20-30% of PDA cases[17]. Tobacco use is especially harmful for those with genetic risk factors where the risk is doubled compared to the general population[17].

b.) <u>Alcohol Consumption</u>

Heavy alcohol use of 3 or more alcoholic beverages a day can increase the risk of pancreatitis, which in turn increases the risk of developing PDA[7, 17]. The alcohol metabolite, acetaldehyde, and ethanol are both carcinogens found to induce pancreatic inflammation as seen in pancreatitis which can then contribute to the development of PDA[17]. Aside from the association of the alcohol-pancreatitis-pancreatic cancer axis, alcohol abuse can also directly increase the risk of PDA by almost 1.3-fold[17].

c.) Chronic Pancreatitis

As previously mentioned, CP increases the lifetime risk of developing PDA. However, a diagnosis of CP does not confer an absolute fate of developing PDA. Patients with idiopathic CP are reported to have a 13-fold increased risk of PDA based on meta-analysis[17]. Hereditary CP puts a patient at risk, but depending on the mutation and if they engage in lifestyle risk factors such as smoking or drinking, determines the increased risk for developing PDA.

1.4) Biology of Pancreatic Ductal Adenocarcinoma (PDA)

Identification of genetic and environmental risks has contributed to our understanding of the etiology of PDA and can help in the prevention of PDA within high-risk populations. However, a majority of PDA patients do not have a genetic predisposition and are diagnosed at a fatal stage due to non-specific symptoms[13]. Recent advancements in novel technologies such as endoscopic ultrasound (EUS), computed tomography (CT), and magnetic resonance imaging (MRI) have helped to detect a pancreatic mass, but individuals who are eligible for scans is debatable[13]. Patients who engage in modifiable risk factors such as tobacco smoke and alcohol abuse can be screened more often, but these are not absolute factors nor are they specific to pancreatic cancer. Regardless, even if the cancer is caught at a prognostically favorable timepoint, candidates for resection have about an 80% chance of recurrence[13]. Other current therapeutic options such as chemotherapy agents and radiation remain largely ineffective leaving PDA as one of the most lethal cancers.

Despite the frustratingly stagnant numbers for the outcome of PDA, there has been immense progress in understanding the tumor biology. Clinical studies from surgical resection and biopsies suggest that a majority of pancreatic cancers start at the head as opposed to the body or tail[15]. Closer examination at the microscopic level reveals that pancreatic cancer can potentially be derived from several precursor lesions: pancreatic intraepithelial neoplasia (PanIN), mucinous cystic neoplasia (MCN), and intraductal papillary mucinous neoplasia (IPMN)[2, 13]. PanINs are the most studied pre-cancerous lesions and are closely associated with progression to PDA[13]. Through surgical resection and autopsy studies, almost 30% of adults present with varying degrees of PanINs, which are graded from low to high grade[15]. However, not all patients with PanIN formations progress to pancreatic cancer; this depends on the acquired genetic aberrations present in patients[15].

Next generation sequencing (NGS) has helped identify the genetic landscape that influences the transition from PanIN to PDA. From these studies it was found that over 90% of patients diagnosed with PDA had an acquired activating *KRAS* mutation[20]. *KRAS* is a small GTP-ase responsible for the activation of several downstream pathways including Raf/ERK and PI3K signaling needed for cell proliferation, migration, and survival[13, 15]. Oncogenic *KRAS* is considered one of the initiating factors of PDA that is seen highly activated from low to high grade PanINs and PDA[2, 13, 15]. The most common aberration found in *KRAS* is the missense mutation G12D (c.35G>A) that results in the constitutive activation of *KRAS* and therefore activates further signaling of downstream effectors that promote tumor initiation and progression[13]. Mutations in *KRAS* are typically followed by subsequent somatic alterations in the tumor suppressor

genes *CDKN2A, TP53, and SMAD4/DPC4*[2, 13, 15]. The loss-of-function in *CDKN2A* which encodes for $p16^{ARF}$, a protein necessary for cell cycle arrest, is found in low grade PanINs[21]. As PDA progresses to moderately differentiated PanIN lesions, mutant p53 becomes more prevalent[15, 21]. This is followed by mutations in *SMAD4/DPC4*, which is associated with TGFβ signaling and often seen in high-grade PanINs and malignant disease[2, 21]. In addition to the genetic alterations defined in tumor cells, the surrounding microenvironment undergoes a gradual increase in collagen deposition that contributes to the characteristic desmoplastic response found in PDA patients (Fig. 1.4A)[2, 15, 21].

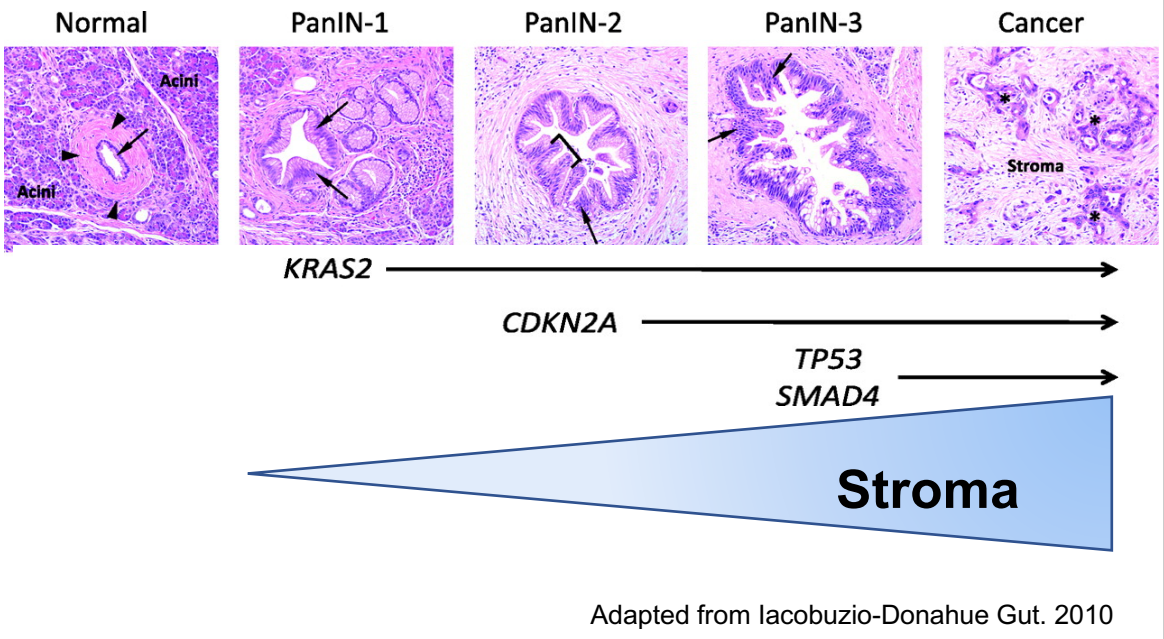

Adapted from Iacobuzio-Donahue Gut. 2010

Figure 1.4.): Histological representation of human PDA progression. Normal tissue is comprised primarily of acini with the occasional islet and ductal cell (arrow) surrounded by collagen (arrow heads). PanIN-1 (low grade) lesions present with mucinous hyperplasia (arrows)[2]. PanIN-2 are distinguished from PanIN-1 by papillary folded indentations (brackets)[2]. High-grade, or PanIN-3, lesions are poorly differentiated lesions with abnormal growth, loss in cell polarity (arrows), and increased stromal response[2]. Cancer presents as undifferentiated cells (asterisks) with a distinct collagen-dense stromal response [2] (blue gradient triangle).

Although patients with PDA may appear to be histologically similar with a predictable genetic landscape, response to therapy and clinical outcomes varies. Advancements in large-scale molecular testing have helped further characterize PDA into several molecular subtypes for better clinical diagnostic, therapeutic, and prognostic outcome. Bailey *et al.* identified four molecular subtypes termed as squamous, abnormally differentiated endocrine exocrine (ADEX), pancreatic progenitor, and immunogenic molecular subtypes based on transcriptomics from untreated PDA patients that had high cellularity (40% tumor cells present), which correlates with previous studies[20, 22]. However, in 2018 Puleo *et al.* performed transcriptomics on over 300 PDA formalin fixed paraffin embedded samples and classified PDA into "Basal-like" and "Classical"[23]. Classical was further divided into immune classical and pure classical[23]. Samples that had low-cellularity were classified into stromal-activated and desmoplastic[23]. The variations in nomenclature for the classification of PDA have recently been reconciled into two main categories based on cell-lineage and identity: "Squamous" and "Classical-Pancreatic". Regardless of the nomenclature, these labor-intensive genomic studies have advanced our understanding of PDA with potential improvements in patient therapeutic options that better align with the subtype presented at diagnosis.

1.5) Mouse Models of Pancreatitis and PDA

Analysis of patient data is a useful tool to understand the development of human pancreatic cancer and tumor biology. However, obtaining enough quality samples for

clinical significance and obtaining samples from early stage PDA in humans are limitations to consider. Alternatives to studying PDA include the use of mouse models, primary or immortalized pancreatic human cell lines, cell-derived xenograft models and organoid cultures that have assisted in defining the molecular events and biology that promote pancreatic disease. These model systems are also important for the initial steps in analyzing therapeutic targets to be translated to humans for clinical trials.

i.) Mouse Models of Pancreatitis

Similar to humans, murine models of pancreatitis can be categorized as acute or chronic. There are several ways to study acute and chronic pancreatitis in mice, however, cerulein-induced methods are the most reliable, reproducible, and economical[24]. Cerulein is the amphibian peptide hormone orthologue to cholecystokinin (CCK), which binds to the CCK-2 receptor to induce the release of digestive enzymes from acinar cells[25]. When given to animals as intraperitoneal injections at supramaximal doses, cerulein stimulates acinar cell stress, necrosis, and an inflammatory response without affecting ductal or endocrine cells[25, 26]. To distinguish between acute and chronic experimental pancreatitis, the amount and duration is adjusted to an extent that the phenotype reflects the correlated human disease.

The protocol for acute pancreatitis varies, but in general, cerulein is given to mice for several hourly injections at 50μg/kg[27]. In our lab we inject mice with 7 hourly injections then harvest pancreata one hour after the last treatment[24, 25]. Following the acute cerulein-induced pancreatitis protocol, pancreata exhibit similar

pathophysiological clinical findings in humans including activation of pancreatic enzymes, immune infiltration, pancreatic edema, and acinar cell vacuolization[24, 25]. These features resolved shortly after cerulein-cessation making this model a reliable method for studying acute pancreatitis.

Chronic pancreatitis can also be mimicked in murine models using a modified protocol. Similar to acute, the chronic pancreatitis protocol varies among labs, however, the overall theory is that repeated bouts of acute pancreatitis can develop into a chronic pancreatitis-like disease[24, 25]. Our lab has established a protocol of cerulein injections at 250μg/kg twice daily for 2 consecutive weeks[27, 28]. Mice are then sacrificed at several timepoints post-cerulein treatment. The extended cerulein protocol reproduces many of the features seen in human disease such as tissue atrophy and a progressive increase in a fibrotic response[24, 25]. Additionally, acinar cells undergo a process termed acinar-ductal metaplasia (ADM) in which acinar cells transdifferentiate into a ductal-like cell[10, 11]. ADM serves as a protective event during injury in which acinar cells reprogram transcriptional targets to avoid further cell death and damage[10, 11]. However, unlike in humans, where chronic pancreatitis results in permanent damage and ADM can progress to neoplasia, mice do recover from cerulein-induced pancreatitis a few weeks after withdrawal. For this purpose, experimental chronic pancreatitis can also be referred to as severe-acute pancreatitis.

ii.) <u>Models of PDA</u>

Developing effective models of PDA that accurately reflect the human disease is crucial in improving patient outcome. Several models are used to study PDA, each

with their own advantages and shortcomings towards basic and translational research. The main preclinical models to study PDA include:

a.) <u>Human PDA Cell Lines</u>

Several human PDA cell lines have been characterized and established over the past 5 decades[29]. Cell lines provide a homogenous population of cells that grow at a relatively quick and predictable rate, indefinitely in the proper media[30, 31]. They are typically well-suited for *in vitro* drug screening or genetic manipulations before moving into more complex systems[30, 31]. Although the use of cell lines are convenient for time and financial purposes, a number of limitations exists such as the lack of the presence of the tumor microenvironment, genetic drift from the initial primary tumor, absence of tumor heterogeneity and the limited number of PDA cell lines available for culture that need to be considered for translational purposes[30].

b.) <u>Cell Line and Patient-Derived Xenograft Models of PDA</u>

Patient-derived Xenograft models involve human transformed cells or patient-derived tumor pieces to be injected into immune-compromised mice either subcutaneously or orthotopically[30]. Subcutaneous injection is a relatively quick method with palpable masses forming 2-6 weeks after implantation and can be used to easily measure tumor growth following manipulation prior to implantation[30]. The orthotopic model involves implantation of patient tumors directly into the pancreas of the mouse in order to mimic the natural surrounding microenvironment as well as preserve the appropriate avenues for metastasis to secondary site[30]. Both methods represent the tumor biology and morphology more effectively than 2D cultures. A major consideration

for xenograft models, whether cell line or patient-derived, is that the stroma that forms is murine derived while the injected cells are from human cell lines[30, 31]. Additionally, the absence of an immune response from using immune-compromised mice affects the interpretation of results and limits the use of testing for immunotherapeutic drug options[31].

c.) <u>Organoid Cultures</u>

Another method to the basic biology of PDA is the use of organoid culture systems. 3D organoid cultures are *in vitro* systems that utilize artificial extracellular matrices to embed primary cells directly extracted from tumors for growth and analysis[30, 31]. The morphological features of PDA are recapitulated after embedded cells adjust to the artificial matrices that mimic the tumor-stromal environment[30]. Common 3D matrices used for organoid cultures are collagen type I and Matrigel (a combination of basement membrane collagen IV, laminin, and growth factors) [31]. Organoid cultures can be used as preclinical models for patient-derived tumor drug screenings as a mode of precision medicine. However, a challenge presented by using organoid systems is that protocols vary among labs and the number of cells obtained directly from the pancreas through biopsy specimen or fine needle biopsies (FNB) are low in quantity and quality which decreases organoid success rates[30]. Additionally, it takes weeks to months for cells to grow and stabilize in culture as well as interpret results from drug screening[30, 31]. However, with further optimization and streamlining of the organoid culture system, it has the potential to serve as a clinical benefit to patients and maintains tumor heterogeneity better than 2-D culture systems.

d.) Genetically Engineered Mouse Models

Genetically engineered mouse models (GEMMS) are a useful tool to study the initiating and metastatic events of PDA in a relatively controlled *in vivo* environment. There are several GEMMS to study PDA that target different mutations seen throughout disease development as previously described[32]. However, since *KRAS* is the most frequent and earliest activated oncogene associated with PDA, most GEMMS are based on mutant *KRAS*[32, 33]. To study the initiating events of PDA, mice have been engineered to express the activating *Kras* mutation G12D at the endogenous locus[34]. To direct oncogenic *Kras* in a time and pancreas specific manner, a STOP cassette flanked by loxP sites precedes *Kras*, annotated as *Lox-STOP-Lox-Kras*$^{G12D/+}$ [34]. The STOP cassette prevents transcription and translation of oncogenic *Kras* until Cre recombinase is introduced into the system which is accomplished by crossbreeding with animals that contain a Cre transgene under the control of the pancreas-specific promoters of either *PDX1* or *Ptf1a*[32, 34]. Cre recombinase recognizes the loxP sites and recombines out the STOP cassette which in turn activates expression of oncogenic *Kras* in pancreatic progenitor cells. This model is referred to as the "*KC*" model of tumorigenesis[32]. The *KC* model recapitulates the initiating events of PDA from ADM to high-grade neoplasia with a concomitant gradual increase in a collagen-dense desmoplastic response as animals age[32, 34]. It is possible to find PDA sporadically in *KC* mice, but expression of oncogenic *Kras* alone is usually not sufficient for carcinoma. For a more robust, metastatic model of PDA, the *"KPC"* mouse incorporates both oncogenic *Kras* and alterations in the tumor suppressor gene *Trp53* with either introduction of an R172H (*LSL-Trp53*$^{R172H/+}$*)* mutation or deletion of a

wild-type allele (*Lox-p53-Lox*)[35]. Depending which *Trp53* is used in the *KPC* system, introduction of Cre-recombinase will either recombine out the STOP cassette for mutant *Trp53* expression or recombine out an allele of *Trp53*[35]. On average, *KPC* mice develop invasive tumors and become moribund in a range from 4-6 months[35].

The *KC* and *KPC* models have expanded our knowledge on the events that initiate and contribute to the development of PDA. However, since Cre is driven by a pancreatic parenchyma promoter, studies of conditional knockout alleles of other genes to determine their contribution in the development of PDA are limited to manipulation within the pancreatic epithelium. To overcome this issue our lab has established a dual-recombinase system to study the significance of genes expressed by cells in the tumor microenvironment (TME) while mice develop PDA. In this model, Flp-Frt system is used to drive tumorigenesis and invasive PDA, while the Cre-LoxP technology is used to interrogate genes outside of the pancreatic epithelium such as fibroblasts or immune cells. In this case, *Kras* is preceded by a STOP cassette flanked by Frt sites, annotated as *Frt-STOP-Frt-Kras*$^{G12D/+}$. The STOP cassette prevents transcription and translation of oncogenic *Kras* until FlpO recombinase, a codon-optimized yeast recombinase, is introduced into the system which is accomplished by crossbreeding with animals that contain a FlpO transgene under the control of the pancreas-specific promoters of either *PDX1* or *Ptf1a*[36]. FlpO recombinase recognizes the Frt sites and recombines out the STOP cassette which in turn activates expression of oncogenic *Kras* in pancreatic progenitor cells. This model is referred to as the "*KF*" model of tumorigenesis[36]. To be able to interrogate cells in the TME in a more robust model, our lab also generated the *KPF* model which consist of *Frt-STOP-Frt-Kras*$^{G12D/+}$;

Frt-STOP-Frt-Trp53; Ptf1a$^{FlpO/+}$ annotated as "*KPF*". Using this dual-recombinase system is a multistep approach in the next generation of GEMMs in elucidating the significance of targets in the TME during the development of PDA.

GEMMS are useful tools to recapitulate the gradual progression of PDA with a co-evolving collagen-dense stromal reaction that mimics human disease *in vivo*. However, the major considerations for using GEMMS are time and cost. It can take months to obtain the correct genotype for studies and months for tumors to develop in order to observe a distinguishable phenotype[32]. Additionally, maintaining mice and obtaining enough mice for statistical power for accurate interpretation of results can be a financial burden[32].

1.6) Current and Emerging Therapeutic Targets of PDA

Advancements in technology and research have elucidated the risk factors that contribute to PDA and the tumor biology. Unfortunately, revealing the molecular events that contribute to PDA have not significantly improved preventative methods or treatment options, leaving PDA as one of the most lethal and aggressive cancers[14]. Only 20% of patients diagnosed with PDA are eligible for surgical resection followed by adjuvant chemoradiation to help reduce the recurrence of disease[37-39]. However, surgical resection is not a curative option and patients have almost an 80% chance of recurrence[39]. A majority of patients are not eligible candidates for surgical procedures due to the presentation of invasive cancer[37, 38]. This limits therapeutic options to help alleviate symptoms rather than actually treat the disease with either a short list of ineffective chemotoxic agents or palliative care[37]. In general, chemotherapy is aimed

to target proliferative cells which includes both healthy and cancer cells that can have adverse side effects[37]. In PDA, however, successful delivery of therapeutic agents to the site is compromised by the collagen-dense stromal response that encapsulates the cancer and forms a barrier for effective drug delivery[38]. The fibrotic, stromal reaction accounts for almost 90% of the tumor volume and consists primarily of collagen secreted from activated fibroblasts, but also features an overproduction of extracellular matrix (ECM) factors and an immunosuppressive microenvironment (Figure 1.6)[38]. Throughout the development of PDA, the stroma and cancer cells coevolve through intricate signaling pathways creating an avascular, hypoxic environment that promotes tumor growth and metastasis[40]. Consequently, understanding the molecular crosstalk between the stroma and cancer cells is necessary to improve disease outcome.

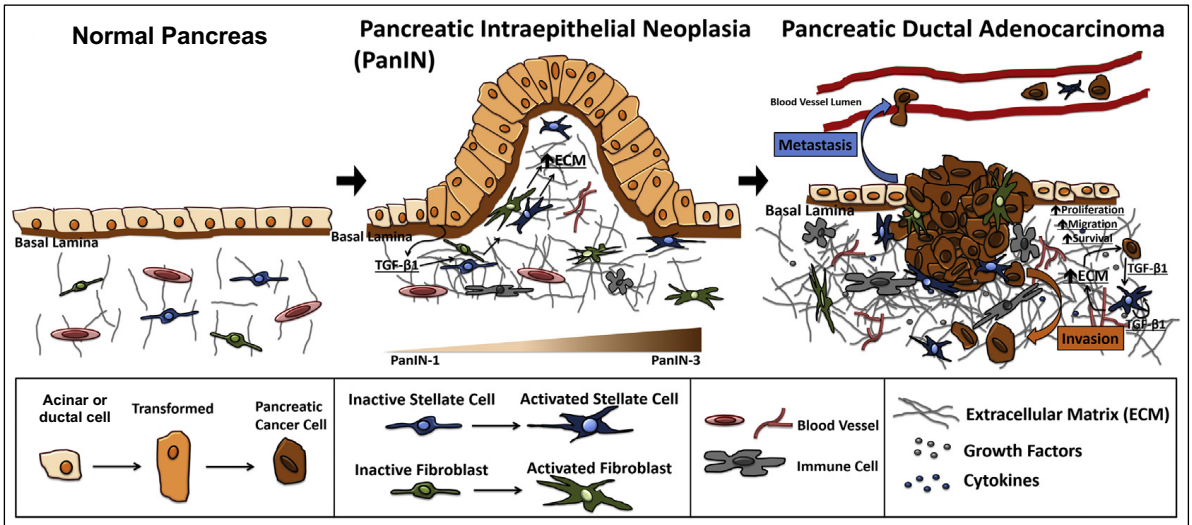

Figure 1.5A) Tumor and stromal landscape of PDA (read from left to right). Healthy pancreatic epithelium is intact. At the onset of tumorigenesis, the epithelial cells undergo morphological changes during acinar-ductal metaplasia (ADM) followed by low-grade neoplastic transformation (PanINs). As more mutations are acquired and the extracellular matrix adapts to the morphological changes in the epithelium, neoplasia can advance to cancer. The release of growth factors and cytokines further exacerbates the affected area and promotes tumor cells to proliferate, migrate and metastasize to the liver or lung.

i.) Inhibiting Neoplastic Cell Signaling

Over the past few decades, studies have aimed at inhibiting the molecular pathways that drive tumorigenesis in epithelial cells. The neoplastic transition of the epithelium in the presence of an injury or mutation works in concert with the stroma to promote tumor growth and progression[37, 38, 40]. Therefore, further studies of the molecular networks that initiate tumorigenesis within the epithelium are crucial in understanding and potentially targeting early events of PDA.

a.) Direct Targeting of Oncogenic *KRAS*

In PDA, mutant *KRAS* is detected in over 90% of patients[41, 42]. Acquisition of oncogenic Kras is confined to the epithelial compartment of the pancreas and is considered the genetic initiating event that drives tumorigenesis[42]. *KRAS* is one member of the Ras GTP-ase family that are responsible for cell proliferation and migration[41-43]. GTP-ases, such as *KRAS*, cycle between a GTP-bound "active" state and GDP-bound "inactive" state. In quiescent cells, *KRAS* is bound to GDP in the inactive state[41, 43]. As a consequence of ligand-receptor activation events, *KRAS* is activated due to guanine nucleotide exchange factors (GEFs) that facilitate signaling by catalyzing the exchange from GDP to GTP bound *KRAS* for mitogenic activities[41, 43]. GTP-ase activating proteins (GAPs) terminate signaling through GTP hydrolysis, thus releasing GTP-bound *KRAS* (active) back to GDP-bound *KRAS* (inactive). However, the cycling between the active and inactive state is disrupted when *KRAS* is mutated and prevents GTP hydrolysis, leaving *KRAS* in the GTP-bound active state[41]. Oncogenic *KRAS* results in unbridled cell proliferation that stimulates further signaling

networks to promote tumor growth and metastasis[42]. Based on this evidence and the overwhelming number of patients with a *KRAS* mutation, the National Cancer Institute has set forth to prioritize the development of treatments against *KRAS*[42].

Although pharmacological inhibition of oncogenic *KRAS* appears to be a logical strategy in combating PDA, it has proven to be a difficult task. One approach to target *KRAS* is by inhibiting the activation site[41-43]. This approach is especially challenging due to the lack of information of the physical structure of the activation binding site for the development of a small molecule that can bind to the nucleotide binding pocket [41-43]. To date, inhibitors against *KRAS*(G12D) have proven unsuccessful, but targeting *KRAS*(G12C) has made some headway. $KRAS^{G12C}$ is a common mutation among non-small lung cancer patients, but is detected in ~3% of PDA patients[41]. Ostrem *et al*. reported a new binding pocket within the G12C mutation that is targetable and have developed a small molecule inhibitor that irreversibly binds to mutant $KRAS^{G12C}$ to induce GDP-bound inactive *KRAS*[44]. This targeted therapy is a hopeful option for PDA patients with an acquired $KRAS^{G12C}$. Another approach in targeting *KRAS* is to block it from docking to the intracellular membrane that is required for its activation[41, 43]. Membrane stabilization is achieved by post-translational modifications that can be targeted to inactivate oncogenic *KRAS*[41, 43]. Again, this approach has proven to be unsuccessful and drugs that tried to inhibit the post-translational modifications that facilitate RAS membrane binding did not show any survival benefits in patients.

b.) Indirectly Targeting *KRAS* Activation

Besides direct targeting of oncogenic *KRAS*, several methods of indirect targeting have been employed. *KRAS* is activated by several upstream receptors, including Epidermal Growth Factor Receptor (EGFR) which is required for pancreatic tumorigenesis[43, 45]. However, EGFR inhibitors show a mild response in PDA patients that quickly become resistant[45]. The most widely used and clinically approved method to disrupting *KRAS* activation is by targeting downstream factors. There have been eleven Ras-related effector families identified. Two of the most commonly studied and targeted pathways are the Raf-MEK-ERK mitogenic signaling and PI3K-Akt-mTOR for cell survival pathways (Figure 1.6B).

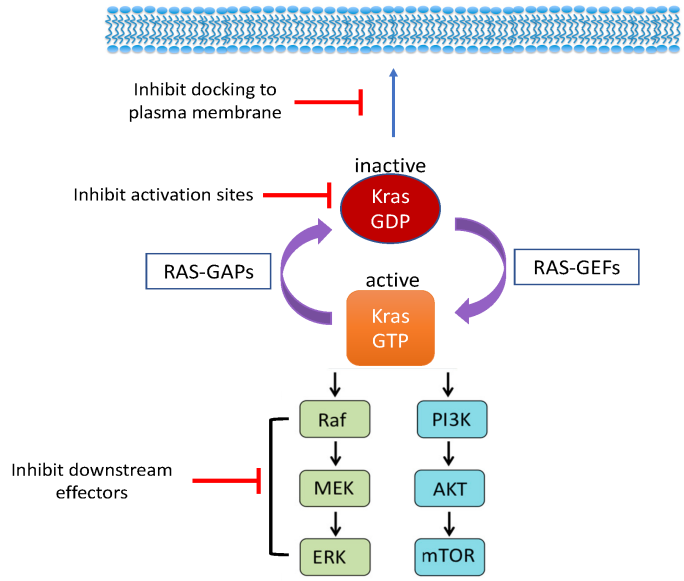

Figure 1.5B.) Points of intervention to inhibit Kras signaling. Activation of *KRAS* form upstream receptor-ligand binding regulates GTPase activation of Kras. Kras activation triggers several downstream cascades, with Raf-MEK-ERK and PI3K-AKT-mTOR being two of the most well-defined pathways. Several points of inhibition to inactive oncogenic *KRAS* have been developed including inhibiting *KRAS* from the required docking sites to the plasma membrane, directly inhibiting the *KRAS* activation site and inhibiting downstream effectors.

1.) RAF-MEK-ERK

RAF is a serine/threonine kinase directly downstream of *KRAS* with 3 isoforms: ARAF, BRAF and CRAF, in which selective BRAF inhibitors have shown to be successful in melanoma patients[43]. However, in *KRAS*-driven cancers such as PDA, the small subset of PDA patients with a BRAF mutation were refractory to BRAF inhibitors. One explanation for the drug failure in PDA is due to the "RAF inhibitor paradox"[42, 43]. Raf isoforms require homo- or heterodimerization for activation stimulated by upstream Ras activation[5, 25]. By inhibiting BRAF in these patients, this indirectly binds and stabilizes CRAF that activates the MEK-ERK kinases[42, 43]. Pan-RAF inhibitors have been developed and are currently being tested for specificity and efficacy in preclinical models[41].

An alternative to bypass the Raf inhibitor paradox is to inhibit the downstream effectors of Raf, MEK or ERK. Again, as with Raf inhibitors, inhibiting MEK or ERK in RAS-driven cancers have had insignificant effects on pancreatic tumors[41-43]. Although inhibiting the RAF-MEK-ERK axis has had minimal success in PDA, it has led to further studies in understanding the signaling networks that drive tumorigenesis and the enhanced resistance to current drug options.

2.) PI3K-Akt-mTOR

PI3Ks are a family of plasma membrane-associated lipid kinases consisting of three classes based on their heterodimerization among several subunits including: p110 catalytic subunit and p55, p84, p85 regulatory subunits[46]. Vps34 exist as a single catalytic subunit within the Class III PI3K family[46]. Regardless of the class, PI3Ks are

stimulated by *KRAS* activation[42]. In PDA, the *PI3CA* gene is the most commonly mutated isoform[42]. For this purpose, drug development has aimed at targeting the p110α subunit. The other isoforms have also been found to be hyperactivated in PDA, in which the thought of using a pan-PI3K inhibitor would be more beneficial. Unfortunately, the pan-PI3K drugs have shown high toxicity and alternative methods of inhibiting the PI3K pathway have come into play[41]. To bypass the issue of toxicity, AKT inhibitors can be used to stop further downstream activation of mTOR. However, inhibiting AKT can lead to an increase in PI3K activity due to the loss of a negative feedback mechanism[15, 41, 42]. Lastly, targeting mTOR has been studied in several cancers. As with targeting the upstream factors of mTOR, inhibiting mTOR can eventually result in hyperactivation of PI3K and/or Akt due to the loss of mTOR as a negative regulator of these effector proteins in *KRAS*-driven cancers[41, 42]. A hypothetical approach to utilize the information gathered from these studies and drug development is to combine inhibitors of the Raf-MEK-ERK pathway with PI3K-AKT-mTOR signaling. Further studies with preclinical models will help elucidate the mechanisms that result in drug resistance and identify the most efficient and least toxic combination of inhibitors for PDA patients.

ii.) Targeting Stromal Factors in PDA

a.) Directly Targeting the Stroma

Due to the presence of the overwhelming collagen-dense stromal response observed at the onset and progression of PDA, several studies have aimed at targeting various components of the stroma in efforts to improve drug delivery and thereby

patient outcome. Initially, studies focused on targeting activated fibroblasts, which produce a majority of the collagen that contributes to the distinct stromal response seen throughout the development of PDA[14]. Olive *et al*. attempted to disrupt the stromal response that would in theory facilitate vascular reconstruction for better drug delivery by using a Hedgehog signaling pathway inhibitor, IPI-926[47]. Sonic hedgehog (Shh) is overexpressed in PDA neoplastic cells[48]. Shh binds to Patched (PTCH) on fibroblasts that results in a conformational change in PTCH releasing Smoothened (Smo) from the membrane to activate the transcription factor Gli, which feeds back to tumor cells in a paracrine loop that ultimately promotes tumor growth[48]. IPI-926 inhibits Smo and thereby the activation of Gli disrupting the crosstalk between tumor cells and fibroblasts to dampen the stromal reaction[47]. Inhibiting stromal hedgehog signaling proved effective in increasing chemotherapy delivery in *KPC* mice measured by a transient decrease in proliferation and an increase in both apoptosis and endothelial cells in the tumor[47]. Unfortunately, when IPI-926 was introduced into clinical trials, it did not show any overall survival benefits in humans[49]. This negative result encouraged further studies into understanding the role of the collagen-dense stromal response in PDA. Rhim *et al*. used both genetic and pharmacological inhibition of Hh signaling to deplete the stroma in *KPC* mice[50]. This study demonstrated that targeting Hh signaling does reduce stromal content, but resulted in poorly differentiated, more aggressive tumors[50]. Ozdemir *et al.* took a slightly different approach by studying the genetic depletion of αSMA cells, or myofibroblasts that secrete collagen, in *KPC* mice[51]. Depleting an entire stromal cell population proved to have negative effects with a more aggressive tumor phenotype and reduced survival[51]. Collectively, these studies

provided insight on the complex role the stroma plays throughout the development of PDA.

Rather than deplete an entire population of fibroblasts or chronically inhibiting a significant factor in stromal signaling, other studies have tried to modify activation states of myofibroblasts. Activation of the vitamin D receptor (VDR) reprograms signaling networks in fibroblasts from an active into a quiescent state[52]. Reprogramming fibroblasts into a quiescent state in pancreatitis and PDA reduced fibrosis and enhanced intratumoral drug delivery in preclinical models[52]. These encouraging results from preclinical models led to the support of clinical trials combining both Vitamin D agonist (paricalcitol) with standard chemotherapy[52]. Unfortunately, clinical trials did not show the same success as seen in mouse models[53]. Another approach to relieving the physical constraints of the stroma that restrict therapeutic delivery is to target components of the ECM. Overproduction of ECM products increases tumor rigidity and contributes to the high interstitial pressure that impairs intratumoral drug perfusion[54]. DuFort *et al.* concluded that hyaluronan (HA), an ECM protein upregulated in a subset of PDA patients, significantly contributes to the high interstitial pressure[54, 55]. To relieve the interstitial pressure and thereby improve drug delivery, the study aimed at depleting HA with pegylated recombinant hyaluronidase (PEGPH20)[55]. PEGPH20, in combination with standard chemotherapy, alleviated tumor pressure and aided in successful intratumoral drug delivery that reduced tumor size and increased survival in *KPC* mice[55]. The positive results from this study translated into clinical trials in patients with high HA expression, but again, did not show the same success rate as seen in the preclinical models[53, 55].

In addition to the physical barrier against treatment, the stroma also presents as an immunosuppressive environment that is resistant to immunotherapy options. Several approaches to reprogram the immune response in cancer include monoclonal antibodies, checkpoint inhibitors, and vaccines[56]. As with other studies that target the components of the stroma, preclinical models have shown limited success with immunotherapy and translating into patients has proved challenging[56]. Although immunotherapy has not had a significant benefit for PDA patients yet, there is promise in the molecular profiling of patient tumors. Obtaining the genetic and stromal composition of tumors can help guide which clinical trial is appropriate and the potential success of the treatment that is available, including immunotherapy.

b.) <u>Indirectly Targeting the Stroma</u>

The crosstalk between the stroma and tumor cells forms a complex relationship in pancreatic disease. A majority of cell surface receptors expressed on tumor cells bind and respond to small molecules such as growth factors or cytokines secreted by stromal constituents[57]. However, the most abundant stromal factor present throughout the development of PDA is collagen[58]. Understanding the influence of collagen and how neoplastic cells respond to the collagen-rich desmoplastic reaction is important in developing strategies to improve patient outcome.

There are two separate families of cell surface collagen receptors: integrins and discoidin domain receptors (DDRs)[59]. Integrins are transmembrane heterodimer cell surface receptors formed by a combination of (18) α and (8) β chains that mediate cell adhesion and migration[59]. There are 24 different integrin family members that respond

to ECM proteins, but only 4 of them bind to collagen with the remaining combination of integrins binding to other ECM products such as fibronectin and laminin [59]. Integrins have been implicated in cancer progression and studied in the context of pancreatic disease, however, little progress has been made in inhibiting their activation in cancer and disease due to issues with drug specificity in targeting integrins[59, 60].

Recently, the non-integrin collagen-binding family of receptor tyrosine kinases (RTK), DDR1 and DDR2, have become of interest in fibrotic disease and cancer. Aberrant activation of DDR1 has been shown to contribute to lung and kidney fibrosis[61, 62]. It is also overexpressed in lung, breast, and pancreatic cancer[63-65]. DDR2 is less studied, but evidence shows that it is a contributing factor of epithelial-to-mesenchymal transition (EMT) and metastasis in breast cancer[66-68]. Although DDRs have limited data in the context of pancreatic disease, they are an attractive feature to study due to their collagen specific binding and their nature as RTKs that have the potential to be druggable targets. Based on the current published data and our preliminary data that shows DDRs play a differential role during pancreatitis and PDA progression, we hypothesize that DDRs contribute to the pathogenesis of pancreatic disease following a fibrotic response. To test this hypothesis, we have developed transgenic mouse models along with the use of cell culture and organoid model systems to study the significance of DDRs in several pancreatic disease states.

1.7.) Physiological Function of Discoidin Domain Receptors and Their Role in Pathological Conditions

i.) Structural Composition of Discoidin Domain Receptors

Discoidin domain receptors are a two-member family, DDR1 and DDR2, with closely related structural features to that of other RTKs [57, 59, 69]. Both DDR1 and DDR2 are transmembrane proteins that contain an extracellular, transmembrane, cytosolic juxtamembrane, and kinase activity domains (Figure 7)[57]. DDR1 exist as 5 isoforms at ~125kDa. DDR1a and DDR1b are the most common and active isoforms[57, 59]. DDR1c is less abundant, but is also an active isoform. DDR1d and DDR1e are present, but exist as truncated proteins that are kinase-deficient and inactive[57, 59]. DDR2 only exist as 1 known active isoform at ~125kDa[57, 59].

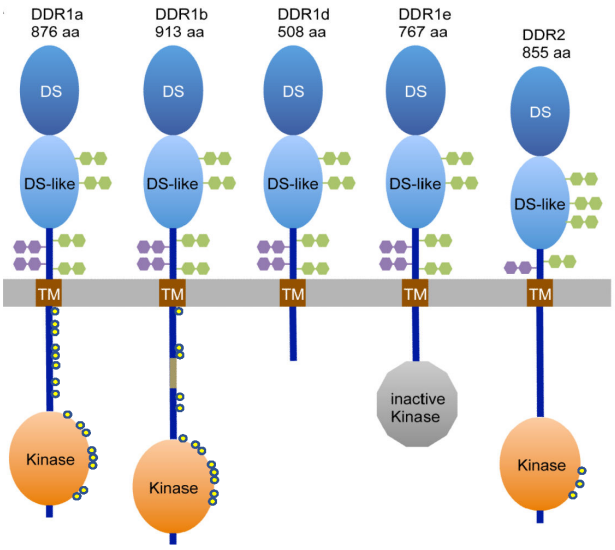

Adapted from Leitinger Intrn Rvw of Cell and Molec Bio. 2014

Figure 1.6) DDRs Structure and phosphorylation sites. Featured are DDR1a, b, d, e (DDR1c not shown) and DDR2. Extracellular domains: DS, DS-like, and JM domain. Green symbols are predictive N-glycosylation; purple symbols are predicted O-glycosylation sites. Gray horizontal bar represents plasma membrane. Intracellular domains: TM, kinase domain (if available), and short cytoplasmic tail.

ii.) Collagen Binding Properties of DDRs

Most RTKs bind to relatively small, soluble factors that activate and modulate downstream effectors through their phosphorylation[59]. DDRs, however, are unique in their ability to be activated by collagens to regulate cell proliferation, migration, adhesion, and ECM remodeling[57, 59, 69]. There are 28 types of collagen, but all collagens are characterized by homotrimeric or heterotrimeric triple helical α-chains[59]. Of the 28 known collagens, it has been shown that DDR1 and DDR2 respond to fibrillar collagens I, II, and III, but only DDR1 binds to non-fibrillar basement membrane collagen IV[59, 69].

DDRs only recognize collagens in their native helical structure; denatured collagen, such as gelatin, cannot induce activation with DDRs[59]. The specificity of DDR-collagen binding has been linked to a 6-amino acid motif, GVMGFO (O stands for hydroxyproline) in collagens I,II,III[57, 59]. Other collagen binding sites have not been mapped out yet, but suggest that the function of each collagen and binding site is relevant for different cell activities[57, 59].

iii.) Signal Transduction of DDRs

DDRs can exist as monomers or pre-existing dimers in the inactive state[59]. Upon collagen stimulation, DDRs homodimerize and are autophosphorylated for activation of cell processes [59]. The activation of DDRs is slow and sustained with peak phosphorylation taking hours in comparison to the kinetics of other RTKs that range from seconds to a few minutes[57, 59, 69]. The basis of the slow activation rate is unclear,

but suggest DDR activation is dependent upon cell activities or involves removal of an inhibitory protein[59].

Recent phospho-proteomic studies have identified DDR1 and DDR2 phosphorylation sites and revealed the docking sites for adaptor proteins, in which most contained either a Src-homology 2 (SH2) or phosphotyrosine-binding (PTB) domain[59]. Additional proteomic studies used glioblastoma and placenta cells to confirm the interactions of DDR1 with Src-homology and collagen-2 (Shc2), C-terminal Src kinase (Csk), Src-homoogy protein-2 (SHP-2, the p110 catalytic subunit of PI3K), non-muscle myosin heavy chain -IIA, Pyk2 (the focal adhesion kinase (FAK) homolog protein), and members of the Signal Transducers and Activators of Transcription (STAT) family[57, 59]. Other proteins that have been associated with DDR1 include the neuronal phosphoprotein DARPP32, Hippo pathway protein KIBRA, Syk, Notch1, and cell polarity regulator proteins Par3/6[57]. As with DDR1, it has been reported that ShcA is recruited to DDR2 docking sites following DDR2 collagen activation[57, 59]. However, unlike DDR1, the extensive list of downstream activation proteins is mostly unknown for DDR2. Potential binding partners include SHP-2, Nck1, Lyn (Src family kinase member), phospholipase C-like 2 (PLCL2), and phosphatidylinositol-4-phosphate 3 kinase (PI3K3C2A), but further studies are needed to validate their status in DDR2 activation[57, 59, 69].

Despite the recent studies that have revealed portions of the DDRs interactome, the signal transduction that follows is not as well defined as other RTKs. Studies using cell lines have exposed potential pathways that are cell-type dependent. For example, in nonmalignant cells, DDR1 activates ERK1/2 of the MAPK pathway in vascular

smooth muscle cells, but inhibits signaling in mesangial cells[57, 59, 69]. In breast and colon cancer cells, upregulated DDR1 activation lead to an increase in pro-survival processes via the MAPK and PI3K pathways[57, 59]. Another study in colon cancer cells supports DDR1 activation as a pro-survival mechanism by regulating Notch1 cleavage that results in translocation of Notch1 to the nucleus to upregulate the pro-survival genes, Hes1 and Hey2[57, 59]. In addition to regulating mitogenic and pro-survival pathways, DDR1 activation was reported to inhibit integrin-α1β1 in EMT-related processes by stabilizing E-cadherin in Madin-Darby canine kidney (MDCK) cells[59, 69]. In contrast, however, DDR1 activation was also found to promote EMT in pancreatic cancer cells through the pCAS130/JNK pathways that results in N-cadherin upregulation and EMT-like cell scattering[57, 59, 69].

Similar to DDR1, DDR2 activation supports EMT activity, but through a different mechanism. Zhang *et al*. showed that DDR2 activation stabilizes SNAIL1, a main driver of EMT, in breast cancer cells and orthotopic xenograft mouse models, which promotes cancer cell invasion[68]. Evidence for other DDR2-induced pathways require further analyses to identify the role of DDR2 in a disease setting.

iv.) Physiological Role of DDRs

DDRs are expressed in a wide variety of organs during development and adult tissue. DDR1 is expressed in epithelial cells of the kidney, lung, gastrointestinal tract, and brain, while DDR2 is expressed in cells of mesenchymal origin such as fibroblasts and connective tissue[59]. To better understand the functional role, mouse models of

either DDR1 or DDR2 genetic ablation have been generated to study the significance of DDRs during embryogenesis and adult development.

DDR1 knockout (*DDR1*$^{-/-}$) were generated by genetic deletion of exon 5 that renders the gene non-functional and does not get expressed. Phenotypically, *DDR1*$^{-/-}$ mice are viable and smaller in size compared to wild-type littermates[59, 70]. Further analysis of *DDR1*$^{-/-}$ mice provides evidence of reproductive defects and a delay in mammary gland growth[59, 70]. A majority of female *DDR1*$^{-/-}$ mice display fertility defects due to impaired blastocysts implantation[59, 70]. Furthermore, female *DDR1*$^{-/-}$ mice feature a delay in mammary gland branching and ductal growth that impairs milk secretion for pups; this can be corrected by using older female *DDR1*$^{-/-}$ mice to breed. Besides playing a role in reproduction and lactation, DDR1 is also important for kidney and inner ear architecture[59, 70]. Mice lacking DDR1 demonstrate altered cell morphology that affects their auditory functions and results in hearing loss[71]. In the kidney, DDR1 deficient mice acquire proteinuria with a disrupted glomerular basement membrane and localized increased collagen synthesis[37, 72]. Collectively, these data provide a role for DDR1 in epithelial cell structure, motility, and collagen production that are important considerations for studying DDR1 in disease states.

In humans, germline DDR2 missense mutations are associated with spondylo-meta-epiphyseal dysplasia (SMED-SL), a rare genetic disorder characterized by short stature, premature calcifications, and bone abnormalities[73]. There have been 4 detected missense mutations in DDR2 related to SMED-SL, in which 3 mutations result in obstructions to the trafficking of DDR2 outside the endoplasmic reticulum and only 1 known mutation shows a defect in collagen binding[74]. Mouse models support the

evidence that DDR2 is required for skeletal bone growth and development[73]. Targeted deletion of DDR2 in mice disrupts chondrocyte proliferation that results in dwarfed mice with short long bones and shortened snouts, concluding DDR2 is necessary for bone growth[75]. *Slie* mice are another mouse model to study DDR2. This model was generated due to a spontaneous, autosomal dominant mutation acquired when a majority of the DDR2 gene is deleted[75]. Studies in *slie* mice suggest DDR2 is required for gonadal development as all females are anovulatory and a majority of males have defects in spermatogenesis[75]. To overcome the complications sustained with genetic DDR2 deletion during embryogenesis, Corsa *et al.* developed a conditional DDR2 knockout mouse[67]. This allows for time and organ specific deletion of DDR2 to study the functional role of DDR2 during the pathogenies of various diseases in the future.

v.) Pathophysiology of DDRs in Cancer

DDRs are implicated in a wide variety of pathological disorders including fibrosis, osteoarthritis, and atherosclerosis[57, 59]. However, a considerable effort has been made in understanding their role in malignant transformation. Both DDRs have been shown to be overexpressed in cancer that typically correlates with an unfavorable outcome[57, 59]. Their identification as RTKs in combination with their dysregulation in cancer makes DDRs attractive therapeutic targets. Several small molecule kinase inhibitors against DDR1 and DDR2 have been developed with limited success due to the lack of specificity between the DDRs and other receptor kinase activities[57]. Therefore, understanding their exact role in the development and progression of cancer is crucial in developing more specific and selective drugs against DDRs to

improve disease outcome. Several approaches have been employed to study the role of DDRs in the context of cancer. Both genetic and pharmacological inhibition of DDRs have helped define their functional role in cancer, while large scale genetic and proteomic human studies have allowed for the detection of mutations, phosphorylation, and dysregulation of DDRs in various cancers.

Lung cancers have been the most widely studied in terms of DDRs. DDR1 is upregulated in Non-Small Cell Lung Carcinoma (NSCLC) and correlates with poor survival[76, 77]. Phospho-proteomic studies found DDR1 as one of the top 3 most phosphorylated kinases in NSCLC[69]. To further support DDR1 as a potential drug target in lung cancer, DDR1-null animals were used in a model of lung adenocarcinoma and showed a reduction in tumor burden and metastasis with increased survival when combined with a Notch inhibitor[65]. Using genomic studies in a relatively small cohort of small cell carcinoma (SCC) and lung adenocarcinomas, somatic mutations were detected in both DDR1 and DDR2[57]. These findings were followed by another study that confirmed DDR2 mutations in SCC and mapped them back to the collagen-binding and kinase domains that may be oncogenic[78]. The acquired DDR2 mutations in SCC lines were more sensitive to the Src-kinase inhibitor, dasatinib[79]. These findings encourage further investigation of DDRs to understand and treat lung cancers.

DDRs have also been well-characterized in breast cancer cell lines and found to be dysregulated in breast cancers. Expression of DDRs vary depending on the tumor type and grade. Additionally, experimental models of breast cancer report conflicting results on the role of DDRs in breast cancer progression. DDR1 is overexpressed in

several lines of breast carcinoma cells in which DDR1 inhibition may pose as a logical target[80]. Conversely, *Takai et al.* showed DDR1 ablation in the mammary gland tumor model promotes fibrosis, necrosis, and a more aggressive tumor[63]. DDR2 has also been targeting in breast cancer, and has shown more promising results. *Zhang et al.* confirmed that DDR2 stabilizes SNAIL1 during EMT which implies DDR2 is not only associated with EMT, but with tumor cell invasion and metastasis[68]. Conditional DDR2-knockout mice in a mammary gland tumor model supports the idea that DDR2 is necessary for metastasis[67]. More studies are necessary to obtain a more comprehensive understanding of the role of DDRs in breast cancer progression, however, results so far have shown DDRs as likely targets.

Expression of DDRs is not confined to lung and breast cancers. DDR1 is overexpressed in brain, prostate, esophageal, hematological and ovarian cancers[57, 59]. DDR2 is overexpressed in thyroid, nasopharyngeal, and some lymphomas[57, 59]. In pancreatic cancer, where collagen is a dominant feature and serves as a natural reservoir for DDR activation, there is currently limited data that defines the expression and functional role of DDRs in pancreatic disease. *Aguilera et al.* showed that DDR1 is upregulated in human samples of PDA and that pharmacological inhibition of DDR1 in combination with the standard chemotherapeutic agent gemcitabine, reduced tumor burden and increased survival[64]. DDR2, on the other hand, has not been defined in a pancreatic disease setting. Our preliminary data shows DDRs are differentially expressed during the onset and progression of pancreatitis and pancreatic cancer. Based on the current literature and our preliminary results that will be discussed, we

hypothesize that activation of DDRs promotes the progression of PDA following the fibrotic response after injury.

Chapter 2: Defining the Role of Discoidin Domain Receptor 1 (DDR1) In the Pathogenesis of Pancreatic Disease and Pancreatic Ductal Adenocarcinoma

Introduction

Pancreatic ductal adenocarcinoma (PDA) is currently the 3rd leading cause of cancer deaths in the United States affecting over 57,000 adults each year[81]. Only 10% of PDA patients survive up to 5 years, with a majority of patients succumbing to the disease within a year of diagnosis[22, 81]. The high mortality of PDA is attributed to the absence of distinct clinical symptoms, a lack of early detection methods, and ineffective therapeutic options[82]. Over the past few decades considerable advancements have been made in studying the development of PDA, but the prognostic outcome has improved only marginally. Consequently, further understanding of the molecular events that contribute to the initiation and progression of PDA is essential for the prevention and early discovery of this lethal disease.

Chronic pancreatitis (CP) increases the lifetime risk of developing PDA[9]. CP is characterized by permanent damage to the pancreas with progressive loss of exocrine cell function, inflammation, and a prominent fibrotic response accompanied by acinar-ductal metaplasia (ADM) [9, 10]. ADM is a transdifferentiation event where acinar cells acquire a ductal cell-like phenotype that plays a reparative role in pancreatic injury[10, 11].

With the acquisition of activating *KRAS* mutations, ADM can progress to premalignant pancreatic intraepithelial neoplasia (PanIN)[83, 84]. As additional mutations accumulate, PanINs are hypothesized to advance to invasive PDA[2, 13].

Both CP and *KRAS* driven tumorigenesis share similar morphological features such as the prominent collagen-dense desmoplastic response that displaces the normal epithelium[2, 13, 85]. The overproduction of collagen, in concert with the deposition of other extracellular matrix (ECM) proteins, creates a largely impenetrable, hypoxic, and nutrient-deficient environment that is influenced by ECM remodeling and impedes drug delivery[86]. The overwhelming desmoplastic response has propelled studies targeting components of the stroma, such as hyaluronan, to enhance drug delivery[87]. Other studies have targeted the desmoplastic fibroblasts, which are a major source of collagen production [47, 50-52]. Unfortunately, widespread depletion of fibroblasts or deletion of specific signaling networks in fibroblast activation accelerates PDA progression[50, 51]. However, reprogramming fibroblasts to a quiescent state after tumors have formed improves drug delivery in preclinical models of PDA[52]. Although the extensive collagen deposition is a hallmark of pancreatic disease, its role during the onset and progression of CP and PDA remain inconclusive. The discrepancies in the current literature provide evidence for not only the complex role the stroma plays in pancreatic disease, but also showcase the diverse interactions of stromal factors that can have opposing roles in PDA progression.

Discoidin domain receptor 1 (DDR1) is a type-1 transmembrane receptor tyrosine kinase that uses collagens as cognate ligands to regulate cell proliferation, adhesion, and migration, and plays a role in ECM remodeling[59]. Aberrant activation of

DDR1 contributes to a number of pathological conditions such as lung and kidney fibrosis[61, 62]. DDR1 is also upregulated in various cancers, including PDA, and has been shown to play a role in tumor growth, progression and metastasis[63-65]. Pharmacological inhibition of DDR1 prolongs survival in a PDA mouse model, but its role in pancreatitis and early neoplasia, has not been explored [64]. In this study, we used DDR1-null *(DDR1$^{-/-}$)* mice to elucidate its functions during the onset and progression of pancreatic cancer as well as pancreatitis. Our data demonstrates a novel role for DDR1 as a gatekeeper of tissue homeostasis, as its ablation in each of these models leads to severe tissue atrophy marked by reduced proliferation and altered ECM dynamics.

Methods and Materials

Mouse Models

The following mice were used: *DDR1*$^{-/-}$ mice have been previously characterized[88]. *Kras*$^{LSL\text{-}G12D/+}$; *Ptf1a*$^{Cre/+}$; *R26R*$^{LSL\text{-}YFP}$ for tumorigenesis studies and *Kras*$^{LSL\text{-}G12D/+}$; *Trp53*$^{R172H/+}$ *Ptf1a*$^{Cre/+}$; *R26R*$^{LSL\text{-}YFP}$ for metastasis[34, 50, 89]. All animal protocols were reviewed and approved by the University of Michigan Institutional Animal Care and Use Committee (IACUC).

Cell Culture

Human pancreatic cancer cell lines (AsPC-1, PANC-1, MiaPaCa-2, Capan-1, CFPAC-1 and BxPC-3) were purchased from the ATCC. Cells were cultured in DMEM (Thermo Fisher) or RPMI (Thermo Fisher) containing 10% FBS and maintained at 37°C in a humidified incubator with 5% CO_2 and 95% air.

Acinar Cell Explant Cultures (3-D and Suspension)

The acinar cell isolation protocol has been previously described[90]. Briefly, the pancreas was harvested and minced with sterile scissors, digested with Collagenase P (Roche), passed through polypropylene mesh (Spectrum Laboratories, Rancho Dominguez, CA), and then pelleted through a fetal bovine serum gradient. The pelleted cells were resuspended in complete Waymouth's MB 752/1 medium (Sigma-Aldrich # W1625-1L) and plated in petri dishes for 3 hours to allow for cell debris and non-acinar cells to settle out of acinar clusters. Acinar cells were then removed from the petri dish into 6-well non-tissue culture plates in suspension or embedded in Cultrex rat tail Collagen 1 (Trevigen #3443-100-01, 3mg/ml) cultured with complete Waymouth's MB

752/1 medium in 12-well tissue treated plates and maintained at 37°C in a humidified incubator with 5% CO_2 and 95% air.

Cerulein Treatment

Experimental pancreatitis was induced, as previously described[27], by administering 250 µg/kg cerulein (46-1-50; American Peptide Company, Inc, Sunnyvale, CA) intraperitoneally twice daily for 2 weeks and allowed to recover for 1,3,7 and 14 days in control and *DDR1*$^{-/-}$ littermates. Mice used in this study were 8-12 weeks with weights between 18-25 grams. Saline (Sigma-Aldrich #07982-100TAB-F) was used as a negative control for cerulein. For pancreatitis-induced tumorigenesis, 6-week old *Kras*$^{LSL\text{-}G12D/+;}$ *Ptf1a*$^{Cre/+}$ (*KC*) and *DDR1*$^{-/-}$*; KC* littermates were treated with 250 µg/kg cerulein once daily for 5 consecutive days and allowed to recover for 1, 4 and 6 weeks before tissue harvesting.

Immunohistochemistry (IHC), Immunofluorescence (IF), and Quantification

Distribution and use of all human samples were approved by the Institutional Review Boards of Mayo Clinic. For IHC, pancreata were removed and fixed in Z-fix (NC9050753; Anatech, Ltd, Battle Creek, MI) overnight. Tissues were processed using a Leica ASP300S tissue processor (Buffalo Grove, IL). Paraffin-embedded tissues were sectioned at 4 µm and stained for specific target proteins using the Discovery Ultra XT autostainer (Ventana Medical Systems, Inc, Tucson, AZ) with antibodies as shown in Table 1 and counterstained with Mayer's hematoxylin (NC9220898; Sigma-Aldrich). H&E staining was performed using Mayer's hematoxylin solution and Eosin Y

(HT110116; Fisher, Pittsburgh, PA). Picrosirius red staining was performed according to the manufacturer's instructions (Polysciences, Inc, Warrington, PA). Gomori's Trichrome stain was performed by manufacturer's instructions (Thermo Scientific™ Richard-Allan Scientific™). IHC slides were then scanned on a Pannoramic SCAN scanner (Perkin Elmer, Seattle, WA). Scanned images were quantified using algorithms provided from Halo software (Indica Labs, Corrales, NM).

IF was performed on pancreata that were fixed in Z-fix for 2 hours, followed by an overnight float in 30% sucrose. Pancreata were incubated in a 1:1 mixture of 30% sucrose and optimal cutting temperature embedding medium (OCT) for 1 hour, embedded in OCT, frozen in liquid nitrogen, and stored at -80°C. Tissue sections (7 µm) were permeabilized in 1× phosphate-buffered saline (PBS) supplemented with 0.1% Triton X-100 (T9284; Sigma-Aldrich, St. Louis, MO) for 1 hour and blocked in 1× PBS supplemented with 5% donkey serum and 1% bovine serum albumin for 1 hour. Sections then were incubated with primary antibody diluted in 1× PBS supplemented with 0.1% Triton X-100 and 1% bovine serum albumin overnight at room temperature, followed by 3 washes in 0.1% Triton X-100/PBS for a total of 1 hour. Sections were incubated with secondary antibodies conjugated with Alexa Fluor (Invitrogen, Carlsbad, CA) for 1 hour at room temperature, followed by 3 washes in 0.1% Triton X-100/PBS. Hoechst 33342 stain (#62249, Thermo Scientific) was used for nuclear stain at 1:10,000 dilution in 1x PBS solution for 20 minutes. Slides were rinsed in deionized water and mounted with Prolong Diamond antifade mount (P36961; Fisher). Images

presented were acquired on a confocal microscope LSM800 (Zeiss, Oberkochen, Germany). IF slides were scanned and quantified as with IHC stained slides.

Immunoblotting

Mouse pancreas whole tissue lysates for protein analysis were obtained by removing a small piece of the pancreas from mice after euthanasia and snap freezing in liquid nitrogen. Tissue samples were then homogenized using the Pro 250 Homogenizer (Pro Scientific Inc, Oxford, CT) in RIPA buffer supplemented with protease inhibitor cocktail (PIA32965; Thermo Fisher Scientific) and PhosSTOP phosphatase inhibitor cocktail (4906845001; Sigma-Aldrich). Lysates were cleared by centrifugation and stored at –80°C. Human cell lines were lysed with RIPA buffer and cleared by centrifugation. Protein concentrations were determined using the BCA Protein Assay Kit (PI23228; Thermo Fisher Scientific). Proteins were separated using SDS-PAGE and transferred to a polyvinylidene difluoride membrane (IPVH00010; VWR, Radnor, PA). Primary antibodies used are listed in Table 1 . Secondary antibody coupled to horseradish peroxidase (GE Healthcare, Pittsburgh, PA) and the enhanced chemiluminescence detection system (BioRad Clarity™ and Max™ Western ECL Substrate) were used to visualize proteins using the BioRad ChemiDoc™ Imaging System.

Second Harmonic Generation (SHG) of Polarized Light, Microscopy

Imaging acquisition of polymerized/fibrillar collagen was attain using the Leica SP8 DIVE confocal/multiphoton microscope system (Leica Microsystems, Inc., Mannheim, Germany) mounted with a 25X HC FLUOTAR L 25x/0.95NA W VISIR water-immersion

objective and illuminating, at 850 nm, with IR laser Chameleon Vision II (Coherent Inc., Santa Clara, CA). Backward emission settings were utilized to generate signals collected, via a non-descanned detector configured to register between 410-440 nm wavelengths. Three areas were selected, per sample H&E stained slide (see methods above). Each selected area was acquired by collecting three images/regions (e.g., n=9 per H&E slide). Acquired regions used identical settings and were recorded as monochromatic, 16-bit image, stacks set to 4µm Z distances, using the Leica Application Suite X 3.5.5 software. Digital imaging analyses were conducted with FIJI (Image 1.52p). Raw image stacks were three-dimensional reconstituted as maximum projections. Signal to noise thresholds were set identically for all images. Positive (e.g., threshold) signal areas were used to calculate integrated SHG intensities (e.g., SHG signal/SHG area). WT mean integrated intensity values were used for normalization; results represent arbitrary units compared to WT controls. Selected, representative, images shown in figures correspond to SHG signal "intensity maps" in which the reconstituted monochromatic images are shown as pseudo colored representations in which cold colors indicate high SHG signal.

Pathology

Human TMA and murine PDA samples were graded blindly by Dr. Yaqing Zhang, a certified gastrointestinal pathologist.

Statistical Analysis

Individual data points were plotted using Prism8.0.2 (San Diego, CA) GraphPad software where the mean and standard deviations were calculated. Significance was determined using a two-tailed Students *t*-test for the comparison between 2 groups. P <0.05 was considered statistically significant.

Table 1: List of Antibodies

Antibody	Company	Catalog #	Concentration	Method
DDR1 (C-20)	Santa Cruz	sc532	1:250	Human TMA
DDR1 (D16G) XP	Cell Signaling Technologies	5583	1:250 1:1000	IF Western Blot
Ki67	Abcam	ab15580	1:1000	IHC
Cleaved-caspase 3	Cell Signaling Technologies	9664	1:200	IHC
Phosphor-histone H3 (Ser10)	Cell Signaling Technologies	9701	1:100	IHC, IF
Amylase	Sigma	A8273	1:1000	IHC
Amylase	Santa Cruz	sc12821	1:250	IF
Cytokeratin 19	TROMA	Max Plank	1:1000	IHC
E-cadherin	BD Pharmingen	610182	1:100	IF
P21	Santa Cruz	sc471	1:100	IHC
DDR2	Cell Signaling Technologies	12133	1:1000	Western Blot
Collagen1a	Abcam	Ab34710	1:250	IHC
Collagen1a	Millipore	Ab765p	1:1000	Western Blot
Alpha smooth muscle actin	Abcam	Ab5694	1:20,000	Western Blot
Podoplanin (Biotinylated)	Biolegend	127403	1:100	IF

Results

2.1. DDR1 is Expressed in Tumor Epithelia in Human PDA and Murine Models of PDA

To evaluate the expression of DDR1 in PDA, we performed immunohistochemistry (IHC) on human pancreatic cancer tissue microarrays. Consistent with previous studies, we found robust DDR1 expression at the plasma membrane of neoplastic lesions (Fig.2.1A upper panels and lower left) and low to no expression of DDR1 in poorly-differentiated tumors (Fig.2.1A, lower right)[64]. DDR1 was also expressed in several established human PDA cell lines, with the lowest expression being found in the poorly-differentiated MiaPaCa-2 and Panc-1 lines (Fig.2.1B)[64].

To explore the function of DDR1 in a metastatic PDA model, we used the *Kras$^{LSL\text{-}G12D/+}$; Trp53$^{LSL\text{-}R172H/+}$; Ptf1a$^{Cre/+}$; Rosa26R$^{LSL\text{-}YFP/+}$ (KPCY)* mouse [50, 89]. The *KPCY* model recapitulates many of the key features of the human disease, including progression through precancerous neoplasia together with a co-evolving collagen-dense fibrotic stroma and metastasis primarily to the liver and lungs[50, 89]. The *ROSA26R$^{LSL\text{-}YFP}$* allele allows for lineage tracing of the epithelial cells throughout tumor progression[50]. In the *KPCY* pancreas, DDR1 was expressed at the membrane of well- to moderately-differentiated PDA, similar to what we observed in human samples (Fig.2.1C).

2.2. DDR1 Promotes Tumor Growth and Progression

To define the role of DDR1 in PDA progression, we crossed DDR1-null (*DDR1*$^{-/-}$) mice into the *KPC* model (Fig.2.2A)[88, 89, 91]. *DDR1*$^{-/-}$ animals have been previously characterized and do not display evident defects in pancreas development[88, 91]. To study the effects of DDR1 ablation in PDA, *KPC* and *DDR1*$^{-/-}$*; KPC* mice were aged until moribund, then sacrificed. Within these parameters, control animals succumbed to complications of PDA between 24-39 weeks. Two *DDR1*$^{-/-}$*; KPC* mice were sacrificed due to hind limb paralysis at 26 weeks of age, an independent morbidity occasionally evident with the *Ptf1a*$^{Cre/+}$ driven *KPC* model due to brain and spinal tumor development (unpublished data). The remaining *DDR1*$^{-/-}$*; KPC* mice became moribund between 21-40 weeks of age with one mouse that remained symptom free up to 42 weeks, at which point we chose to terminate the experiment (Fig.2.2B).

Although we observed no differences in overall survival between the two cohorts, gross examination and quantitation of relative pancreatic mass revealed that *DDR1*$^{-/-}$*; KPC* mice had significantly smaller pancreata compared to *KPC* controls of the same age (Fig.2.2C, D). Western blot analysis of pancreatic tissue lysates confirmed DDR1 expression in *KPC* cohorts and its absence in *DDR1*$^{-/-}$*; KPC* tissue (Fig.2.2E). Necropsy revealed that 4/6 *KPC* mice had visible liver metastases, compared to only 1/7 *DDR1*$^{-/-}$*; KPC* mice (1/5 that made it to endpoint without paralysis, Fig.2.2F). Histological examination showed that all *KPC* tumors had progressed to either moderately- or poorly-differentiated adenocarcinoma (Fig.2.2G, 2.3A). *DDR1*$^{-/-}$*; KPC* mice, in contrast, presented with well- to moderately-differentiated adenocarcinoma, with the exception of the one animal with liver metastases which also

presented with a poorly-differentiated primary tumor (Fig.2.2F, G). While the paralysis co-morbidity limited our cohort size, these data support a role for *DDR1* in PDA progression, consistent with the finding that pharmacological inhibition of DDR1 inhibits PDA progression in a similar mouse model [64].

2.3. DDR1 is Required for Tumor Growth and Proliferation in PDA

On the basis of the consistent phenotype of a smaller pancreas found in the *DDR1$^{-/-}$; KPC* cohort regardless of histological grade, we hypothesized that *DDR1$^{-/-}$* tissue had a defect in cell proliferation or survival. To avoid bias when comparing poorly-differentiated tumors from *KPC* mice with predominantly well- to moderately-differentiated tumors from *DDR1$^{-/-}$; KPC* mice, we compared only differentiated tumors from both genotypes in our comparative analyses (Fig.2.3B); although histology from poorly-differentiated *KPC* tissue is included in Fig.2.3A. After careful quantitation, we found that *DDR1$^{-/-}$; KPC* tumors had significantly fewer Ki67+ proliferative cells than *KPC* tumors (Fig.2.3A, B). Phosho-histone H3 (p-hH3) staining was used as an independent measure of cell proliferation and confirmed that *DDR1$^{-/-}$; KPC* tumors were less proliferative than *KPC* controls (Fig.2.3A, B). *DDR1$^{-/-}$; KPC* tumors also had drastically fewer CC3+ cells, suggesting that tissue atrophy was not due to greater apoptotic cell death in these pancreata (Fig.2.3A, B).

To help determine a possible mechanism behind the smaller, less proliferative tissue we examined the expression of EGFR in *KPC* and *DDR1$^{-/-}$; KPC* animals. EGFR is required for tumorigenesis and can promote proliferation through the regulation of cyclin D1[45]. Additionally, recent unpublished data from phospho-proteomic

studies in pancreatic cancer cell lines that overexpress DDR1b have a reduction of phosphorylation at the inhibitory S1166 site in EGFR, suggesting the possibility of a synergistic effect between both receptors. Western blot analysis of whole tissue lysates revealed the activating p-EGFR (Y1068) site is upregulated in *KPC* mice, with an obvious decrease in *DDR1$^{-/-}$; KPC* mice supporting the EGFR/DDR1 synergistic relationship (Fig.2.3C). Collectively, these data suggest that DDR1 ablation delays tumor progression and that the associated subsequent smaller, less proliferative pancreas observed in the *DDR1$^{-/-}$; KPC* mice may be associated with a lack of EGFR signaling that is required for tumor growth and progression.

2.4 DDR1 Ablation Promotes Fibrosis During Spontaneous Tumor Formation

In addition to the morphological changes within the epithelium, PDA is defined by a collagen-dense fibrotic response associated with tumor progression and malignancy[40]. To determine if the loss of DDR1 affects fibrosis, we stained tissues with Gomori's Trichrome (blue) and Picrosirius Red. The relative amount of both stains was significantly elevated in *DDR1$^{-/-}$; KPC* mice compared to controls (Fig.2.4A, B), suggesting more overall collagen and fibrosis in the tissue. We then used Second Harmonic Generation (SHG) of polarized light microscopy to visualize polymerized (e.g., mature) collagen fibers. The overall SHG integrated intensity was found to be higher in *DDR1$^{-/-}$; KPC* mice consistent with the histological collagen-indicative stains (Fig.2.4C).

Collectively, these data suggest that the presence of DDR1 interacts with collagens to promote tumor progression. The associated subsequent smaller, less

proliferative pancreas observed in the *DDR1*$^{-/-}$*; KPC* mice may lead to pancreatic insufficiency potentially associated with a tumor restraining type of tissue fibrosis, contributing to their decline even with low metastatic disease.

2.5 DDR1 Ablation Induces Tissue Atrophy in Early Pancreatic Neoplasia

A possible explanation for the observed pancreatic atrophy in the *DDR1*$^{-/-}$*; KPC* mice is that normal pancreatic tissue is dying at an earlier point in tumor progression; this possibility would be missed by analyzing tissue only at endpoint. To test this hypothesis, we investigated the effect of DDR1 ablation during early tumor development. For this purpose, we used the *Kras*$^{LSL\text{-}G12D/+}$*; Ptf1a*$^{Cre/+}$ *(KC)* model of pancreatic neoplasia, which is known to recapitulate the early stages of carcinogenesis in a predictable manner [34]. In this model, endogenous expression of DDR1 is relatively low within healthy acinar regions (Fig.2.5A, top panels). However, DDR1 was found to be highly expressed in the epithelia of ADM and PanINs (Fig.2.5A, bottom panels)[34].

To study the role of DDR1 during the onset of pancreatic tumorigenesis, we crossed the *DDR1*$^{-/-}$ mouse into the *KC* model, to generate *DDR1*$^{-/-}$*; KC* mice (Fig2.5B). Pancreas mass (PM) relative to total body weight (BW) was used as an indirect measure of neoplastic burden. At 2 months old, when minimal transformation had occurred, *KC* and *DDR1*$^{-/-}$*; KC* mice presented with similar PM/BW ratios of ~2%. Over the period of a year, this ratio reached ~3.5% in *KC* animals (Fig.2.5C). The PM/BW ratio in *DDR1*$^{-/-}$*; KC* mice, in contrast, decreased to ~1.5% at the age of one year (Fig.2.5C). The decreased pancreatic mass in *DDR1*$^{-/-}$*; KC* mice did not reflect a delay in the onset of transformation as both cohorts displayed a similar burden of ADM and

PanIN lesions, as determined by H&E staining (Fig.2.5D). However, the two cohorts exhibited significant differences in other measures of pancreatic transformation. For instance, *DDR1$^{-/-}$; KC* mice at 12 months of age showed a greater reduction in normal acinar cell mass, as determined by IHC for the acinar cell marker Amylase, compared to controls (Fig.2.5E, I). To determine the total area occupied by ADM and neoplasia, IHC for the duct cell marker Cytokeratin-19 (Ck19) was used, but revealed no difference between the two cohorts. (Fig.2.5F, I). This suggests that the reduced pancreatic mass in *DDR1$^{-/-}$; KC* animals is primarily due to the loss of normal acinar tissue. *DDR1$^{-/-}$; KC* mice also displayed fewer proliferating epithelial cells (p-hH3^{+}) as mice aged to 12 months, compared to *KC* animals (Fig.2.5G, J), a result similar to what we found in *DDR1$^{-/-}$; KPC* tumors (Fig.2.3A, B). Moreover, we did not observe any differences in epithelial apoptosis (CC3^{+}) between the cohorts at any age, again implicating an overall loss of proliferation as a primary cause of the difference in pancreatic mass (Fig.2.5H, K).

2.6 DDR1 Ablation Promotes a Dynamic Fibrotic Response During Spontaneous Tumor Formation

To examine fibrosis within the tissue, we stained both *KC* and *DDR1$^{-/-}$; KC* tissue with Trichrome and Picrosirius Red, revealing no significant differences in fibrotic area at any time point (Fig.2.6A, B). We also stained for collagen 1a (Col1a), the most prominent fibrillar collagen within the fibrotic stroma and a DDR1 ligand[59]. Again, no quantitative differences were observed in the total area of collagen deposition as measured by IHC for Col1a between the two cohorts as they aged to 12 months (Fig.2.6C). While there was no significant difference in fibrosis or Col1a staining, SHG

microscopy revealed that levels of polymerized collagen fibers were significantly lower in *DDR1*$^{-/-}$*; KC* mice at 12 months of age (Fig.2.6D). This suggests that in comparison to the utility of DDR1 in tumor progression (as shown in Fig.2.4C), this ECM receptor may play a distinct, but still important role in collagen remodeling/polymerization in the stroma surrounding early neoplasia.

2.7 DDR1 is Necessary for Tissue Homeostasis and Recovery Following Pancreatitis-Induced Tumorigenesis

Experimental pancreatitis works synergistically with oncogenic Kras expression to accelerate tumorigenesis[45, 85]. Consequently, we examined the role of DDR1 in pancreatitis-associated tumorigenesis. In this model, *KC* and *DDR1*$^{-/-}$*; KC* mice were administered supramaximal doses of cerulein, a cholecystokinin orthologue, to induce acinar cell damage, resulting in pancreatitis[45]. Mice were treated once daily for 5 days with cerulein and sacrificed at 1, 4, and 6 weeks after the last injection (Fig.2.7A). One week after cerulein treatment, both cohorts had PM/BW ratios of ~3-4% (Fig. 2.7B). However, as mice were allowed to recover, *KC* mice maintained a ratio of ~3%, while *DDR1*$^{-/-}$*; KC* mice showed a significant drop in the PM/BW ratio, stabilizing at ~1% (Fig.2.7B). H&E staining showed a similar degree of tissue transformation at 1 week of recovery, but revealed a failure to resolve tissue damage at 6 weeks after treatment in *DDR1*$^{-/-}$*; KC* mice compared to *KC* mice (Fig.2.8A). Loss of acinar tissue and its replacement by ADM/PanIN lesions in both *KC* and *DDR1*$^{-/-}$*; KC* mice were measured by IHC for Amylase and Ck19, respectively (Fig.2.7C, D, G). Amylase^{+} and Ck19^{+} areas indicated that *KC* animals experienced widespread tissue damage and

transformation, but regained normal-appearing Amylase^{+} acinar tissue by 6-weeks post-cerulein (Fig.2.7C, G). In contrast, *DDR1$^{-/-}$; KC* mice showed little recovery of acinar tissue with a concomitant increase in Ck19^{+} ductal cells (Fig.2.7D, G), again suggesting the loss of nearby normal tissue contributes to the observed tissue atrophy.

2.8 Absence of DDR1 Promotes Fibrosis in the Recovery Following Pancreatitis-Induced Tumorigenesis

These data reinforce that, in the absence of DDR1, a loss of normal tissue in a background of tumorigenesis and tissue damage contributes significantly to tissue atrophy. Similar to what we observed in the *KPC* (Fig.2.3A, B) and spontaneous *KC* (Fig.2.5G, J) models, ablation of DDR1 led to a less proliferative epithelium (p-hH3^{+}, Fig.2.7E), but no measurable difference in apoptotic cell death (CC3^{+}, Fig.2.8B). Tissue atrophy and the absence of acinar cells in *DDR1$^{-/-}$; KC* pancreata was accompanied by a significant increase in Trichrome and Picrosirius red positive stained area (Fig.2.7F, I, Fig.2.8C). SHG signals revealed a more dynamic collagen polymerization and recovery rate in response to cerulein aggravation in the absence of DDR1, highlighting the fact that DDR1 is important for maintaining polymerized collagen stability (Fig.2.8D). Taken together, the data from the spontaneous and pancreatitis-associated tumorigenesis models suggest that DDR1 is necessary for acinar cell homeostasis and regeneration, as well as for regulation of ECM deposition and polymerization.

2.9 DDR1 is Necessary for Tissue Regeneration Following Experimental Pancreatitis

Ablation of DDR1 in the *KPC* and *KC* mouse models consistently resulted in extensive tissue atrophy accompanied by stunted proliferation and an overall depletion of acinar cells. To further examine the effects of DDR1 ablation on pancreatic tissue homeostasis in a model of pancreatic injury in the absence of oncogenic *Kras*, we used supramaximal doses of cerulein to induce severe acute pancreatitis in wild-type (WT) and *DDR1*$^{-/-}$ mice (Fig.2.9A). This treatment induces extensive ADM accompanied by a fibrotic response, similar to that found in CP. Unlike true CP, however, damage resolves over a period of several days following cerulein withdrawal.

After severe acute pancreatitis induction, Western blotting showed that DDR1 expression was increased in *WT* mice during the tissue repair phase (Fig.2.9B). We used PM/BW ratios as an indirect measure of tissue injury and regeneration following cerulein treatment. On average, healthy pancreata from both WT and *DDR1*$^{-/-}$ mice have PM/BW ratios at ~1.0% (Fig.2.9C). This ratio decreased to ~0.7% in *WT* mice 1-day post-cerulein treatment, but gradually recovered to ~1.0% after 2 weeks (Fig.2.9C). In comparison, *DDR1*$^{-/-}$ mice showed a more dramatic decrease in relative pancreas mass, dropping below 0.5% with little recovery in tissue mass 2 weeks after cerulein cessation (Fig.2.9C). Gross anatomy reflected smaller pancreata in *DDR1*$^{-/-}$ mice (Fig.2.9D). H&E staining showed comparable initial damage between *WT* and *DDR1*$^{-/-}$ mice, as indicated by the presence of ADM (Fig.2.9E). However, *DDR1*$^{-/-}$ mice showed prolonged pancreatic damage at 7 days post treatment, which failed to return to a histologically normal phenotype until 2 weeks of recovery. Amylase^{+} staining

confirmed that *DDR1*$^{-/-}$ pancreata recovered their acinar cell population more slowly, with the most significant difference compared to *WT* pancreata at 7 days post-cerulein (Fig.2.9F).

2.10 DDR1 Proliferation is Delayed in the Epithelium of DDR1-deficient Mice During Tissue Recovery

To examine the acute tissue atrophy and acinar cell loss in *DDR1*$^{-/-}$ mice, we next measured proliferation. In *WT* mice, an increase in Ki67^{+} epithelia are evident 1-day post-cerulein treatment and eventually subsides after 2 weeks when the tissue has recovered (Fig.2.10A). In contrast, *DDR1*$^{-/-}$ mice experience a delay in proliferation measured by fewer Ki67^{+} epithelial cells at 1 and 3 days post-cerulein. Strikingly, the number of Ki67^{+} epithelial cells significantly increases 7 days after cerulein cessation, the timepoint that features the most significant decrease in pancreatic acinar mass, but also when the tissue mass is stabilized in *WT* mice (Fig.2.10A). To test if DDR1 ablation affected acinar proliferation, we performed co-IF for E-cadherin (epithelial marker), amylase (acinar cell marker) and p-hH3 (mitosis) (Fig.2.10B). p-hH3 staining was primarily located in nuclei of E-cadherin^{+}; amylase^{+} cells in both *WT* and *DDR1*$^{-/-}$ mice. As indicated by the extent of Ki67 positivity, proliferative cells were numerous in *WT* pancreata during the early recovery time points, but progressively decreased as homeostasis was restored. *DDR1*$^{-/-}$ mice, however, had fewer proliferative epithelial cells at 1 and 3 days, which dramatically increased after 7 days of recovery (Fig.2.10B). As with the other models, we did not find a significant difference in the amount of apoptotic cell death between the cohorts, as measured by CC3 staining (Fig.2.10D).

After confirming a delay in cell proliferation following cerulein treatment in *DDR1*$^{-/-}$ animals, we hypothesized that this delay was due to a disruption in the regeneration potential of acinar cells during recovery. To test this hypothesis, tissues were stained for Stathmin1 (STMN1), which marks a subset of acinar cells that are uniquely capable of proliferation following pancreatic injury[92]. Co-staining for STMN1 and PCNA (marker of proliferation), showed that *WT* and *DDR1*$^{-/-}$ mice had similar numbers of STMN1^{+} cells at baseline (saline control, Fig. 2.10C). However, after injury, WT mice showed a large expansion of STMN1^{+} cells, an expansion that was delayed and then quickly subsided in *DDR1*$^{-/-}$ mice (Fig.2.10C). Moreover, most PCNA^{+} proliferative cells were also STMN1^{+}. These data suggest that the STMN1^{+} subset of acinar cells is dependent on DDR1 expression for its regenerative function, further reinforcing the critical role that DDR1 plays in restoring pancreatic tissue homeostasis after injury.

2.11 DDR1 Deficient Mice Develop Extensive Fibrosis after Pancreatic Injury

The collagen-dense fibrotic response observed in pancreatic cancer is also a key feature in experimental and clinical pancreatitis[9, 27, 28]. To examine this, tissues from *WT* and *DDR1*$^{-/-}$ mice were stained with Trichrome and Picrosirius Red. Both cohorts showed an initial increase in Trichrome and Picrosirius staining 1 day following the experimental pancreatitis protocol (Fig.2.11A, 2.11F). As expected, *WT* tissues showed a decrease in fibrosis as pancreata recovered from cerulein treatment associated with tissue remodeling and homeostatic equilibrium (Fig.2.11A, 2.12A). In contrast, *DDR1*$^{-/-}$ mice failed to resolve the initial fibrosis after 2-weeks post-cerulein, as

indicated by the significantly higher amount of Trichrome and Picrosirius positive staining (Fig.2.11A, 2.12A) and Col1a positive staining (Fig.2.11B) in *DDR1*$^{-/-}$ mice during the recovery phase. Finally, when assessing collagen polymerization dynamics via SHG microscopy we confirmed that collagen fibrillogenesis was initially increased in *DDR1*$^{-/-}$ animals, 1-day post-treatment. However, SHG signals decreased significantly at 3 and 7-days after cerulein cessation in *DDR1*$^{-/-}$ mice, but failed to fully resolve compared to controls 2 weeks after treatment (Fig.2.11C, D). We also examined the expression of several markers of fibrosis including DDR2, Col1a, and α-smooth muscle actin (α-SMA, activated fibroblasts). Western blot analysis revealed increased amounts of these fibrotic markers in *DDR1*$^{-/-}$ animals compared to wild-type cohorts (Fig.2.11E). Furthermore, co-staining for fibroblastic activation markers, podoplanin (PDPN) and α-SMA, indicated a relative increase in the number of these collagen-producing fibroblasts in *DDR1*$^{-/-}$ animals during recovery following cerulein treatment, possibly explaining the failure of the tissue to fully resolve following injury (Fig.2.11G)[93, 94].

Discussion

The ECM is a three-dimensional network of protein polymers that are essential for the physical, biochemical, and mechanical support of organs[58]. In pancreatitis and PDA, the ECM undergoes a series of remodeling events that are orchestrated with the morphological changes that occur in the epithelia throughout disease progression[58]. These changes are associated with an upregulation of the expression of ECM proteins, infiltration of immune cells, and the activation of pancreatic stellate cells (PSC) that secrete collagen to form the characteristic desmoplastic response observed in patients[14, 58]. The desmoplastic reaction can influence the crosstalk between the microenvironment and tumor cells, affecting pancreatic disease progression[14, 58, 82]. However, selectively targeting stromal signaling pathways that promote pancreatic tumor progression without disturbing those that help constrain the tumor remains a challenge[50, 51].

Due to the late presentation of PDA, most patients are diagnosed with metastatic disease where the normal epithelium has been largely replaced by the collagen-rich desmoplasia which subsequently increases organ stiffness and interstitial pressure, creating a barrier to the delivery of chemotherapy [14, 58, 82]. Several approaches have been employed to target specific components of the ECM in pancreatic cancer. While some show therapeutic promise, they have also revealed the complexity of the relationship between the stroma and cancer cells. Ablation of collagen-producing fibroblasts leads to a more aggressive tumor phenotype in both experimental and clinical studies[47, 51]. As a result, other studies have attempted to modulate fibroblast activity and their production of ECM proteins, especially collagen,

by targeting the inactivation of pancreatic stellate cells with Vitamin D agonists[52, 95]. Another approach in improving therapeutic delivery is to alleviate intra-tumoral pressure responsible for the collapse of the tumor vasculature by degrading hyaluronic acid (HA), which is a prominent feature of the ECM of some PDA patients[96]. The positive results from these preclinical studies led to clinical trials, culminating in a Phase III trial in patients with high HA content, ultimately showing no benefit[97]. The lack of translational success so far emphasizes the need to better understand the complex dynamics of the tumor-stromal response in PDA progression.

The unique feature of the DDR family of type-1 receptor tyrosine kinases, namely the ability to signal in response to collagen ligands, suggest they may be a useful target for treating fibrotic diseases including pancreatic cancer where collagen is a dominant feature[59]. DDR1 is upregulated in several cancers and fibrotic diseases, correlating with a worse prognosis. However, its role in cancer progression is complex and ill-defined[59]. Takai *et. al*. ablated DDR1 in the MMTV-PyMT metastatic luminal-type mammary tumor model and showed that *DDR1*$^{-/-}$ tumors are more aggressive, fibrotic, and necrotic compared to controls[63]. In contrast, Ambrogi *et. al*. used *DDR1*$^{-/-}$ animals in the inducible *Kras*^{G12V} model of lung cancer, finding increased survival and reduced tumor size in *DDR1*$^{-/-}$ mice[65]. Similarly, the use of the DDR1 inhibitor, 7rh, in this model showed a significant reduction in tumor size when used in combination with Notch inhibitors[65]. Similarly, Aguilera *et. al.* used 7rh to inhibit DDR1 in pancreatic cancer xenografts and the autochthonous *KPC* model and showed improved drug delivery in combination with gemcitabine, accompanied by a reduction in tumor burden

and metastases[64]. Together, these results suggest that the roles of DDR1 in cancer are context/organ dependent and require more studies.

In our current studies, we used genetic ablation of DDR1(*DDR1*$^{-/-}$) in several models that recapitulate the molecular and histological events associated with pancreatitis, pancreatic neoplasia and pancreatic cancer. Utilizing the metastatic *KPC* mouse model supported a role for DDR1 in pancreatic carcinoma progression to a poorly-differentiated phenotype generally associated with an aggressive form of the cancer. Overshadowing possible effects on progression, we found that tumor progression was accompanied by an unexpected and severe loss of pancreatic mass in the absence of DDR1. In neoplasia, we found that while DDR1 ablation had no obvious effects on transformation or fibrosis, but revealed severe tissue atrophy marked by a significant loss of normal acinar tissue. This effect was enhanced by accelerating transformation via induction of acute pancreatitis. The observed tissue atrophy was reminiscent of the phenotype seen when DDR1 was ablated in a mammary cancer model, in which the absence of DDR1 conferred a more fibrotic and necrotic tumor[63]. However, unlike that study we did not observe clear evidence of tissue necrosis (data not shown). Finally, focusing solely on tissue damage, we found that inducing severe acute pancreatitis in *DDR1*$^{-/-}$ animals recapitulated the severe tissue atrophy and acinar cell drop-out that was similar to our observations in the cancer and neoplastic models. In these cases, fibrosis and collagen deposition remained unresolved in the *DDR1*$^{-/-}$ mice for over a week after cerulein treatment compared to controls, suggesting DDR1 is necessary for ECM remodeling, to attain normal homeostatic equilibrium following injury.

Exploring the tissue atrophy common to each model, we found no difference in the apoptotic index, measured by cleaved-caspase 3 IHC, or necrosis by H&E (data not show). While there are several other mechanisms of cell death we did not measure (e.g. Ferroptosis, necroptosis), we did see a modest increase in possible cellular senescence, as measured by p21 IHC (data not shown). Most prominently, we consistently observed a decrease in epithelial proliferation in each DDR1 ablated model of pancreatic disease, which likely contributed to overall organ atrophy.

While fibrosis constitutes a known feature of PDA onset and progression, stroma normalization (as opposed to desmoplastic elimination) is a highly sought out clinical avenue[52, 98]. However, it has also been reported that fibrosis can be a predictor of improved survival in patients that underwent neoadjuvant therapy prior to surgery; in this case increased levels of fibrosis observed at time of surgery rendered improved outcomes in PDA patients[99]. Additionally, other studies suggest that the fibrotic stromal signatures could be indicative of improved or detrimental patient outcomes[100, 101]. The varying outcomes from these studies suggest distinct pro- and anti-tumor types of fibrosis that are evident throughout our investigation of DDR1 activity in this study. The results attained from our study suggest a role for DDR1 in maintaining tissue homeostasis and demonstrate that the absence of DDR1 promotes dynamic ECM deposition/remodeling, but prevents complete resolution after injury. Furthermore, our results encourage the notion that a tumoral homeostatic equilibrium is needed at each stage of tumorigenesis (e.g., tumor onset and progression) and the absence of DDR1 prevents tissues from reaching these equilibria.

Collectively, our data indicate that DDR1 is an important signaling factor during pancreatic injury, tumor development and progression. Our studies show that DDR1 is necessary for tissue homeostasis following an injury whether it be physical or oncogenic. Indeed, the ablation of DDR1 in our pancreatic disease models had an impact on the surrounding desmoplasia, which exhibited a more persistent stromal response and altered rates of ECM remodeling. Altogether, the overexpression of DDR1 and the extensive collagen production in pancreatic diseases strongly suggest that DDR1 is a putative therapeutic target. Our results suggest that chronic and systemic inhibition of DDR1 could induce tissue atrophy primarily by inhibiting proliferation in an environment of chronic cell stress and tissue repair and should be taken into consideration as a therapeutic target.

Miscellaneous Data and Future Directions

2.12 Miscellaneous Data: Results without Conclusions

The previous data confirms that DDR1 is upregulated in the epithelium during the process of ADM and in the recovery, phase following an injury to the pancreas (Fig.2.5A, 2.9B). Furthermore, it shows that DDR1 is necessary for the reparative events and homeostasis of tissue after pancreatic injury. However, the functional role of DDR1 during the process of ADM and tumor transformation was not defined. Consequently, understanding the active contributors in DDR1 signaling would provide insight into a potential mechanism of the significantly smaller, less proliferative pancreata observed in the multiple mouse models of pancreatic disease. The following are a list of experiments performed to define the potential mechanism of DDR1 in the process of pancreatitis and pancreatic tumorigenesis. While the results from these studies did not confirm a mechanism to explain the DDR1-null phenotype, they did define areas that are necessary to explore for future studies using different techniques and methods.

i.) Downstream Effectors: A Look at Mitogenic and Survival Pathways

As a member of the RTK superfamily, DDR1 was shown to be directly upstream of Src kinase and regulate the activation of downstream effectors, ERK and Akt, of the mitogenic and cell survival pathways, respectively[59]. To determine if Src, ERK or Akt signaling was disrupted during injury and recovery in the absence of DDR1, *WT* and *DDR1*$^{-/-}$ mice were analyzed following the experimental pancreatitis protocol. Protein expression from whole tissue lysates show that p-Src, p-ERK and p-Akt are elevated

during the recovery phase in both cohorts (Fig.2.12i-A). However, as *WT* mice recover the expression of p-Src, p-ERK and p-Akt is mitigated, whereas *DDR1*$^{-/-}$ mice remain elevated up to 2 weeks post-cerulein. Since whole tissue lysates are a combination of all pancreas cell types such as acini, ducts, endothelial cells and fibroblasts that have the potential to activate the Raf-MEK-ERK and PI3K-Akt-mTOR pathways, I performed IHC to decipher which cell type presented with ERK or Akt expression was detected in immunoblot results (Src was not detected by IHC). Results from IHC were unable to identify which cell type expressed p-ERK or p-Akt and was generally very difficult to quantitate accurately (Fig.2.12i-B). Immunofluorescence (IF) was also used to address the issue presented by IHC, but p-Src, p-ERK and p-Akt antibodies were not able to be detected by IF. Although the source of p-Src, p-ERK and p-Akt was not confirmed, it is still relevant to highlight that *DDR1*$^{-/-}$ animals have extended fibrosis and a spike in epithelial proliferation 1-week after cerulein treatments. This may account for the elevated protein levels of activated Src, Erk and Akt detected in the lysates coming from the acinar compartment that are necessary for tissue repair.

ii.) DDR1 in the Hippo Pathway

The Hippo pathway is a central regulator of organ size by regulating tissue homeostasis, regeneration, and ECM remodeling that affects organ growth[102]. The key players in Hippo signaling include the serine/threonine kinases Mst1/2, large tumor suppressor kinases Lats1/2, and transcriptional co-activators YAP and TAZ[102]. The Hippo “on” or active state retains YAP and TAZ in the cytoplasm primed for ubiquitination by a series of upstream phosphorylation events[102]. Phosphorylation of

MST1/2 leads to phosphorylation of Lats1/2 and subsequent phosphorylation of Yap/Taz, which in turn tags them for ubiquitination[102]. During the Hippo "off" or inactive state, MST1/2, Lats1/2, and Yap/Taz protein are not phosphorylated which results in nuclear localization of Yap/Taz followed by transcriptional activation of genes required for proliferation, migration, and survival[102]. The substantial loss in pancreatic mass and delay in proliferation in both pancreatitis and PDA suggest the Hippo pathway may be altered in the absence of DDR1. To test this, immunoblot, IHC, and IF analysis was used to determine the expression of the downstream effectors in the Hippo signaling, Yap/Taz. Examination of whole tissue lysates from mice during recovery after experimental pancreatitis revealed inconsistent results (Fig.2.12ii-A). IHC proved to be more complicated to interpret due to non-specific p-Yap, total Yap, p-Taz and total Taz antibody staining (data not shown). IF shows non-specific staining of Yap and Taz, but the amount of expression of either protein did not differ between *WT* and *DDR1*$^{-/-}$ mice (Fig.2.12ii-B).

Observations in experimental pancreatitis provided a basis for potential factors and pathways that may contribute to pancreatitis and possibly PDA. However, in the cerulein-induced model of pancreatitis the inconsistencies were not resolved to make firm conclusions which can be due to the area of tissue obtained for lysate or the turnover of nuclear Yap/Taz, which would be better analyzed by cell fractionation and examination of nuclear proteins rather than whole tissue lysates.

To test whether the Hippo pathway is altered in a homogenous, controlled model, I examined Yap and Taz in AsCP-1 and BxPC3 DDR1-knockdown human PDA cell lines. Cells were grown to 80% confluence and then serum starved for 16 hours

before adding 30μg/ml of soluble rat tail collagen to the media. Protein was collected at time 0, time 5 hours, and time 8 hours after cells were treated with collagen to allow for DDR1 activation. Detection of p-YAP implies Hippo signaling is active and Yap is not in the nucleus regulating transcription. In AsCP1 lines not treated with collagen, p-YAP is elevated and goes down after cells have been treated with collagen regardless of DDR1, but is elevated again 8 hours after the addition of collagen in both DDR1-knockdown (Fig.2.12ii-C). This expression pattern is the reverse in total Yap levels and TAZ is unaffected by the status of DDR1. In BxPC3 lines, the p-YAP, YAP, and TAZ are unaffected by DDR1 status or collagen (Fig.2.12ii-C). Collectively, these results suggest DDR1 is not associated with the Hippo pathway is these models of pancreatitis and PDA. However, I only focused on the YAP and TAZ in these models and it is possible upstream factors such as MST1/2 or LATS1/2 are associated with DDR1. Additionally, other methods such as RNA analysis of transcription factors regulated by Hippo signaling may be more informative in determining an association between DDR1 and the Hippo pathway.

iii.) DDR1 and Autophagy

Autophagy (self-eating) is a catabolic process that is necessary for the normal physiology of a cell. The process of autophagy can be induced by cell stress to prevent cell damage and promote cell survival and involves a highly regulated sequence of events. For autophagy to occur cytosolic components such as pathogens, dysfunctional organelles, and cytotoxic protein aggregates must be tagged with ubiquitin (Ub). Ub tagged proteins are then specifically recognized by p62, which then

binds to the membrane-conjugated LC3. The Ub-tagged protein, p62, LC3 complex goes through the process of elongation of the isolation membrane to complete the structure of the autophagosome. The autophagosome can then fuse with the lysosome to form the autolysosome in which a change in the pH causes acid hydrolysis for the degradation of the contents of the autophagosome and recycling of the molecular components back to the cell.

In disease state such as inflammation and cancer, the process of autophagy is disrupted and may assist in the selective survival of cancer cells. Autophagy has been shown to be active in the pancreas of cerulein treated rodents by several methods including IHC, IF, immunoblot, and electron microscopy. To determine if autophagy is dysregulated in the absence of DDR1 during tissue repair after cerulein-induced pancreatitis, I performed both immunoblot and IF analysis of the two prime components in autophagy, p62 and LC3 (Fig2.12iii-A, B). Results from immunoblotting were inconsistent among biological samples and therefore difficult to replicate for interpretation. IF images of p62, represented as red punctate dots in the cytoplasm, were present, but difficult to quantify for analysis. While these analyses were informative in detecting the presence of p62 and LC3 in pancreatitis at a single timepoint, a more quantitative measure of autophagy is to measure autophagic flux. Autophagic flux is the entire process of autophagy from autophagosome formation lysosome fusion, to recycling of cytosolic materials. This can be tracked by infecting a GFP-RFP fusion reporter into cells in which cells will express both GFP and RFP. Fusion with the lysosome with the autophagosome causes an increase in pH that quenches the GFP signal, but RFP remains since it is insensitive to pH changes and

indicates cells that have gone through the flux of autophagy. Utilizing this technology, I transfected primary acinar cells isolated from *WT* and *DDR1*$^{-/-}$ animals with the GFP-RFP fusion reporter and treated with either cerulein or autophagy blocker, Hydroxychloroquine (HQC). Both GFP and RFP were detected in acinar clusters, but tracking autophagic flux at arbitrary timepoints by light microscopy was not an accurate method. Tracking autophagic flux in real time by time-lapse microscopy would prove to be much more useful. The principles of acinar isolation, viral transfection, and observing color changes in acinar clusters undergoing autophagic flux were applied in both suspended or collagen embedded cells for 24-hours under time-lapse microscopy. However, working out the cell numbers, treatment concentrations, keeping acinar cells alive, and general microscopy errors was labor intensive and often affected the imaging resolution. In principle, the assay did work, but mostly recorded acinar cells dying due to the extreme conditions set by the time-lapse chamber and heat created by the lasers for GFP-RFP detection.

iv.) DDR1-Null Acinar Cells During ADM Ex Vivo

A consistent feature observed during tumorigenesis, pancreatitis-induced tumorigenesis, and experimental pancreatitis was not only tissue atrophy, but also a loss in acinar cells in *DDR1*$^{-/-}$ mice compared to controls. This suggested DDR1 is necessary for acinar repopulation following pancreatic injury. Additionally, DDR1 is upregulated during the recovery phase following cerulein treatment and during spontaneous tumorigenesis suggesting DDR1 is also necessary for tissue homeostasis. Based on this data, I hypothesized that DDR1-null acinar cells are more

susceptible to damage and therefore undergo and maintain ADM following a fibrotic response.

To test this hypothesis, I isolated and embedded primary acinar cells in 3D collagen from WT and DDR1-null animals. Cells were then left untreated or treated with cerulein or TGFα to induce ADM *ex vivo*. *Ex vivo* results did not show a significant difference in cyst-like ductal structures after 5 days in culture between WT and $DDR^{-/-}$ animals (Fig.2.12iv-A). To obtain more quantitative results, I aimed to analyze transcript levels of acinar associated transcription factors at baseline in primary acini cells isolated and left in suspension from *WT* and $DDR1^{-/-}$ mice. Unfortunately, I could not isolate sufficient amounts of high-quality RNA from primary acinar cells and moved on to test protein levels of ADM markers. Isolated acinar cells were again either left untreated or treated with 2pmol/ml with cerulein for a period of 3 days (Fig.2.12iv-B). This is typically enough time for ADM markers to be detected before acinar cells undergo cell death in suspended media cultures. Protein analysis from these samples confirmed DDR1 is elevated during the process of ADM, with more Ck19 and DDR2 expression levels in $DDR1^{-/-}$ animals (Fig.2.12iv-C). However, the addition of DDR1 ligand by collagen I or Matrigel matrices may show more robust results between *WT* and $DDR1^{-/-}$ acinar cells during the process of ADM.

2.13.) Future Directions

Extended collagen deposition and ECM remodeling are barriers to overcome in the pathogenesis of PDA. DDR1 is a unique RTK activated by collagen that is upregulated in fibrosis and several cancers suggesting it may be involved in disease

progression[57, 59]. Genetic and pharmacological inhibition of DDR1 contributes valuable information on the role it plays in disease, however, the consensus on whether the activation of DDR1 is pro- or anti-tumorigenic in PDA remains inconclusive.

Prior to the work set out by Aguilera *et al.*, limited knowledge on the role of DDR1 in PDA was known. Aguilera *et al.* established that DDR1-activation stimulates the pro-tumorigenic activation of p-PYK2 and p-PEAK1 in human PDA cells lines[64]. The study also provided detailed data on the beneficial use of 7rh, an ATP-competitive inhibitor, to block DDR1 activation with adjuvant use of gemcitabine[64]. The combination of 7rh with standard-of-care cytotoxic gemcitabine, enhanced drug efficacy in both xenograft and KPC mouse models of PDA that resulted in increased survival and decreased tumor burden[64]. However, we must consider that although 7rh has improved cytotoxic drug therapy in PDA, it is not specific nor selective to DDR1. As an ATP competitive kinase inhibitor, 7rh has the potential to block activation of other ATP kinase binding sites in other receptors which can attribute to its anti-tumor activity. Regardless of the nature of 7rh, these encouraging results offer a foundation for further studies into the role of DDR1 in disease and the development of more selective and specific DDR1 inhibitors.

Germline ablation of DDR1 in the *KPC* model supports the data of pharmacologically inhibiting DDR1 in PDA with markedly smaller, less proliferative and less advanced tumors compared to controls. This phenotype was consistent throughout spontaneous tumorigenesis, pancreatitis-induced tumorigenesis, and cerulein-induced pancreatitis. Additionally, within these models of pancreatic injury, tissue atrophy was accompanied by increased fibrosis, a substantial loss in healthy

acinar cells and delay in proliferation which may explain the lack of tumor progression in *KPC* mice. While these data support the idea of inhibiting DDR1 in pancreatic disease, it does not provide the mechanism or show how DDR1 regulates tumor progression. Observations of reported downstream effectors of DDR1 were mostly unaffected in *DDR1*$^{-/-}$ animals. A possible explanation for this unlikely outcome is the use of DDR1 germline ablation. In this case, mice develop and adapt to the deletion of DDR1 which may create compensatory activation of other pathways to be activated that have redundant downstream effectors. Moreover, the signal transduction of DDR1 is still undetermined and the typical RTK effectors that were examined may not be regulated by DDR1. A more efficient way to study the role of DDR1 activation and signaling in disease is the use of a conditional DDR1 knockout mouse model. Generation of a conditional DDR1 knockout mouse may address the regulatory role of DDR1 in a cell and tissue specific manner and therefore may clarify the results I produced with a germline knockout as well as add to the contribution in disease.

Phospho-proteomics studies and basic research approaches have enhanced our knowledge in understanding the role DDR1 in both physiological and pathophysiological conditions. Despite this progress, detailed information aimed at the molecular mechanisms that DDR1 regulates is limited. A better grasp of the molecular underpinnings of the regulatory events of DDR1 will not only advance our understanding of DDR1 in disease, but also provide a basis for improved drug development. The novel insights I investigated have expanded upon the repertoire of information studied on DDR1 in several models of pancreatic injury and tumor progression. Collectively, DDR1 has the potential to be a valuable molecular target,

however, additional studies and methodologies are needed to understand how and when DDR1 inhibition is required in specific disease settings before heading to the clinic.

Figures

Figure 2.1

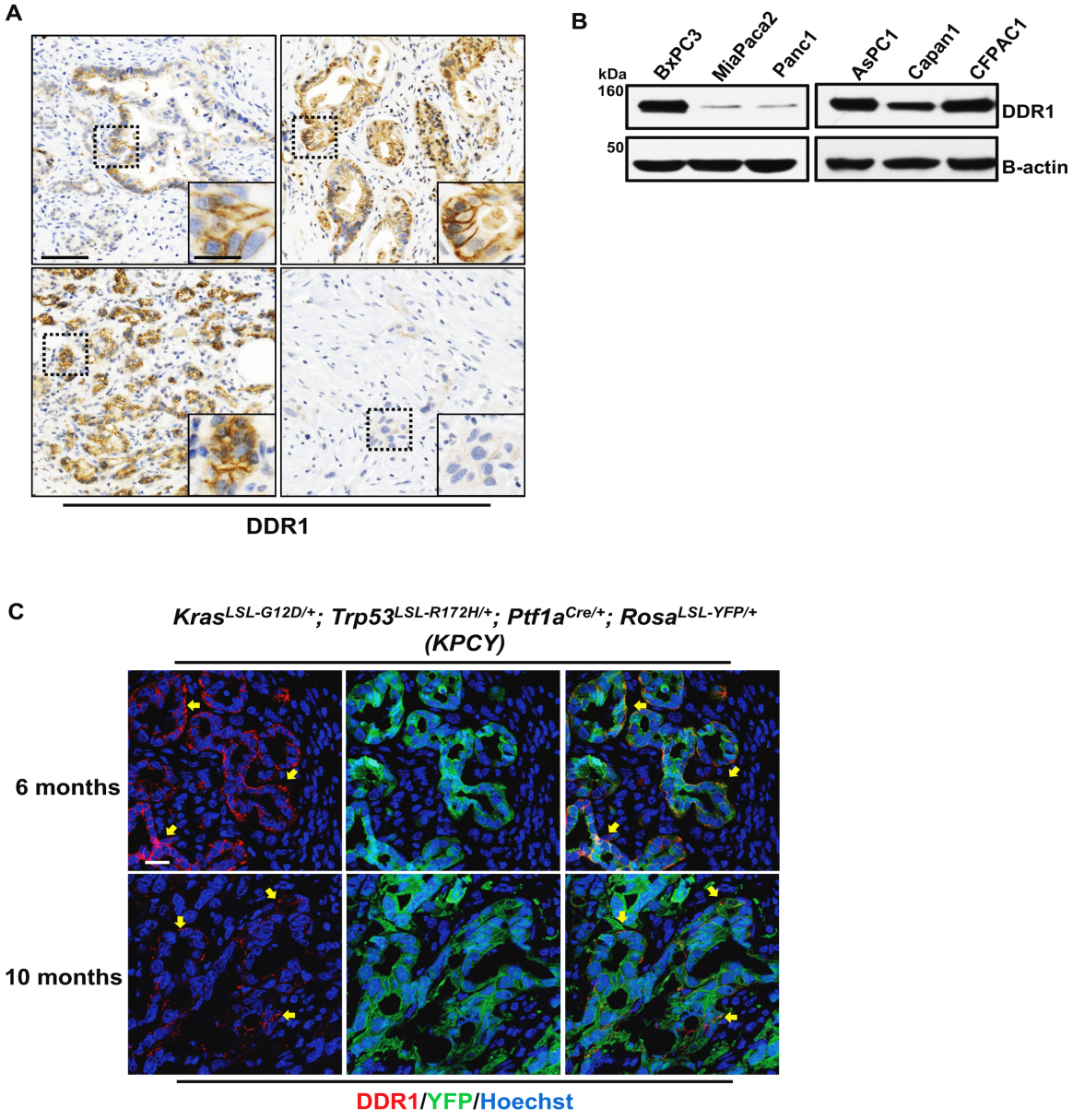

Figure 2.1: DDR1 is upregulated in human PDA and murine models of PDA. A.) IHC expression of DDR1 on representative human PDA samples. B.) Western blot of DDR1 expression in human PDA cell lines C.) Indirect immunofluorescence detection of DDR1 (red), observed localized at the membrane of neoplasia in the *KPCY* mouse model of PDA at 6 and 10 months. Green is YFP lineage tracer. Hoechst (blue) for nuclear staining. Yellow arrows indicate DDR1 positive lesions. Scale bars: 100μm (A, low power); 25 μm (A, insets); 20 μm (C).

Figure 2.2

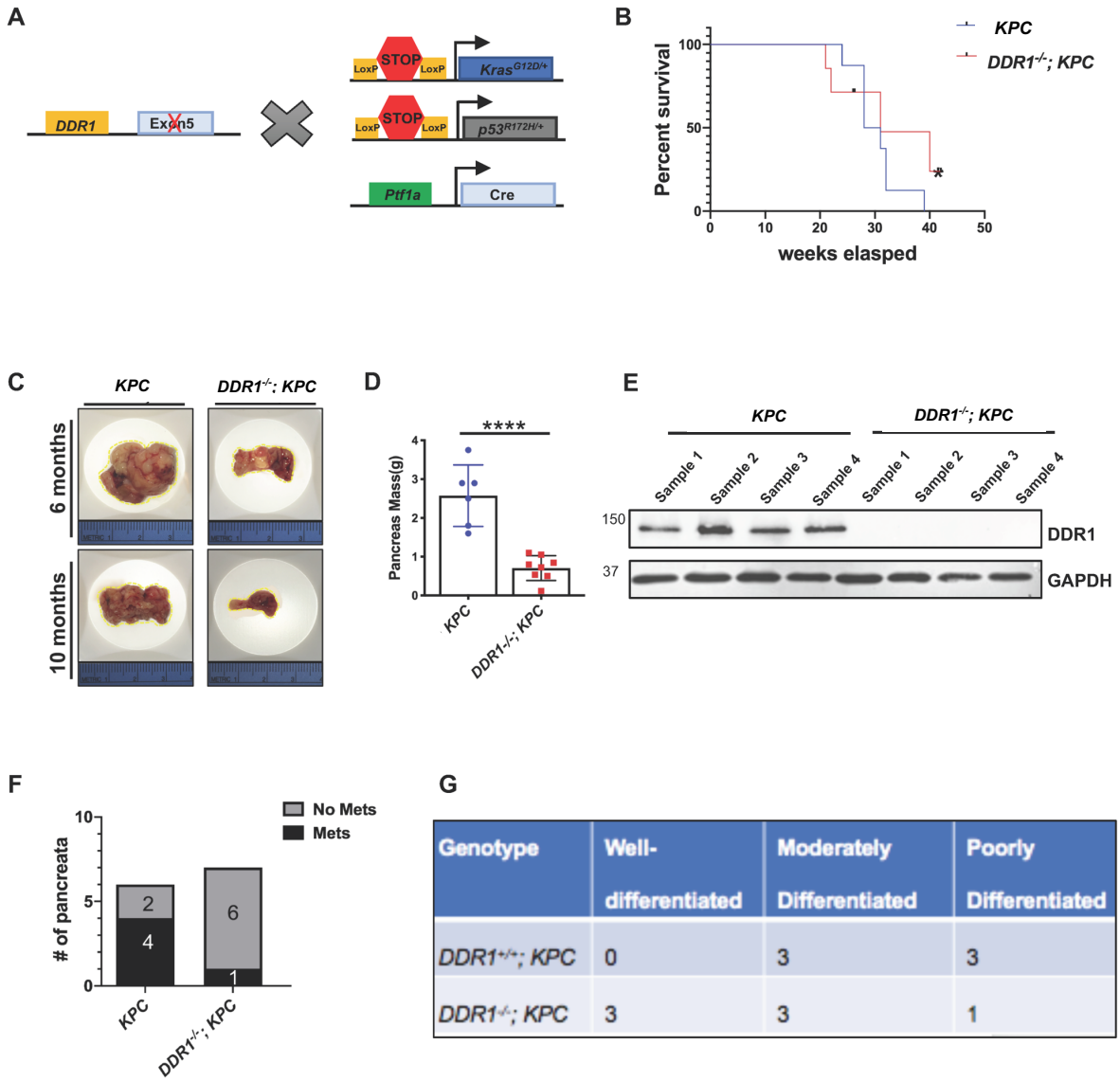

Genotype	Well-differentiated	Moderately Differentiated	Poorly Differentiated
DDR1+/+; KPC	0	3	3
DDR1-/-; KPC	3	3	1

Figure 2.2: DDR1 ablation reduces tumor growth and delays PDA progression. A.) Schematic of DDR-null mice crossed into the *KPC* metastatic mouse model. B.) Kaplan-Meier curve of *KPC* controls and *DDR1$^{-/-}$; KPC* mice. Horizontal lines at 26 weeks indicate censored mice taken down due to hind-leg paralysis. Asterisk indicates 42-week-old mouse used as a time point. C.) Gross anatomy of pancreata from *KPC* and *DDR1$^{-/-}$; KPC* mice aged at 6 and 10 months. Yellow dashed lines outline pancreas D.) Pancreas mass in grams (g) of all *KPC* and *DDR1$^{-/-}$; KPC* mice. E.) Western blot of biological replicates for *KPC* mice (left) and *DDR1$^{-/-}$; KPC* mice (right) for DDR1 expression. GAPDH was used as a loading control. F.) Graphical representation of mice with macro-metastasis to the liver. G.) Table representing tumor grade of *KPC* and *DDR1$^{-/-}$; KPC* mice. Error bars represent mean with standard deviation n > 3. ****P<0.0001.

Figure 2.3

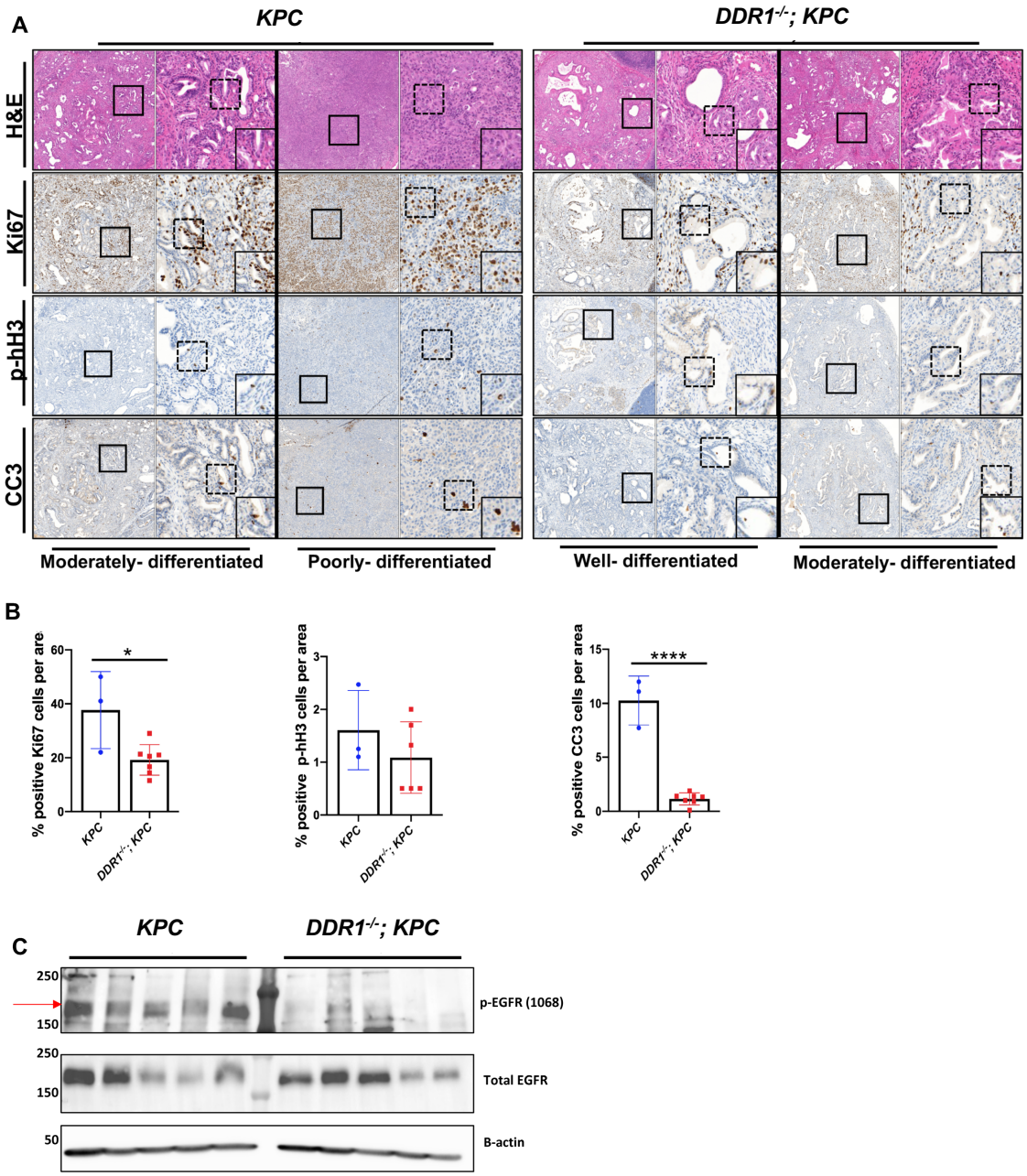

Figure 2.3: DDR1 is required for tumor growth and proliferation in PDA. A.) Histological representation of moderately-differentiated (far left) and poorly-differentiated (middle, left) *KPC* pancreata along with well- (middle, right) and moderately- differentiated *DDR1$^{-/-}$; KPC* pancreata. Low and high-power images of specified areas for H&E (top), Ki67, p-hH3, and CC3 are shown with zoomed in images of each stain. B.) Quantitation of respective staining for each group. C.) Western blot analysis of activation EGFR phosphorylation site Y1068. Total EGFR and β-actin were used as EGFR control and loading control, respectively. Error bars represent mean with standard deviation n > 3. Scales: 100μm (D, all images). *P<0.01, ****P<0.0001.

Figure 2.4

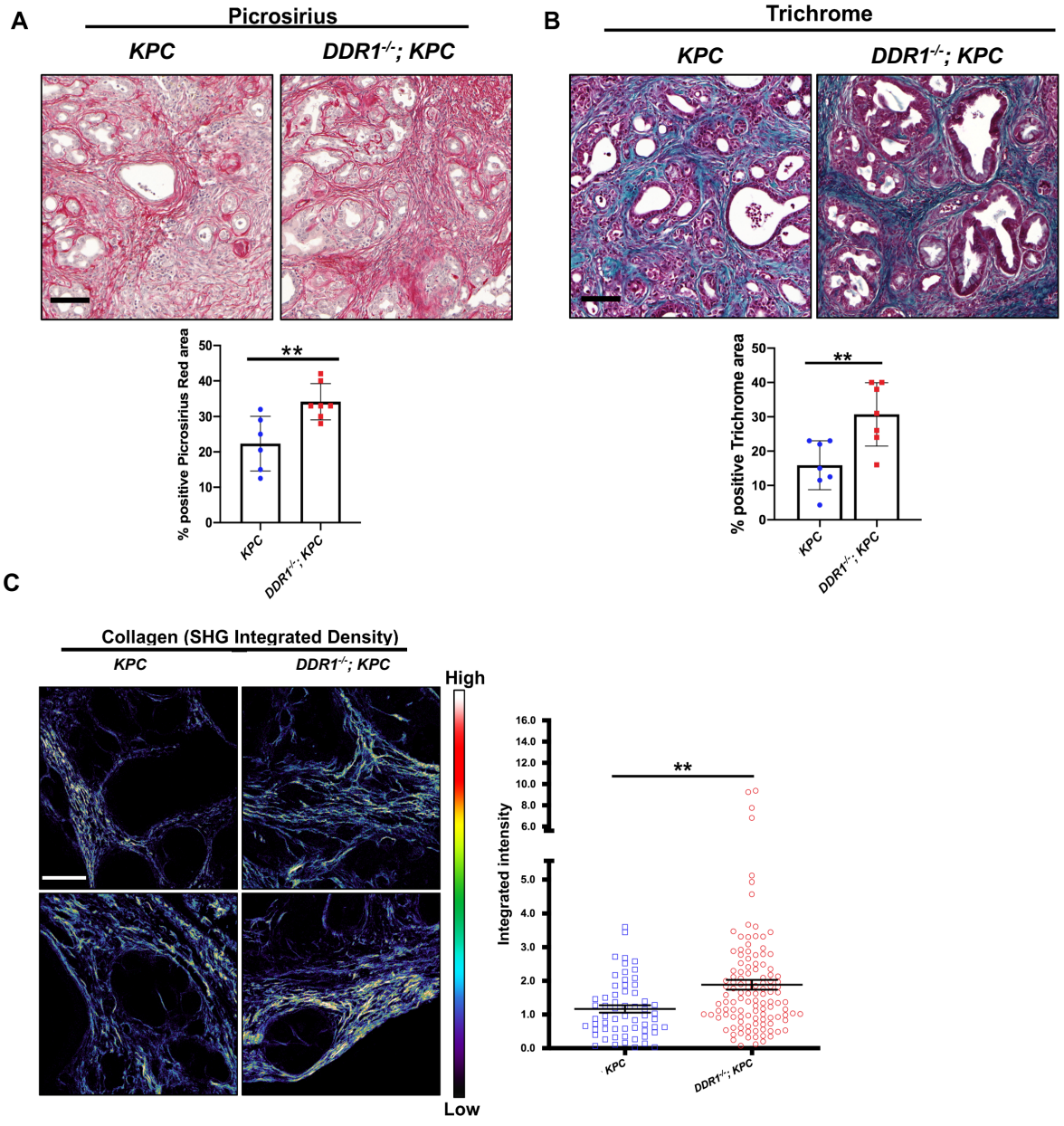

Figure 2.4: The absence of DDR1 alters the fibrotic response in PDA Progression. A, B.) Representative images of Picrosirius red and Trichrome staining from *KPC* and *DDR1$^{-/-}$; KPC* (top), respectively. Quantitative analysis of Picrosirius Red and Trichrome staining per tissue area (bottom). C.) Representative images showing Second Harmonic Generation (SHG) microscopy signatures from (2) *KPC* mice (left panels) and (2) *DDR1$^{-/-}$; KPC* (right panels). Color scale indicates intensity of polymerized collagen fibers "High" (white) and "Low" (black) levels. Quantitative analysis of polymerized collagen signatures (graph on right) obtained as SHG signal intensities divided by positive SHG signal areas (e.g., integrated intensity). Values

presented are relative (e.g., normalized) to *KPC.* Error bars represent mean with standard deviation n > 3 (A). Error bars represent mean with standard deviation n=5 for *KPC* and n=6 for *DDR1$^{-/-}$; KPC.* Three selected areas from an H&E slide from each condition were analyzed and three images/regions (e.g., n=9) were collected per slide (B). Scales: 100μm (A, B). **P<0.01

Figure 2.5

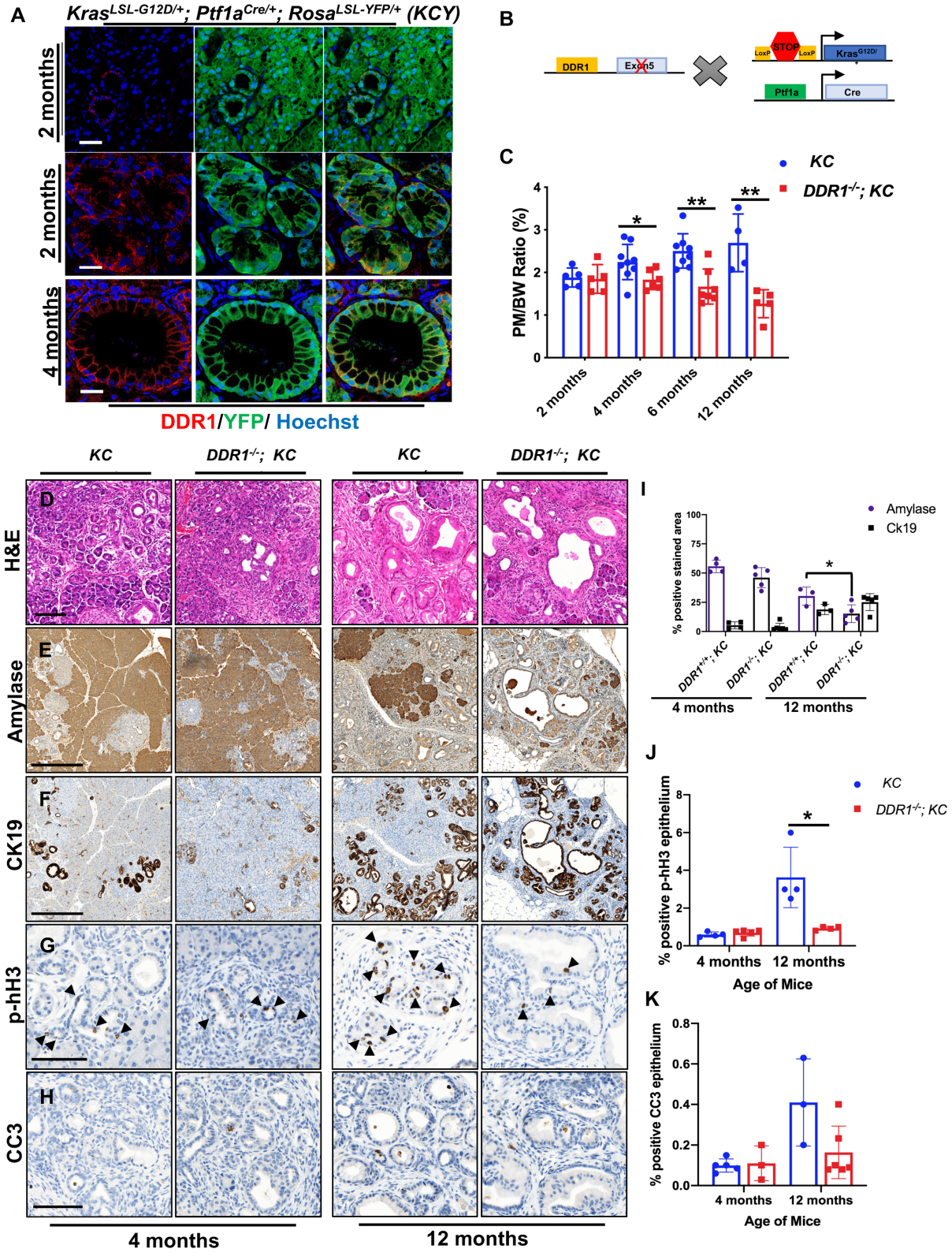
A
Kras LSL-G12D/+; Ptf1a Cre/+; Rosa LSL-YFP/+ (KCY)
2 months
2 months
4 months
DDR1/YFP/ Hoechst
B
DDR1
Ex 5
STOP
LoxP
LoxP
Kras G12D/+
Ptf1a
Cre
C
KC
DDR1-/-; KC
PM/BW Ratio (%)
2 months
4 months
6 months
12 months
KC
DDR1-/-; KC
KC
DDR1-/-; KC
H&E
Amylase
CK19
p-hH3
CC3
4 months
12 months
I
Amylase
Ck19
% positive stained area
DDR1+/+; KC
DDR1-/-; KC
DDR1+/+; KC
DDR1-/-; KC
4 months
12 months
J
KC
DDR1-/-; KC
% positive p-hH3 epithelium
4 months
12 months
Age of Mice
K
% positive CC3 epithelium
4 months
12 months
Age of Mice

Figure 2.5: DDR1 is necessary for tissue homeostasis during tumorigenesis
A.) Immunofluorescence detection of DDR1 (red) at the membrane of ADM in the *KCY* mouse model at 2 and 4 months. Green is YFP lineage tracer. Hoechst (blue) for nuclear staining. B.) Schematic of DDR-null mice crossed into the *KC* model of tumor formation C.) PM/BW ratios of mice from 2,4,6 and 12 months of age. D-H.) Representative IHC images for analysis in horizontal order of H&E, Amylase (brown), Ck19 (brown), p-hH3 (brown), CC3 (brown). I.) Quantitative analysis of Amylase and Ck19 in control and *DDR1$^{-/-}$; KC* mice at 4 and 12 months of age. J.) Quantitation of p-hH3 shows *DDR1$^{-/-}$; KC* mice are less proliferative as they age and progress to neoplasia. K.) Quantitative analysis apoptosis (CC3) in control and *DDR1$^{-/-}$; KC* mice at 4 and 12 months of age. Error bars represent mean with standard deviation n > 3. Scales: 100 μm (D, H); 500 μm (E, F all images); 50 μm (G all images). *P<0.05, **P<0.01.

Figure 2.6

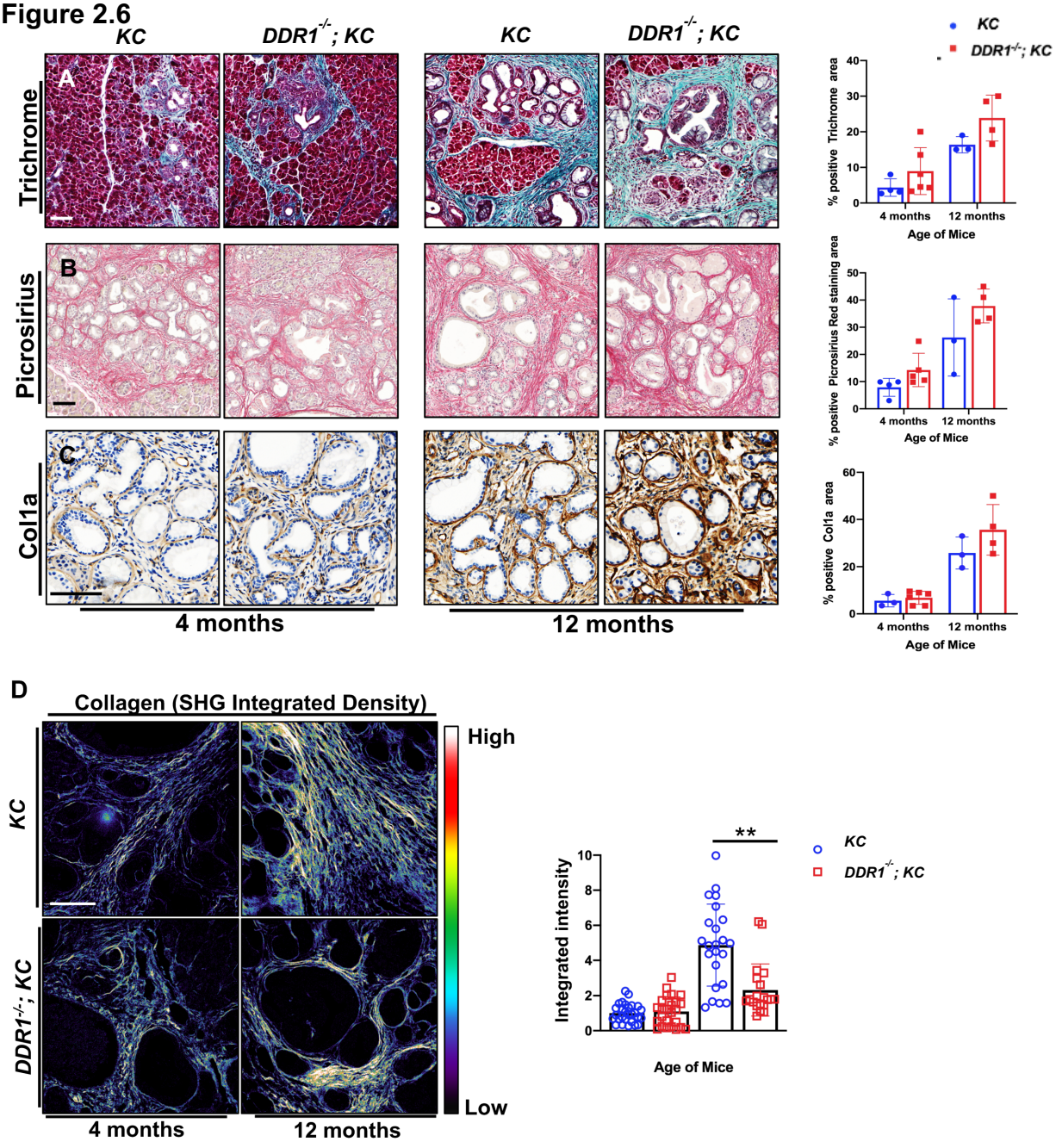

Figure 2.6 DDR1 ablation promotes a dynamic fibrotic response during spontaneous tumor formation. A-C.) Representative IHC images and quantitative analysis in horizontal order of Trichrome (blue/green), Picrosirius (dark red) and Col1a (brown) staining of control and *DDR1$^{-/-}$; KC* mice at 4 and 12 months of age. D.) Representative images of SHG for *KC* and *DDR1$^{-/-}$; KC* (left) and quantitative analysis (right). Error bars represent mean with standard deviation of n > 3 (A-C). Error bars represent mean with standard deviation n=3 for *KC* and n=3 for *DDR1$^{-/-}$; KC.* Three selected areas from each condition were analyzed and 3 images/regions (e.g., n=9) were collected per slide (D). Scales: 100 µm (SFig2 B-E, for all images). **P<0.01.

Figure 2.7

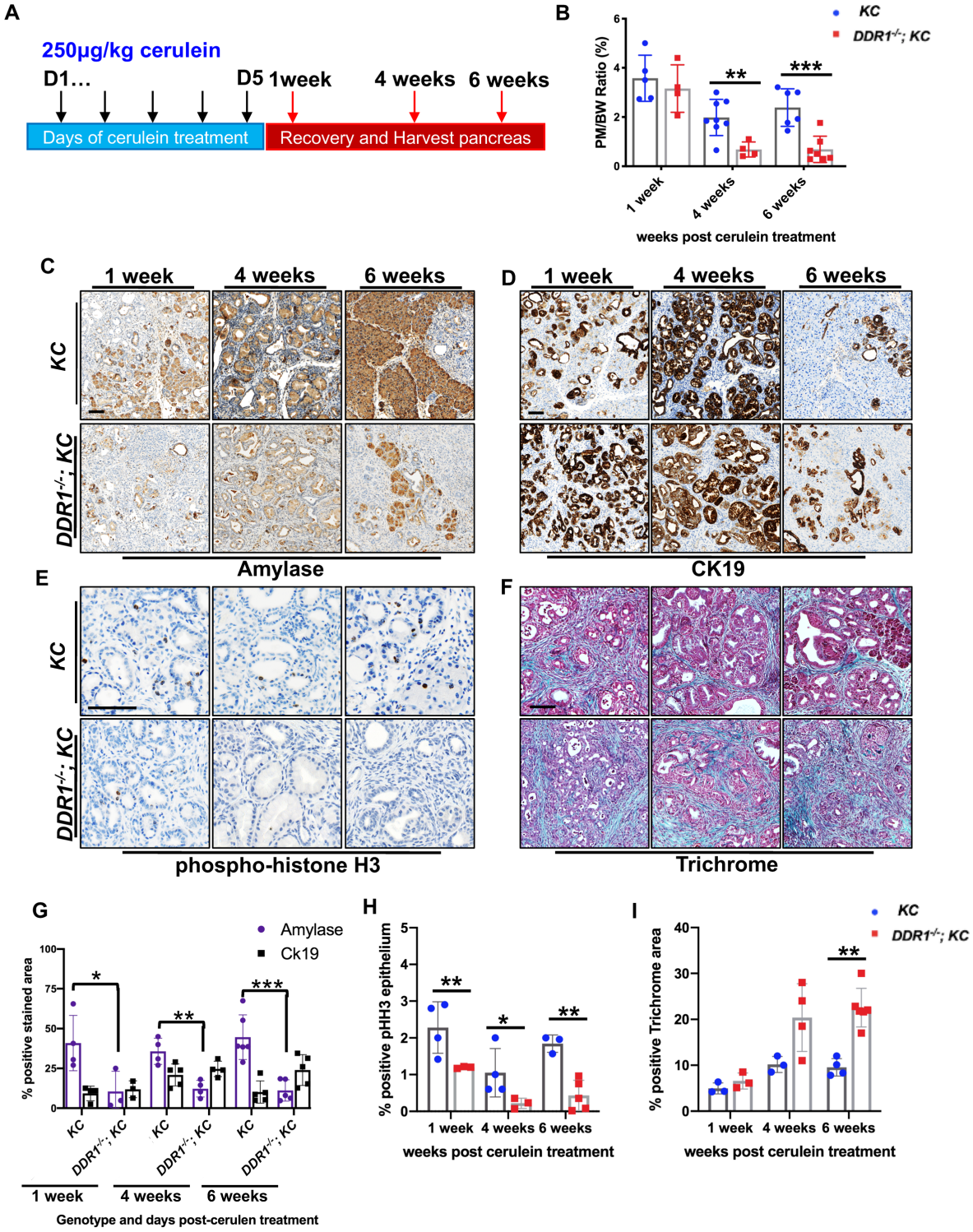
A
250µg/kg cerulein
D1…
D5 1week
4 weeks
6 weeks
Days of cerulein treatment
Recovery and Harvest pancreas
B
KC
DDR1-/-; KC
PM/BW Ratio (%)
1 week
4 weeks
6 weeks
weeks post cerulein treatment
C
1 week
4 weeks
6 weeks
KC
DDR1-/-; KC
Amylase
D
CK19
E
phospho-histone H3
F
Trichrome
G
Amylase
Ck19
% positive stained area
Genotype and days post-cerulen treatment
H
% positive pHH3 epithelium
I
% positive Trichrome area

Figure 2.7. DDR1 ablation disrupts tissue maintenance following pancreatitis-induced tumorigenesis. A.) Schematic of cerulein treatment protocol and recovery period. B.) PM/BW ratios of mice at 1, 4, and 6 weeks post-cerulein treatment C. D.) Amylase and Ck19 staining for control and *DDR1$^{-/-}$; KC* mice after cerulein treatment. Amylase (brown) decreases 1 month after cerulein cessation, but is recovered in controls after 6 weeks. Conversely, Ck19 (brown) increases as Amylase decreases in *DDR1$^{-/-}$; KC* animals that maintain a loss in acinar population. E.) Staining for p-hH3 (brown) shows significantly lower proliferation in *DDR1$^{-/-}$; KC* animals 6 weeks after cerulein. F.) Trichrome (blue) increases during recovery phases for both cohorts, but decreases in control compared to *DDR1$^{-/-}$; KC* animals that maintain higher trichrome after 6 weeks G.) Graph of Amylase and Ck19 area quantitated from IHC images. H.) Quantitation of p-hH3. I.) Quantitation of Trichrome. Error bars represent mean with standard deviation n > 3. Scales: 100 μm (C, D, E, F all images). *P<0.05, **P<0.01, ***P<0.001.

Figure 2.8

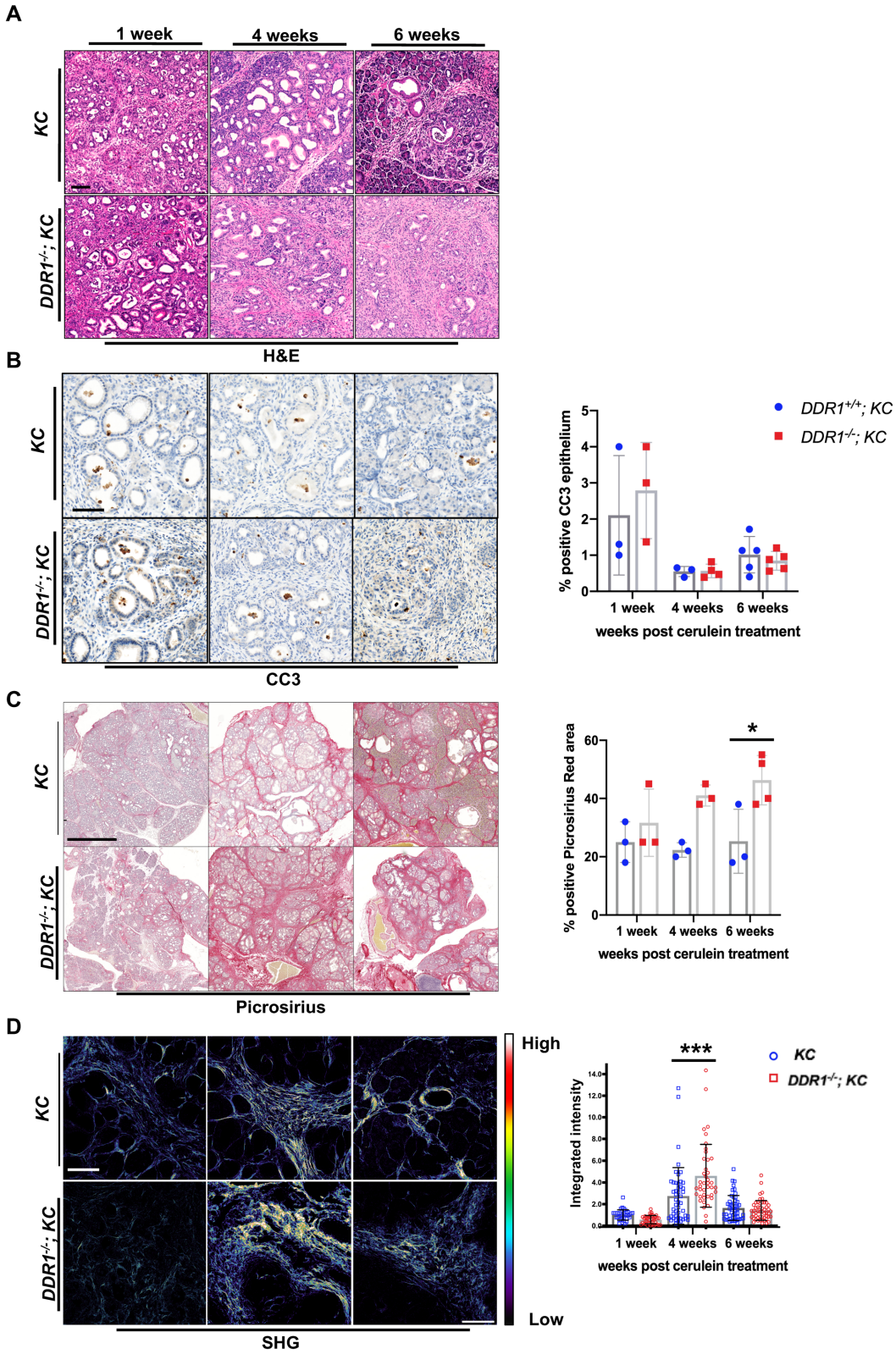
A
1 week
4 weeks
6 weeks
KC
DDR1-/-; KC
H&E
B
KC
DDR1-/-; KC
CC3
DDR1+/+; KC
DDR1-/-; KC
% positive CC3 epithelium
1 week
4 weeks
6 weeks
weeks post cerulein treatment
C
KC
DDR1-/-; KC
Picrosirius
% positive Picrosirius Red area
*
1 week
4 weeks
6 weeks
weeks post cerulein treatment
D
KC
DDR1-/-; KC
SHG
High
Low
***
KC
DDR1-/-; KC
Integrated intensity
1 week
4 weeks
6 weeks
weeks post cerulein treatment

Figure 2.8 DDR1 Ablation Disrupts Tissue Maintenance Following Pancreatitis-Induced Tumorigenesis A.) H&E images showing less recovery of normal acini in *DDR1$^{-/-}$; KC* mice over a month (6 weeks) after cerulein cessation B.) CC3 (brown) staining shows no difference in apoptotic cell death. C.) Picrosirius (dark red) staining in *KC* (left) and *DDR1$^{-/-}$; KC* (right) animals after treated with 5 days of cerulein and left to recover for 1, 4, and 6 weeks with quantitation. D) Pseudo colored images indicative of SHG intensities (e.g., warm colors represent high SHG signal) of *KC* (top) and *DDR1$^{-/-}$; KC* (bottom) animals as above. Graphs shows means of quantitated data shown in images normalized to *KC* animals at Day 1 of recovery. Error bars indicate standard deviation of n > 3 (C). Error bars represent mean with standard deviation n=3 for *DDR1$^{+/+}$; KC* and n=3 for *DDR1$^{-/-}$; KC* per timepoint. Three selected areas from each condition were analyzed and 3 images/regions (e.g., n=9) were collected per slide (D). Scales: 100 μm (A, B, D), 1mm (C). *P<0.05, ***P<0.001.

Figure 2.9

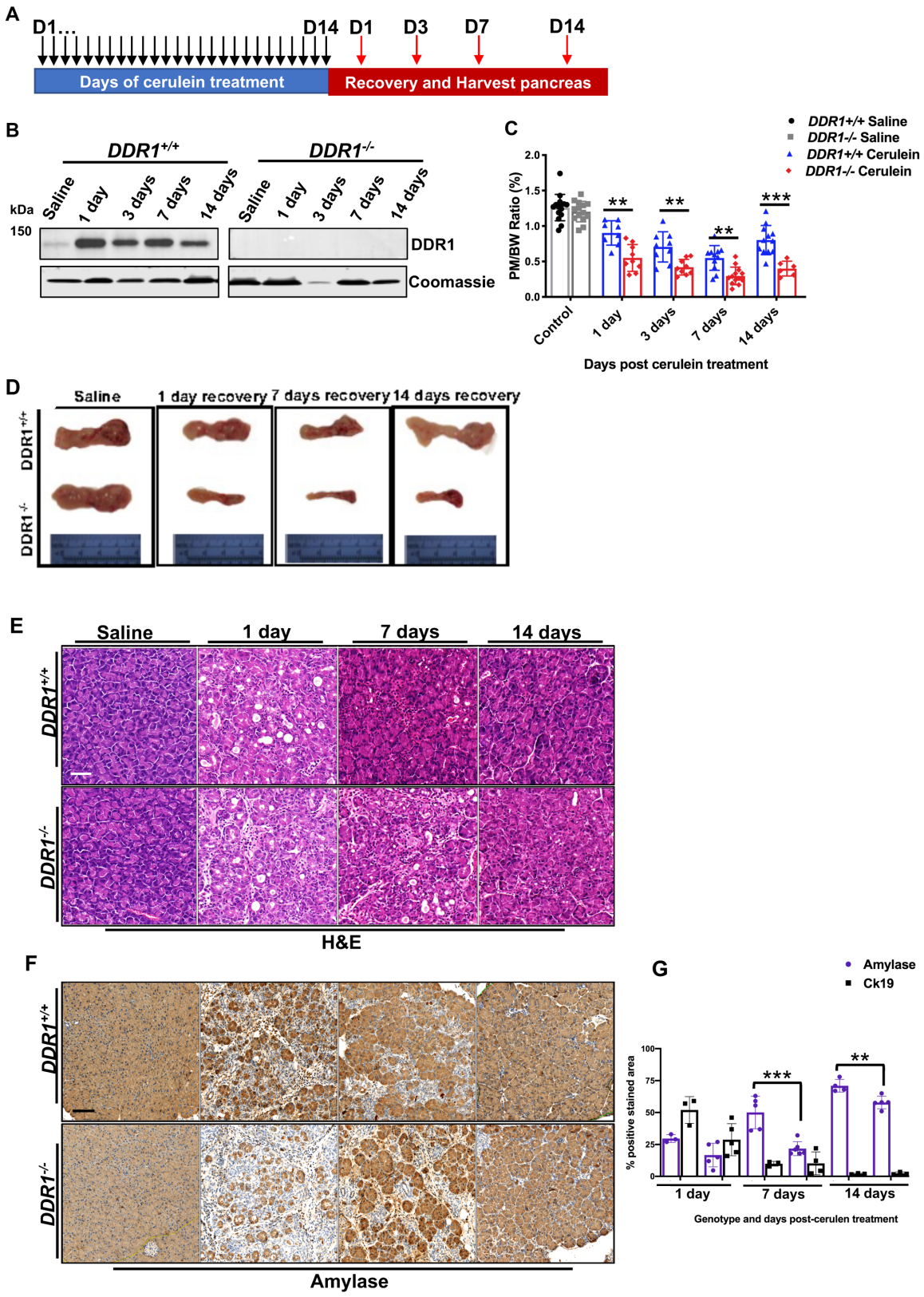
A
D1…
D14
D1
D3
D7
D14
Days of cerulein treatment
Recovery and Harvest pancreas
B
DDR1+/+
DDR1-/-
Saline
1 day
3 days
7 days
14 days
kDa
150
DDR1
Coomassie
C
DDR1+/+ Saline
DDR1-/- Saline
DDR1+/+ Cerulein
DDR1-/- Cerulein
PM/BW Ratio (%)
2.0
1.5
1.0
0.5
0.0
**
**
**
***
Control
1 day
3 days
7 days
14 days
Days post cerulein treatment
D
Saline
1 day recovery
7 days recovery
14 days recovery
DDR1+/+
DDR1-/-
E
Saline
1 day
7 days
14 days
DDR1+/+
DDR1-/-
H&E
F
DDR1+/+
DDR1-/-
Amylase
G
Amylase
Ck19
% positive stained area
100
75
50
25
0
***
**
1 day
7 days
14 days
Genotype and days post-cerulen treatment

Figure 2.9: DDR1 ablation impedes tissue recovery following cerulein-induced pancreatitis. A.) Schematic of experimental pancreatitis protocol. B.) Immunoblot for DDR1 expression in *WT* and *DDR1*$^{-/-}$ animals. *WT* animals have elevated DDR1 during recovery. C.) Pancreas weight (PM)/ body weight (BW) ratios of *WT* and *DDR1*$^{-/-}$ mice at 1,3,7, and 14 days after 2 weeks of cerulein treatment. *DDR1*$^{-/-}$ consistently have lower PM/BW ratios compared to control mice. D.) Gross histology of *WT* (top) and *DDR1*$^{-/-}$ (bottom) mice treated with the established cerulein-induced pancreatitis protocol at indicated time point post-cerulein treatment. Saline was used as a negative control. E.) H&E images show healthy pancreata (top, saline controls) for WT and *DDR1*$^{-/-}$. During recovery after cerulein treatment, controls and *DDR1*$^{-/-}$ show evidence of tissue damage with *DDR1*$^{-/-}$ mice experiencing tissue damage 1-week post-cerulein compared to controls (right, center). F.) Amylase (brown) staining for *WT* and *DDR1*$^{-/-}$ reflects loss of tissue mass contributed towards a loss in amylase staining (acinar cells) during recovery, with more significant loss in staining in DDR1-null animals. G) Quantitation of Amylase and Ck19 positive staining from IHC images. Error bars represent mean with standard deviation n > 3. Scales: 100μm (E, D all images). **P<0.01, ***P<0.001.

Figure 2.10

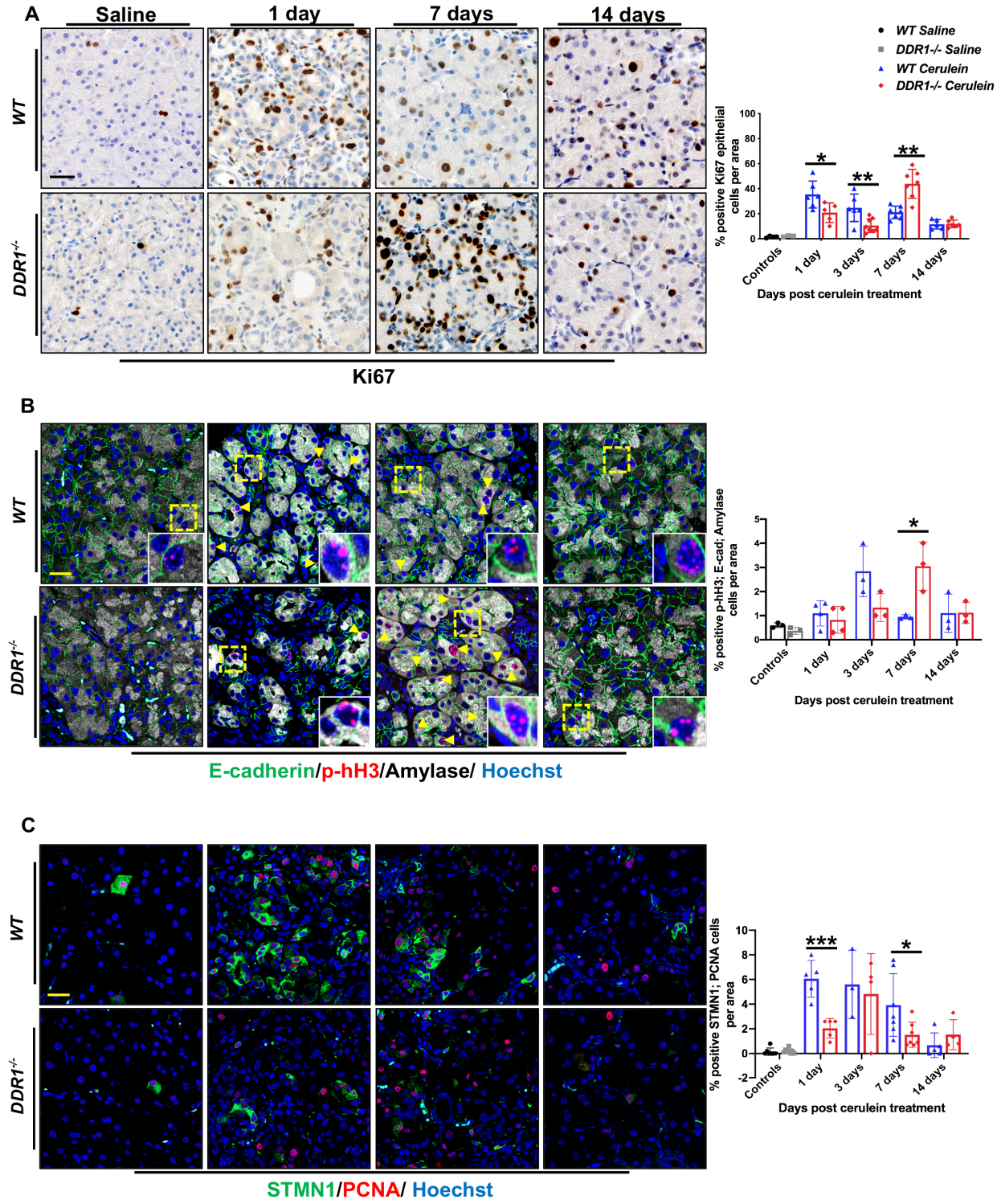
A
Saline
1 day
7 days
14 days
WT
DDR1-/-
Ki67
WT Saline
DDR1-/- Saline
WT Cerulein
DDR1-/- Cerulein
% positive Ki67 epithelial cells per area
Controls
1 day
3 days
7 days
14 days
Days post cerulein treatment
B
E-cadherin/p-hH3/Amylase/ Hoechst
% positive p-hH3; E-cad; Amylase cells per area
C
STMN1/PCNA/ Hoechst
% positive STMN1; PCNA cells per area

Figure 2.10: Proliferation is stunted during tissue recovery following cerulein treatment in DDR1 ablated mice. A) Ki67 (brown) is detected in low amounts in saline controls (top, left). After cerulein, controls have more $Ki67^+$ epithelial up to 3 days of recovery (top, left center). Conversely, *DDR1*$^{-/-}$ animals have lower $Ki67^+$ epithelial cells at 1 and 3 (lower, left center) but a burst of $Ki67^+$ cells 7 days post-treatment (lower, right center). Both cohorts have similar $Ki67^+$ cells 2 weeks after cerulein cessation (top and lower far left). Quantification of Ki67 staining (right). B) Triple staining for E-cadherin (green), amylase (white), p-hH3 (red), and nuclei (blue) to detect acinar cells undergoing mitosis. Yellow triangles indicate triple positive cells. Insets are outlined in yellow dashed-square lines. Quantification of triple positive (E-cadherin$^+$; Amylase$^+$; p-hH3$^+$) cells (right). C) Co-staining for STMN1 (green), PCNA (red), and nuclei (blue) to detect number of cells that contribute to the regeneration of the pancreas after injury. Double positive cells are detected in saline controls at low numbers. During recovery, the amount of STMN1$^+$; PCNA$^+$ cells increases in both WT and *DDR1*$^{-/-}$ mice compared to saline controls, with significantly more cells in *DDR1*$^{+/+}$ mice. Quantitation of dual positive (STMN1$^+$; PCNA$^+$) cell (right). Error bars represent mean with standard deviation n > 3. Scales: 100μm (A, B all images), 20μm (C, lower power) *P<0.05, **P<0.01, ***P<0.001.

Figure 2.11

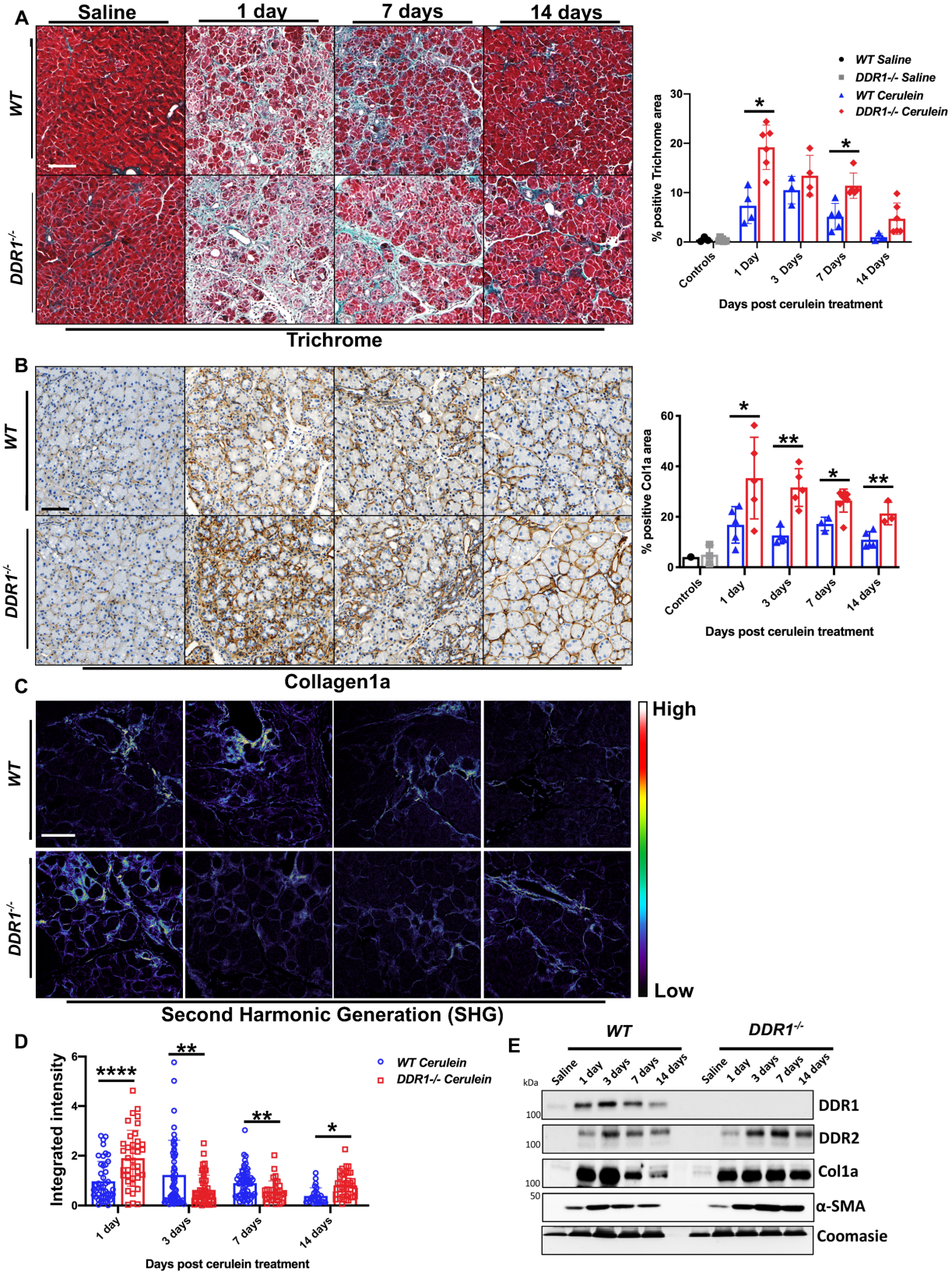
A
Saline
1 day
7 days
14 days
WT
DDR1-/-
Trichrome
WT Saline
DDR1-/- Saline
WT Cerulein
DDR1-/- Cerulein
% positive Trichrome area
Controls
1 Day
3 Days
7 Days
14 Days
Days post cerulein treatment
B
Collagen1a
% positive Col1a area
1 day
3 days
7 days
14 days
C
High
Low
Second Harmonic Generation (SHG)
D
Integrated intensity
WT Cerulein
DDR1-/- Cerulein
Days post cerulein treatment
E
WT
DDR1-/-
kDa
DDR1
DDR2
Col1a
α-SMA
Coomasie

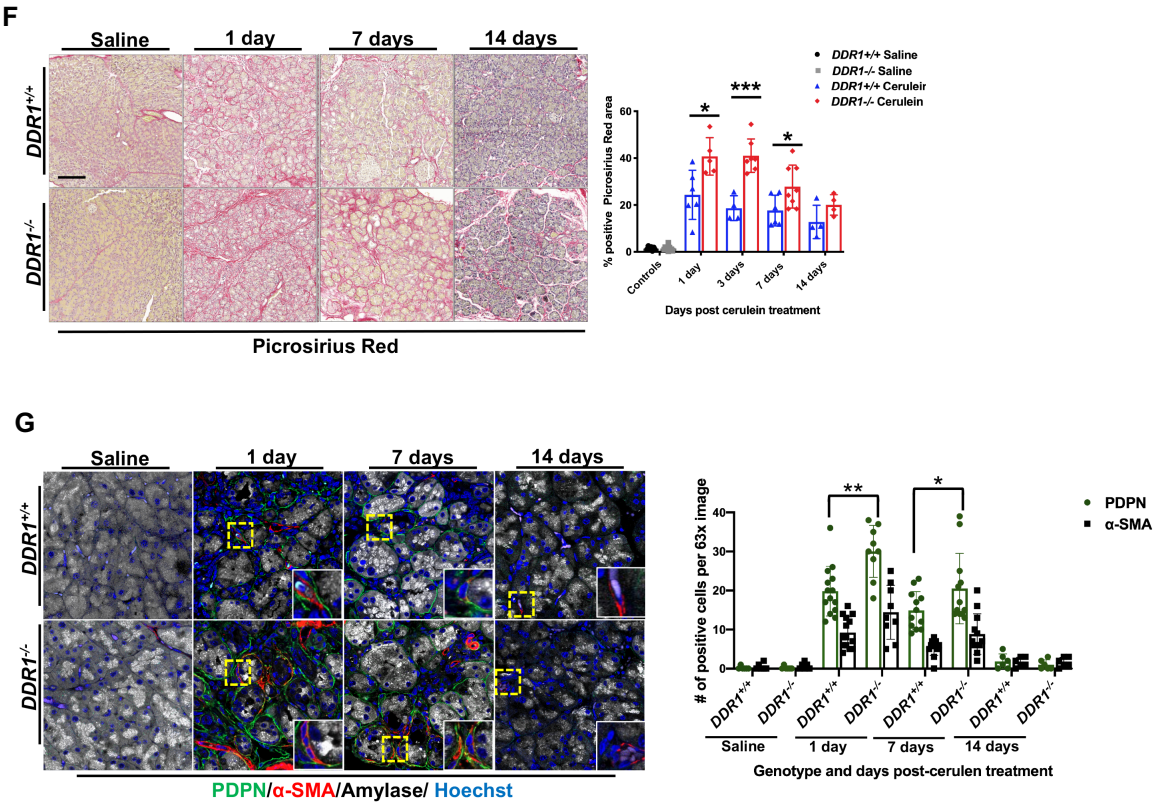

Figure 2.11 DDR1 deficient mice develop extensive fibrosis after pancreatic injury. A) Trichrome (blue/green) staining in both control and *DDR1*$^{-/-}$ animals is elevated (left). Quantitation of Trichrome staining (right). B) Col1a staining during recovery (left). Quantitation of Col1a staining (right). C) Representative images of SHG during recovery after pancreatic injury reveal increased signals indicative of polymerized collagen deposition in *DDR1*$^{-/-}$ mice. D) Quantitation of SHG shows that the increased fibrillogenesis remained unresolved, in *DDR1*$^{-/-}$ mice, 2 weeks after cerulein treatment. E) Western blot analysis of whole tissue lysates for common markers of fibrosis. F) Picrosirius red staining in *WT* (top) and *DDR1*$^{-/-}$ (bottom) animals after treated with the established cerulein-induced pancreatitis protocol at indicated time point post-cerulein treatment. Saline was used as a negative control. Quantitation of Picrosirius red staining (right). G) Co-staining for Podoplanin (PDPN, green), α-SMA (red), Amylase (white), and nuclei (blue) in WT (top) and *DDR1*$^{-/-}$ (bottom) for the detection of fibroblasts. Total number of PDPN^{+} and α-SMA^{+} cells were counted manually from n=2 WT and n=2 *DDR1*$^{-/-}$ biological replicates for each timepoint and an average of n>4 regions/images at 63x (n= 8) per slide condition. Error bars represent mean with standard deviation n > 3 (A, B, F). Error bars represent mean with standard deviation n=3 for *DDR1*$^{+/+}$ and n=3 for *DDR1*$^{-/-}$ per timepoint. Three selected areas from each condition were analyzed and 3 images/regions (e.g., n=9) were collected per slide (D). Scales: 100μm (A, B, C all images). *P<0.05, **P<0.01, ****P<0.0001.

Figures from Miscellaneous Data

Figure 2.12i

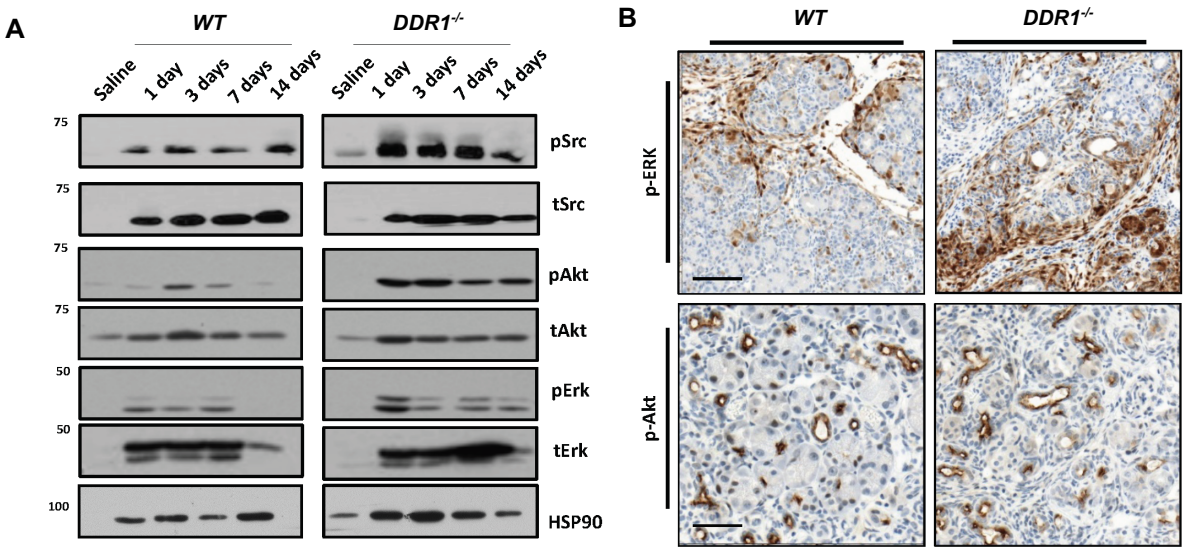

Figure 2.12i Downstream effectors of DDR1. A.) Immunoblot analysis of whole tissue lysates from cerulein treated mice for reported downstream effectors of DDR1 including activated and total amount of Src, Erk, and Akt. HSP90 was sued as a loading control. Saline treated lysates were used as a negative control for baseline levels of proteins. B.) IHC of 7-day recovery animals for activated Erk (p-ERK, brown) and activated Akt (p-Akt, brown).

Figure 2.12ii

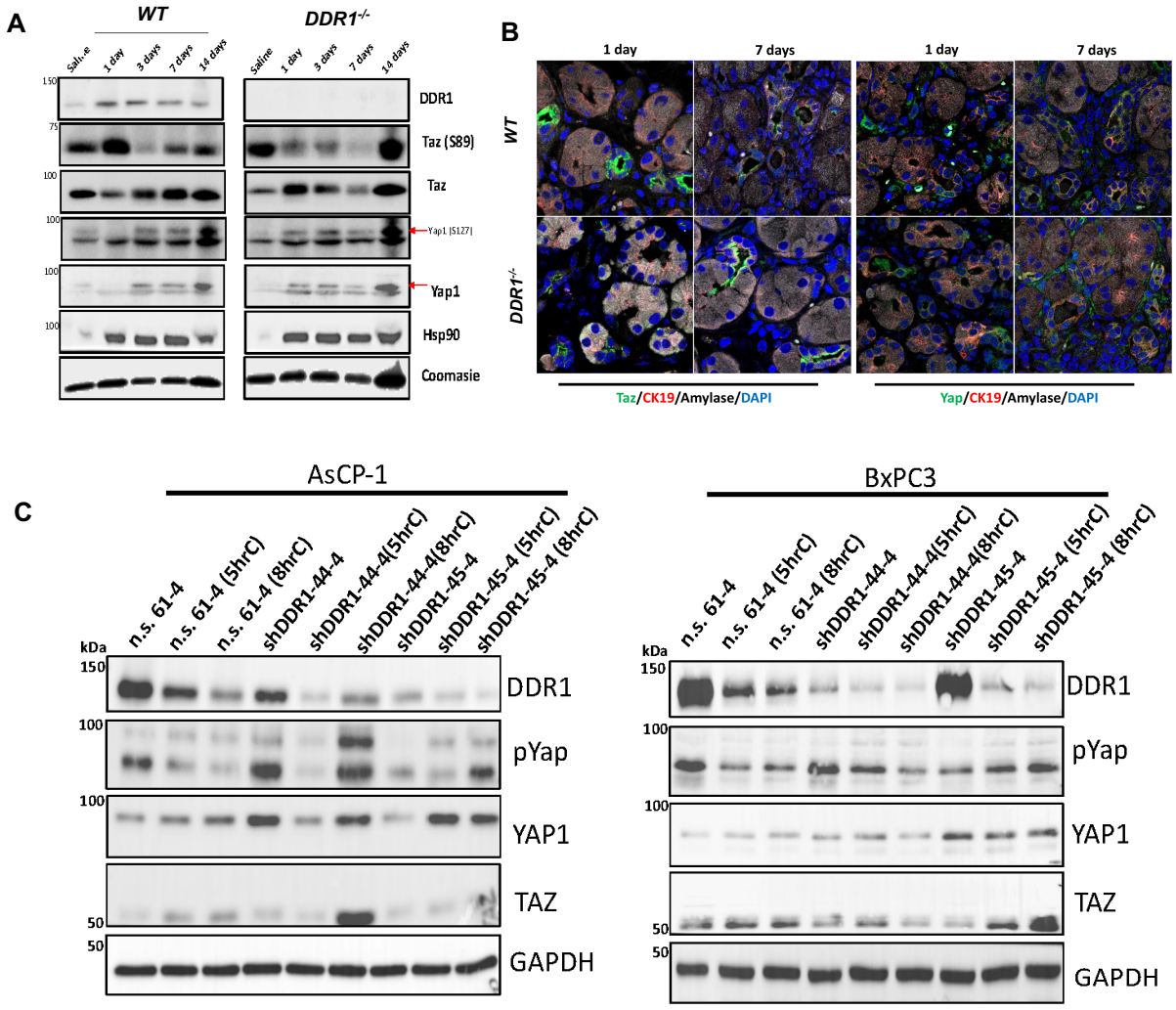

Figure2.12ii DDR1 and its regulation in the Hippo pathway: A.) Immunoblot analysis of whole tissue lysates from cerulein treated mice for downstream Hippo pathway effectors including phosphorylated and total Yap1 and Taz proteins. HSP90 and Coomassie blue stain were used as loading controls. B.) IF detection of Taz (left, panel) and Yap (right panel) in *WT* and *DDR1*$^{-/-}$ cerulein treated mice at 1- and 7-days post-treatment.
C.) Immunoblot analysis on human pancreatic cancer cell lines, AsPC1 and BxPC3, with endogenous or knockdown of DDR1 treated with 5 hours or 8 hours of collagen (5hrC, 8hrC, respectively) before collecting lysates for downstream Hippo pathway effectors including phosphorylated and total Yap1 and Taz proteins. GAPDH was used as a loading control.

Figure 2.12iii

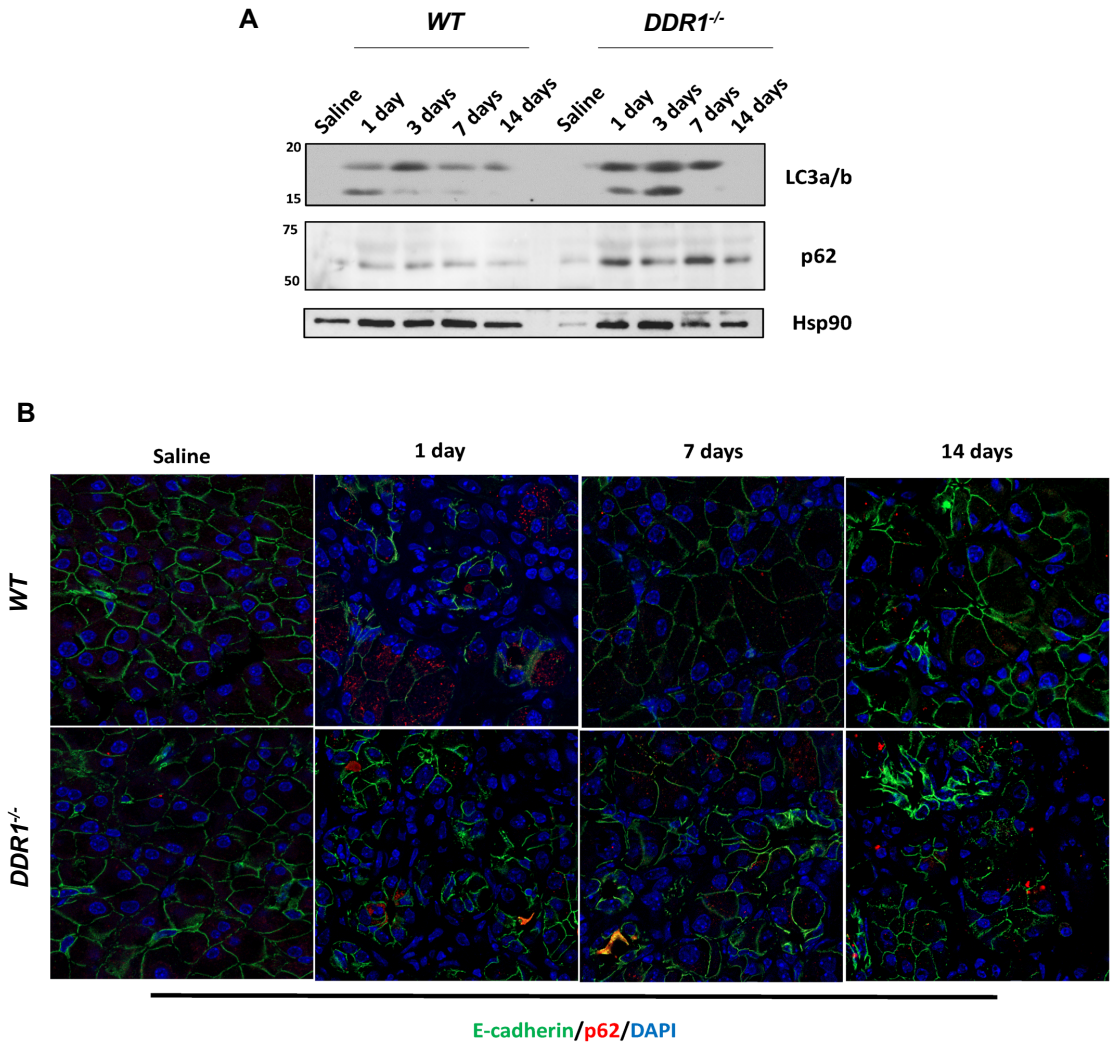

Figure 2.12iii The role of DDR1 in autophagy: A.) Immunoblot analysis of whole tissue lysates from cerulein treated mice for critical components of autophagosome formation, LC3a/b and p62. HSP90 was used as a loading control. B.) Immunofluorescence of Saline control and cerulein treated *WT* and DDR1$^{-/-}$ animals for p62 (red, punctate dots in cytoplasm) within the epithelium (green) of pancreatic tissue after injury. DAPI (blue) was used a nuclear detection.

Figure 2.12iv

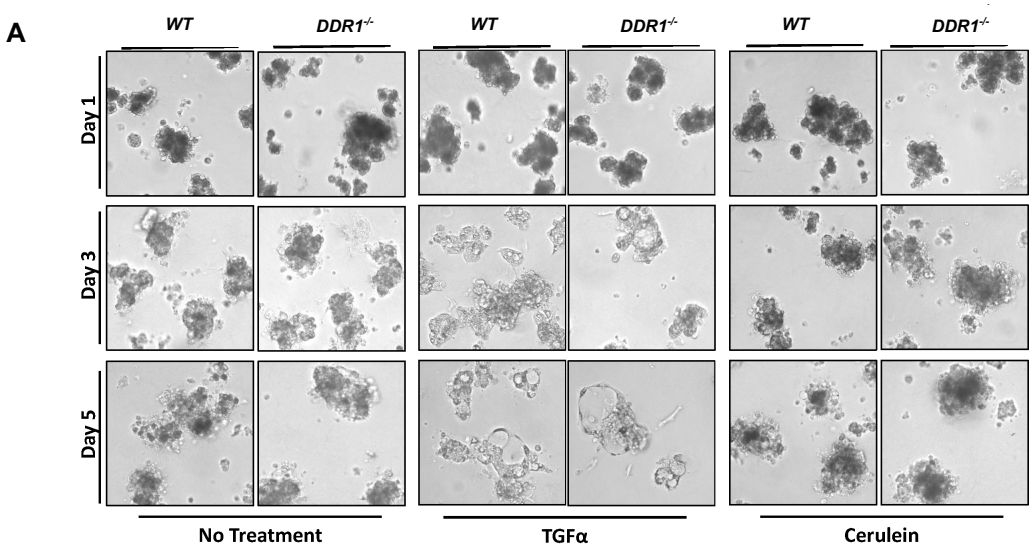

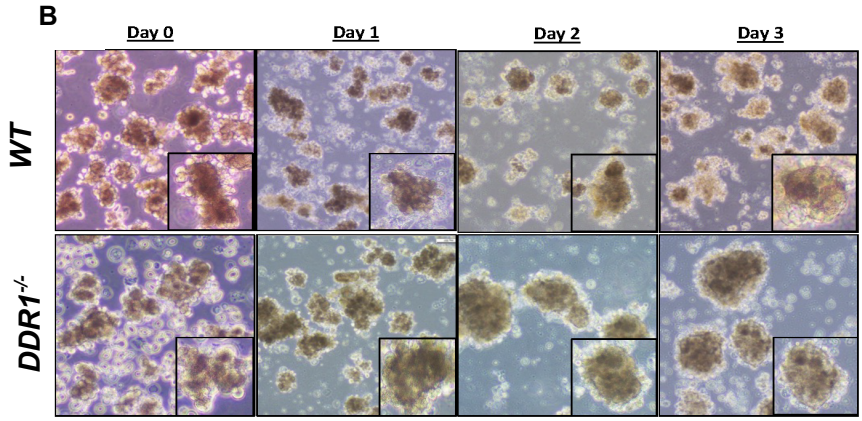

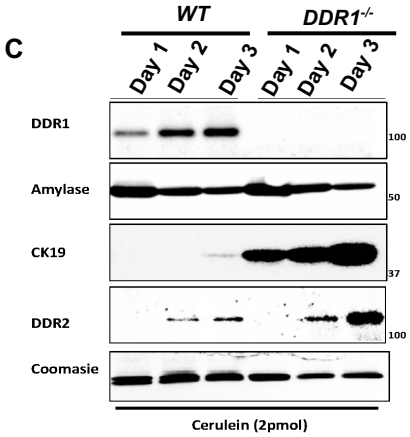

Figure 2.12iv DDR1-null animals during ADM. A.) Acinar cell explants from both *WT* and *DDR1*$^{-/-}$ animals and then embedded in rat tail collagen. Cultures with either sustained in Waymouth media (left, no treatment) or with ADM inducing agents, TGFα (middle) or cerulein (right). B.) Acinar cell explants from both *WT* and *DDR1*$^{-/-}$ animals suspended in media with cerulein to induce ADM. C.) Protein lysates from suspended acinar cultures to demonstrate the elevation of ADM markers CK19 and DDR2. Coomasie was used a loading control.

Chapter 3: Determining the Role of Discoidin Domain Receptor 2 (DDR2) in the Progression of Pancreatic Ductal Adenocarcinoma

Introduction

Metastasis is defined as the colonization of tumor cells from the primary site to distant organs[103]. Recently, a bulk of cancer research has focused on the initiation and progression of localized tumors in efforts to prevent and detect it at an early, treatable stage[103]. However, metastasis is the leading cause of cancer associated deaths in solid tumors for which the molecular events that promote tumor cell invasion remain unclear[104, 105]. A majority of patients diagnosed with PDA present with locally advanced or widespread metastatic disease, in which surgical or standard-of-care cytotoxic agents are largely ineffective[106]. Surgical resection is an option for a small percentage of patients that do not appear to have metastatic disease[103]. Unfortunately, after surgical resection almost 80% of patients present with recurrent, metastatic disease indicating that pancreatic tumor cells may escape the primary site earlier than previously conceived[105, 106]. Placing new efforts into studying and understanding the molecular events that orchestrate metastasis will add valuable insight for potential clinical benefits.

Dissemination of cancer cells from the primary site is not a trivial task. Cancer cells must overcome several obstacles including genetic instability, immune cell

surveillance, and the physical barriers of the stroma[103]. It has been proposed that survival through these conditions implies metastasis is an evolutionary process in which cells that adapt to the selective pressures acquire advantageous properties to colonize other organs akin to "survival of the fittest"[103, 105]. Experimental evidence supports this concept and other processes that influence the metastatic cascade which include epithelial-to-mesenchymal transition (EMT) of tumor cells and the selective pressure created by the collagen-dense tumor microenvironment that stimulates metastatic properties[103, 105]. While these events contribute to malignancies, the molecular signals and cues received by tumor cells to migrate from the primary site are not fully understood and require attention.

Discoidin Domain Receptor 2 (DDR2) is a member of the RTK superfamily that is selectively activated by fibrillar collagens to regulate cell adhesion, migration, and proliferation[59]. Endogenous expression of DDR2 is found in mesenchymal cells and is detected during the wound healing process following an injury[57, 59]. In certain cancers, DDR2 is aberrantly activated and expressed in both the stroma and cancer cells indicating a probable role in tumor progression. Recent studies in breast cancer models have shown that DDR2 facilitates the process of EMT and is a critical component in metastases[67, 68]. In lung cancer, next-generation sequencing (NGS) has identified several point mutations in DDR2 that are currently being considered for targeted therapy[78, 107]. In PDA, patients present with a dominant collagen-rich fibrotic response that can serve as an unlimited source of ligand for DDR2. However, the contribution of DDR2 in PDA progression has not been investigated. Preliminary data from human PDA tissue microarrays (TMA) provide evidence that DDR2 is expressed

in both neoplastic lesions and the surrounding stroma. Lineage-tracing in mouse models of PDA also detected DDR2+ cells in acinar-derived tumor cells and the stroma suggesting DDR2 is associated with a metastatic phenotype, which supports prior studies that show DDR2 is involved with EMT and metastasis[67, 68]. Based on these data, I hypothesized that DDR2 activation is necessary to promote PDA progression and metastasis. To test this hypothesis, a number of *in vitro* assays and mouse models have been generated to determine the functional role of DDR2 in PDA progression.

Methods and Materials

Mouse Models

The following mice were used: *DDR2$^{fl/fl}$; β-actin$^{CreERT2/+}$; Rosa$^{LSL-Tdt}$* mice have been previously characterized and gifts from Dr. Gregory Longmore, Washington University[67]. *Kras$^{LSL-G12D/+;}$ Ptf1a$^{Cre/+}$; R26R$^{LSL-YFP}$* for tumorigenesis studies and *Kras$^{LSL-G12D/+;}$ Trp53$^{R172H/+}$ Ptf1a$^{Cre/+}$; R26R$^{LSL-YFP}$* for metastasis[34, 50, 89]. *Kras$^{LSL-G12D/+;}$ Ptf1a$^{CreERT/+}$; R26R$^{LSL-YFP}$ and Kras$^{LSL-G12D/+;}$ Trp53$^{R172H/+}$ Ptf1a$^{CreERT/+}$; R26R$^{LSL-YFP}$* were used for lineage-tracing studies. *DDR2$^{fl/fl}$; β-actin$^{CreERT2/+}$; Kras$^{FSF-G12D/+}$; Ptf1a$^{FlpO/+}$ and DDR2$^{fl/fl}$; β-actin$^{CreERT2/+}$; Kras$^{FSF-G12D/+}$; Trp53$^{FSF/+}$ Ptf1a$^{FlpO/+}$* were generated internally. Mice were maintained on mixed backgrounds. All animal protocols were reviewed and approved by the University of Michigan Institutional Animal Care and Use Committee (IACUC).

Cell Culture

Human pancreatic cancer cell lines (PANC-1, MiaPaCa-2, and BxPC-3) were purchased from the ATCC. Cells were cultured in DMEM (Thermo Fisher) or RPMI (Thermo Fisher) containing 10% FBS and maintained at 37°C in a humidified incubator with 5% CO_2 and 95% air.

Tamoxifen Treatment

Tamoxifen (Sigma, #T5648-1g) was reconstituted in sterile corn oil at 5mg/ml and incubated for 1-hour (or until dissolved) at 37^{o}C in rocking incubator. 8-week old mice were treated with 250μg/ml one time a day for 5 days by oral gavage.

Cerulein Treatment

Experimental pancreatitis was induced, as previously described (Halbrook et al, 2017), by administering 250 µg/kg cerulein (46-1-50; American Peptide Company, Inc, Sunnyvale, CA) intraperitoneally twice daily for 2 weeks and allowed to recover for 1,3, and 7 in control and *DDR2*$^{fl/fl}$ littermates. Mice used in this study were aged between 8-12 weeks and weights between 18-25 grams. Saline (Sigma-Aldrich #07982-100TAB-F) was used as a negative control for cerulein. For pancreatitis-induced tumorigenesis, 6-week old *Kras*$^{FSF\text{-}G12D/+;}$ *Ptf1a*$^{FlpO/+}$ *(KF)* and *DDR2*$^{fl/fl}$*; KF* littermates were treated with 250 µg/kg cerulein once daily for 5 consecutive days and allowed to recover for 1, 4 and 6 weeks before tissue harvesting.

Immunohistochemistry (IHC), Immunofluorescence (IF), and Quantification

Distribution and use of all human samples were approved by the Institutional Review Boards of Mayo Clinic. For IHC, pancreata were removed and fixed in Z-fix (NC9050753; Anatech, Ltd, Battle Creek, MI) overnight. Tissues were processed using a Leica ASP300S tissue processor (Buffalo Grove, IL). Paraffin-embedded tissues were sectioned at 4 µm and stained for specific target proteins using the Discovery Ultra XT autostainer (Ventana Medical Systems, Inc, Tucson, AZ) with antibodies as shown in Table 1 and counterstained with Mayer's hematoxylin (NC9220898; Sigma-Aldrich). H&E staining was performed using Mayer's hematoxylin solution and eosin Y (HT110116; Fisher, Pittsburgh, PA). Picrosirius red staining was performed according to the manufacturer's instructions (Polysciences, Inc, Warrington, PA). Gomori Trichrome (Green Collagen) stain was performed by manufacturer's instructions

(Thermo Scientific™ Richard-Allan Scientific™ IHC slides were then scanned on a Pannoramic SCAN scanner (Perkin Elmer, Seattle, WA). Scanned images were quantified using algorithms provided from Halo software (Indica Labs, Corrales, NM).

IF was performed on pancreata that were fixed in Z-fix for 2 hours, followed by an overnight float in 30% sucrose. Pancreata were incubated in a 1:1 mixture of 30% sucrose and optimal cutting temperature embedding medium (OCT) for 1 hour, embedded in OCT, frozen in liquid nitrogen, and stored at -80°C. Tissue sections (7 μm) were permeabilized in 1× phosphate-buffered saline (PBS) supplemented with 0.1% Triton X-100 (T9284; Sigma-Aldrich, St. Louis, MO) for 1 hour and blocked in 1× PBS supplemented with 5% donkey serum and 1% bovine serum albumin for 1 hour. Sections then were incubated with primary antibody diluted in 1× PBS supplemented with 0.1% Triton X-100 and 1% bovine serum albumin overnight at room temperature, followed by 3 washes in 0.1% Triton X-100/PBS for a total of 1 hour. Sections were incubated with secondary antibodies conjugated with Alexa Fluor (Invitrogen, Carlsbad, CA) for 1 hour at room temperature, followed by 3 washes in 0.1% Triton X-100/PBS. Hoechst 33342 stain (#62249, Thermo Scientific) was used for nuclear stain at 1:10,000 dilution in 1x PBS solution for 20 minutes. Slides were then rinsed in deionized water and mounted with Prolong Diamond antifade mount (P36961; Fisher). Images presented were acquired on a confocal microscope LSM800 (Zeiss, Oberkochen, Germany). IF slides were scanned and quantified with same methods as IHC.

Immunoblotting

Mouse pancreas whole tissue lysates for protein analysis were obtained by removing a small piece of the pancreas from mice after euthanasia and snap freezing in liquid nitrogen. Tissue samples were then homogenized using the Pro 250 Homogenizer (Pro Scientific Inc, Oxford, CT) in RIPA buffer supplemented with protease inhibitor cocktail (PIA32965; Thermo Fisher Scientific) and PhosSTOP phosphatase inhibitor cocktail (4906845001; Sigma-Aldrich). Lysates were then cleared by centrifugation and stored at –80°C. Human cell lines were also lysed with RIPA buffer and cleared by centrifugation. Protein concentrations were determined using the BCA Protein Assay Kit (PI23228; Thermo Fisher Scientific). Proteins were separated using sodium dodecyl sulfate gel electrophoresis and transferred to a polyvinylidene difluoride membrane (IPVH00010; VWR, Radnor, PA). Primary antibodies are listed in Table 2. Secondary antibody coupled to horseradish peroxidase (GE Healthcare, Pittsburgh, PA) and the enhanced chemiluminescence detection system (BioRad Clarity™ and Max™ Western ECL Substrate) were used to visualize proteins using BioRad ChemiDoc™ Imaging System.

Table 2: List of Antibodies

Antibody	Company	Catalog #	Concentration	Method
DDR2 (C-20)	R&D	AF2538	1:400 1:250	Human TMA IF
DDR1 (D16G) XP	Cell Signaling Technologies	5583	1:1000	Western Blot
DDR2	Cell Signaling Technologies	12133	1:1000	Western Blot
Collagen1a	BioRad	21501410	1:1000	Western Blot
GAPDH	Cell Signaling Technologies	2118	1:2500	Western Blot
Synaptophysin	Sigma	336R-95	1:500	IF

Results

3.1.) DDR2 is Expressed in Both Tumor Cells and the Stroma in Human PDA

The expression and function of DDR2 in pancreatic disease is unknown. To determine the expression and clinical relevance of DDR2 in PDA, I performed IHC on PDA human tissue microarrays (TMA) for DDR2. DDR2 was highly expressed in both the neoplastic lesions and stromal cells of human PDA tumors (Fig.3.1A). DDR2 was also expressed in the human PDA cell lines BxPC3, MiaPaca-2, and Panc-1, for which MiaPaca-2 and Panc-1 are known to exhibit mesenchymal, invasive properties (Fig.3.1B)[29]. To further characterize the expression and activation of DDR2, I analyzed human PDA and fibroblasts cell lines as well as a murine line of PDA after stimulation with soluble collagen. DDR2 expression was detected in the human primary cell line UM5, human cancer associated fibroblasts (CAF), and human pancreatic stellate cells (PSC). DDR2 was also detected in the murine *KPC* line, in which mice harbor both oncogenic $Kras^{G12D}$ and mutant $p53^{R172H}$ to recapitulate the events of tumor progression and metastasis, making it a relevant model to study the functional role of DDR2 for future studies. MiaPaCa-2 lysates were used as a control for DDR2 expression. Of note, Panc-1 did not express DDR2 as it did in Fig3.1B, which may attribute to the characteristic feature of Panc-1 cells to alternate their identity between an epithelial and mesenchymal phenotype. Together, these results establish the expression of DDR2 in multiple human PDA and fibroblasts samples as well as murine PDA lines that can be used to target DDR2 in pancreatic cancer.

3.2) DDR2 is Associated with the Transitional Events of ADM and EMT

DDR2 expression is found primarily in mesenchymal cell types such as fibroblasts[57, 59]. However, DDR2 was found in both neoplasia and stromal cells in human TMA samples of PDA, suggesting DDR2 may play a role in transdifferentiation events of acinar-ductal-metaplasia (ADM) and/or epithelial-to-mesenchymal transition (EMT). To determine if DDR2 is associated with ADM, I isolated primary acinar cells harboring the *Kras*^{G12D} knock-in allele and infected them with adenovirus Cre-GFP to activate Kras and thereby promoting ADM *ex vivo*. Primary acinar cell explants were then harvested on days 1, 2, and 3-post isolation and analyzed by RNA-seq. Gene Set Enrichment Analysis (GSEA) found that Kras-induced ADM resembles an EMT programming where N-cadherin, Snail, and Zeb2 were among several upregulated mesenchymal gene transcripts in ADM (Fig.3.2A). DDR2 was also found to have a significant 3-fold upregulation ($p<0.001$) (Fig.3.2A). Observations from pancreatic cancer cell lines that express DDR2 support the data that DDR2 is associated with an EMT signature. RT-PCR shows that MiaPaCa-2, which holds the highest DDR2 expression, correlates with reported EMT markers such as Lox2, Snail1, and Zeb1 with a loss in the epithelial marker E-cadherin (Fig.3.2B). BxPC3 and Panc-1 have similar expression patterns with expression of E-cadherin and N-cadherin as well as Lox2, Snail1, and Zeb1 (Fig3.2B).

To determine the presence of DDR2 in ADM *in vivo*, I used the neoplastic *KC* mouse model (described in Chapter 2) with the addition of *Rosa*$^{LSL\text{-}YFP}$ to track the source of DDR2+ cells. Immunofluorescence (IF) of DDR2 detected DDR2+ cells within YFP+ ADM and neoplasia (Fig.3.2C). Furthermore, DDR2+; YFP+ cells were

also detected in the aggressive *KPCY* model of PDA (described in Chapter 2) (Fig.3.2C). Collectively, these results suggest DDR2 may facilitate the processes of ADM and EMT that is highlighted by a subpopulation of tumor cells with metastatic potential.

3.3.) Lineage Tracing Confirms Metastatic Potential of DDR2 Positive Cells

The presence of DDR2+ cells in ADM and neoplasia in the *KCY* and *KPCY* models are reminiscent of the DDR2 expression established in neoplastic lesions in human PDA. However, the source of these DDR2+ cells, which are usually associated with mesenchymal cell types, in tumor lesions is unknown. To define the origin of DDR2+ tumor cells, I utilized the $Kras^{LSL\text{-}G12D/+}$; $Ptf1a^{CreERTM/+}$; $ROSA^{LSL\text{-}YFP}$ *(KCert; YFP)* conditional mouse model of neoplasia. *Ptf1a* is expressed in pancreatic progenitor cells during development, which leads to recombination in all pancreatic cell types when Cre is driven by *Ptf1a* during embryogenesis. The *KCert; YFP* model addresses this issue by activating oncogenic *Kras* after mice are treated with tamoxifen as adults (8-weeks old) to induce recombination specifically in adult acinar cells. The YFP tracer helps to define acinar cells that have undergone recombination and can be used to co-stain for additional markers such as DDR2 to determine if they are derived from an acinar origin. Using the *KCert; YFP* model, I found DDR2 is expressed in a small subset of recombined acinar cells associated with ADM and neoplastic lesions, that may acquire EMT and metastatic properties in the presence of activated *Kras* (Fig3.3A).

A feature I observed with the DDR2+ tumor cells in both human and murine models of PDA was the “needle-nose” phenotype that is reminiscent of Synaptophysin+ (SYP) cells, a marker of neuroendocrine cells (Fig.3.3A, B). Cell plasticity and the presence of SYP+ cells in neoplastic lesions of pancreatic cancer is facilitated by MYC oncogene and correlates with a shortened disease-free survival[108]. Based on the evidence that DDR2 is detected in acinar-derived tumor cells implies DDR2 contributes to cell plasticity and may be associated with Synaptophysin. To test if DDR2 and Synaptophysin are co-expressed, I stained *KCert; YFP* tissue for both markers. Lineage tracing confirms DDR2+; SYP+ cells (yellow arrow) comprise a subpopulation of acinar-derived tumor cells (Fig.3.3C). I also detected DDR2+; SYN+ that were not YFP+ adjacent to neoplastic lesions (red arrow). Additionally, not every SYP+ cell expressed DDR2 (white arrow). While these studies outline the expression of DDR2, the functional role of DDR2+ tumor and stromal cells is yet to be determined in pancreatic disease. Model systems that genetically or pharmacologically inhibit DDR2 will help further determine the contribution of DDR2 in the progression of PDA.

Works in Progress

3.4) Mouse Models to Study the Functional Role of DDR2 in the Progression and Metastasis of PDA

High levels of collagen and fibrosis is a distinctive feature throughout the development of PDA that is associated with a poor prognosis and therapeutic resistance[14]. DDR2 is an RTK activated by fibrillar collagen that I have discovered is upregulated in human and murine models of PDA. However, the functional role of DDR2 has not been explored in the pathogenesis of pancreatic disease. This is partially a consequence of limited mouse models available to study the potential functional role of DDR2 in pathological conditions. To address this issue, *Corsa et al*. generated the first conditional DDR2-knockout model in 2016[67]. In this model, exon 8 of DDR2 is flanked by loxP sites (*DDR2$^{fl/fl}$*) and with the expression of Cre recombinase will recombine and render the gene non-functional denoted as "*DDR2$^{d/d}$*"[67]. Mice that are not flanked by loxP sites and have functional expression of DDR2 are denoted as "*DDR2$^{w/w}$*". The Td-Tomato reporter gene was inserted into the Rosa locus as a lineage marker to indicate recombination (*Rosa$^{LSL\text{-}Tdt}$*)[67]. Utilizing this novel mouse model, I have begun to breed them into our models of pancreatic tumorigenesis and metastatic PDA.

i.) The Role of DDR2 at the Onset and Progression of PDA

DDR2 is expressed in mesenchymal cell types, but my preliminary data shows that DDR2 is upregulated in acinar-derived Kras-induced ADM, a partial EMT event, suggesting DDR2 contributes to the transitional, morphological events that promote

tumor transformation[57]. To study the significance of DDR2 in the pancreatic epithelium at the onset of tumorigenesis, I crossed *DDR2$^{fl/fl}$; Rosa$^{LSL\text{-}Tdt}$* mice into the *KC* model to generate *DDR2$^{d/d}$; KCT* mice (Fig.3.4A). In this case, *Ptf1a* regulatory regions drive Cre recombinase and DDR2 is ablated in the pancreatic epithelium to define the influence of DDR2 in neoplastic transformation. I have allowed mice to age to 6 and 12 months in both *DDR2$^{w/w}$; KCT* and *DDR2$^{d/d}$; KCT* colonies. Using pancreas mass/body weight (PM/BW) ratios as measure of tumor progression, *DDR2$^{d/d}$; KCT* at 6 months have slightly higher ratios compared to controls (Fig. 3.4B). At 12 months, PM/BW ratios are significantly higher in *DDR2$^{d/d}$; KCT* mice compared to controls indicating increased tumor burden when DDR2 is ablated from the pancreatic epithelium during tumorigenesis (Fig. 3.4B). However, more mice are necessary to determine any significant differences in tumor growth, transformation, proliferation, cell death, and fibrosis.

DDR2+ cells in the neoplastic lesions of lineage-traced disseminated tumor cells in the *KPCY* model indicate DDR2 may play a role in metastasis. To perform a more robust analysis of the role of DDR2 in PDA progression and metastasis, *DDR2$^{fl/fl}$; Rosa$^{LSL\text{-}Tdt}$* were crossed into the aggressive *KPC* model of PDA to generate *DDR2$^{d/d}$; KPCT* (Fig.3.4C). Generation of *DDR2$^{w/w}$; KPCT* were used as controls. Mice from both cohorts are aging until moribund. Unfortunately, some mice were taken down before endpoint due to events outside of cancer. The 1/1 control mouse was taken down at 18 weeks due to a prolapsed penis. 1/5 *DDR2$^{d/d}$; KPCT* mice was taken down due to hind-leg paralysis. The remaining 4/5 mice were aged to endpoint. Pancreas weights were also recorded, but with only (1) control from the *DDR2$^{d/d}$; KPCT* colony, it

is difficult to determine if DDR2 ablation from the pancreatic epithelium during tumor progression confers a survival advantage or not as well as inhibits tumor growth. Although not ideal nor accurate, I compared *DDR2$^{d/d}$; KPCT* to *KPC* controls from Chapter 2 as an arbitrary method to observe survival in these mice and I found *DDR2$^{d/d}$; KPCT* do not have a survival advantage. On average, *DDR2$^{d/d}$; KPCT* mice are moribund at 4 months compared to 6-8 months in the *KPC* colony. Additionally, I compared pancreas weights of *KPC* mice to *DDR2$^{d/d}$; KPCT* and found that pancreata averaged at about 1(g) in *DDR2$^{d/d}$; KPCT.* This average is significantly lower compared to the *KPC* colony that had an average mass of 4(g). Again, this is not an accurate comparison due to differences in strain, background and colonies of mice. Further analyses and proper controls from the *DDR2$^{d/d}$; KPCT* colony are necessary to make any additional conclusions. Collectively, the results from these studies will define the role of DDR2 at the onset of tumorigenesis as well as the influence of DDR2 during metastasis of PDA.

ii.) <u>Determining the Role of DDR2 in Tumor Cells and the Stromal Compartment of PDA</u>.

Genetic ablation of DDR2 in the *KC* and *KPC* models only addresses the relation of DDR2 in the pancreatic epithelium, however, DDR2 expression is found in mesenchymal cell types during development and disease[57, 59]. To determine the role of DDR2 in both the epithelium and stroma of PDA, collectively, I crossed *DDR2$^{fl/fl}$* mice into the dual recombinase system of global *β-actin^{CreERT2}* to conditionally knockout DDR2 and the *Kras$^{FSF\text{-}G12D/+}$; Ptf1a$^{Flpo/+}$ (KF)* to induce tumorigenesis and *Kras$^{FSF\text{-}G12D/+}$;*

Trp53$^{Frt/+}$*; Ptf1a*$^{Flpo/+}$ *(KPF)* for studies in metastasis. In this system, flippase (FlpO) is driven by the pancreas specific promoter *Ptf1a* to recombine the FRT sites flanking oncogenic Kras and/or loss-of-function (LOF) *Trp53 (Frt-Stop-Frt Kras*$^{G12D/+}$*; Frt-p53-Frt; Flpo*$^{Cre/+}$*)*[36]. Activation of *Kras* and LOF *Trp53* allele by FlpO can then allow for the conditional, ubiquitous knockout of DDR2 in the epithelium and stroma with *β-actin*^{CreERT2}.

Using the dual-recombinase system, I have begun to investigate the role of DDR2 in the pancreatitis-induced model of tumorigenesis. *DDR2*$^{fl/fl}$*; β-actin*^{CreERT2} mice were crossed into the *Kras*$^{FSF-G12D/+}$*; Ptf1a*$^{Flpo/+}$ background to produce *DDR2*$^{d/d}$*; KFβ*$^{ERT/+}$ mice (Fig.3.4A). *DDR2*$^{w/w}$*; KFβ*$^{ERT/+}$ were used as controls. Mice were treated with tamoxifen once daily, for 5 consecutive days at 8 weeks of age to induce recombination, ubiquitously depleting DDR2 as mice undergo tumorigenesis. After tamoxifen treatment, mice were then treated with 5 daily doses of cerulein to promote tumorigenesis to study the significance of DDR2 during tumorigenesis and will be taken down at 1, 4, and 6 weeks post-cerulein (Fig.3.4B). (2) controls and (3) *DDR2*$^{d/d}$*; KFβ*$^{ERT/+}$ mice have been sacrificed at the 4-week timepoint. Pancreas mass/body weight ratios were used as a measure of tumor transformation, in which *DDR2*$^{d/d}$*; KFβ*$^{ERT/+}$ mice had lower ratios compared to controls (Fig.3.4C). However, more mice are being allowed to progress to the additional timepoints to establish the role of DDR2 at the onset of tumorigenesis. Additionally, *DDR2*$^{d/d}$*; KFβ*$^{ERT/+}$ and controls are also being aged to develop spontaneous tumors in the absence of DDR2.

PDA is characterized by a collagen-dense fibrotic response that influences tumor metastasis and is natural source of DDR2 ligand activation. To study the role of

DDR2 in PDA progression and metastasis, I crossed *DDR2$^{fl/fl}$; β$^{ERT/+}$* mice into the *KPF* background (*DDR2$^{fl/fl}$; KPFβ)* (Fig.3.4D). *DDR2$^{w/w}$; KPFβ* used as controls. *KPF* mice are equivalent to the *KPC* model in which tumors and subsequent metastasis typically form between 4-6 months of age. In the *DDR2$^{fl/fl}$; KPFβ* model, mice were treated with tamoxifen at 8-10weeks of age, once daily for 5 consecutive days to genetically ablate DDR2 before metastasis occurs. A number of controls and *DDR2$^{fl/fl}$; KPFβ* have been sacrificed at endpoint when mice appeared moribund. DDR2 ablation did not reduce tumor size, but *DDR2$^{fl/fl}$; KPFβ* did not develop macro metastases, with the exception of (1) mouse (Fig.3.4E). Similar to the *KPC* model, (3) *DDR2$^{fl/fl}$; KPFβ* mice developed hind limb paralysis, an independent morbidity factor that occasionally occurs in *Ptf1a* driven recombinase model due to brain and spinal tumor development (unpublished data). (2) *DDR2$^{fl/fl}$; KPFβ* mice presented with distended abdomens, a common feature observed during metastatic disease. However, at necropsy the distention was due to large fluid filled cyst and not tumor burden. Additionally, (3) *DDR2$^{fl/fl}$; KPFβ* mice were found dead on arrival making it difficult to determine the cause of death. Although not ideal, a Kaplan-Meier curve provides results that indicate DDR2 plays a role in PDA progression, however, the functional role of DDR2 in tumor progression is unclear (Figure 3.4F). Further studies using these models are necessary to determine the contribution of DDR2 in PDA progression and metastasis.

3.5 Miscellaneous Data

i.) Attempted Focus at Generating a Conditional-DDR2 knockout Mouse

Before the advent of conditional DDR2-knockout mice we had tried to develop our own conditional DDR2 knockout mouse at the University of Michigan through the use of Crispr-CAS9 technology. Unfortunately, this method of genomic manipulation by knocking in loxP sites in murine models proved to be difficult to validate due to non-specific targets. While this experiment did not come to fruition, it did serve as a valuable learning experience for the cautions of new technologies and also helped expand my skills in genomics.

ii.) Studying the Role of DDR2 in Cerulein-induced Pancreatitis

A distinct feature of pancreatitis is the collagen-dense fibrotic response[7, 9]. Pancreatitis is often an irreversible, persistent injury that can activate wound healing processes[9]. DDR2 is expressed in mesenchymal cells of the stroma and is known to play a physiological role in wound healing processes[59]. Additionally, in my studies of pancreatitis in DDR1 proficient and DDR1-null animals (Chapter 2), DDR2 expression was elevated during tissue recovery from cerulein-induced pancreatitis. To determine if DDR2 plays a role in pancreatitis, I treated 8-week old *DDR2$^{fl/fl}$; β-actin^{CreERT2}* and *DDR2$^{w/w}$; β-actin^{CreERT2}* mice with tamoxifen for 5 days to allow for efficient recombination to knockout DDR2. Mice were then treated with cerulein twice daily for 2 consecutive weeks and left to recover at 1, 3, and 5 days post-cerulein, the same protocol from Chapter 2 Fig.2.7A. Pancreas mass to body weight measurements were used to define tissue recovery, which in untreated animals stands at ~1%. Following

cerulein treatment these ratios do decrease, however, there was no significant difference between controls and *DDR2$^{fl/fl}$; β-actin^{CreERT2}* treated animals (Fig.3.5A). Histological examination by H&E did not show any differences in injury or recovery (Fig.3.5A). Analysis of Ki67 (proliferation), CC3 (apoptosis), and picrosirius staining (fibrosis) by IHC also did not reveal any significant differences (data not shown). Additionally, immunoblot analysis shows DDR2 is efficiently knocked-out of the pancreas with lower expression of DDR1 compared to controls (Fig.3.5B). However, further analysis of downstream targets of DDR2, and additional staining and biological replicates are is necessary to conclude a role for DDR2 during pancreatic injury.

Discussion and Future Directions

Metastasis is the primary cause of death in many cancers, including PDA[103, 104]. The overproduction of collagen and extensive ECM remodeling in PDA promotes an aggressive, metastatic environment that is refractory to surgical options and current cytotoxic agents[15]. Rhim *et al*. found that lineage-traced tumor cells with an EMT phenotype disseminate to surrounding tissues and are detected prior to the progression of pancreatic cancer[105]. This potentially helps to explain the high recurrence rate of PDA for patients that are rarely diagnosed and treated at early stages. Extensive efforts have established the genetic culprits that initiate and influence the development of PDA, however, details of the actual molecular events between the stroma and tumor cells that permit metastasis are not well-defined. Therefore, defining the molecular mechanisms that promote invasion and metastases is imperative in understanding the aggressive nature of PDA with potential therapeutic targets to improve patient outcome.

DDR2 is a receptor tyrosine kinase (RTK) activated by fibrillar collagen to regulate the properties of cell proliferation, adhesion, and migration in physiological conditions[57, 59]. The functional roles of DDR2 in pathological conditions are largely unknown, however, it has recently been explored in various cancers. Studies in breast cancer have shown that DDR2 stabilizes Snail1, a transcription factor necessary for EMT, that promotes invasion and migration *in vitro* as well as metastasis in orthotopic mouse models[68]. A more recent study utilizing the conditional DDR2 knockout mouse in the aggressive MMTV-PyMT model of mammary gland cancer shows that ubiquitous DDR2 ablation does not prevent primary tumor formation, but reduces metastasis[35, 67].

In a separate, yet related study, stromal DDR2 was found to facilitate the mechano-transduction of tumor stiffness and metastasis in MMTV-PyMT mice[109]. Mutations in DDR2 have also been detected in both lung adenocarcinoma and squamous cell carcinoma that are currently being investigated as potential therapeutic targets[78, 107]. Despite the new research of DDR2 in cancer, the expression and role of DDR2 in PDA, where the overproduction of collagen can serve as an abundant source of DDR2 activation that can contribute to tumor progression, is unknown.

In this study I reveal the expression patterns of DDR2 in both human and murine models of PDA. As expected, DDR2 was expressed in the stromal cells throughout PDA progression. I also observed DDR2+ tumor cells which was a consistent and unexpected feature in both human TMA and mouse PDA tissue. Furthermore, I established DDR2+ tumor cells often correspond to Synaptophysin+ neuroendocrine cells, which are associated with tumor cell plasticity and metastasis in PDA[108]. In line with cell plasticity and the existence of DDR2+ epithelial-derived tumor cells, I also explored the role of DDR2 during ADM, which is considered a partial EMT event. DDR2 was found to be significantly upregulated during ADM *in vitro* and was accompanied by the elevation of other EMT markers and collagen. Together these data support the previously published works that demonstrate the significance of DDR2 in EMT and cancer progression. Moreover, these data initiate a novel research angle to study and target a potential crosstalk of networks between tumor and stroma cells through the activities of DDR2 in PDA. Although the conclusions from these studies are incomplete, I have established multiple permutations of mouse models to study and

define the functional role of DDR2 at the onset, progression, and metastasis of PDA in both a cell specific and universal knockout manner for future experiments.

Figures

Figure 3.1

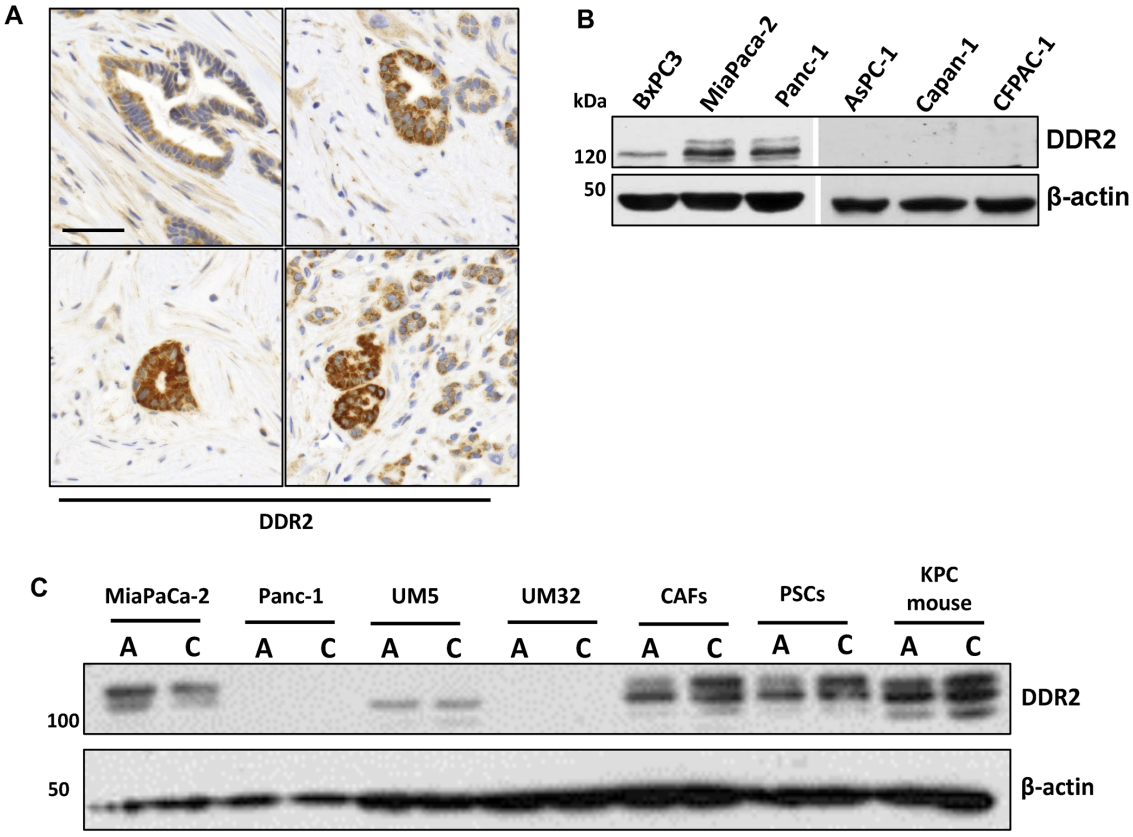

Figure 3.1. Expression of DDR2 in Human TMA and cell lines of PDA. A.) IHC of DDR2 expression in 4 different patients from a TMA. B.) Expression of DDR2 (~125kDa) in the human pancreatic cancer lines of BxpC3, MiaPaCa-2, and Panc-1. β-actin was used as a loading control C.) Human pancreatic cancer lines (MiaPaCa-2, Panc-1), primary human cell lines (UM5, UM32), human CAFs, human PSCs and murine KPC cells treated with soluble collagen. The presence of 3 separate bands indicates the 3 separate phosphorylation sites. Acetic acid was used as a control for collagen. β-actin was used as a loading control. Scale bar = 50μm

Figure 3.2

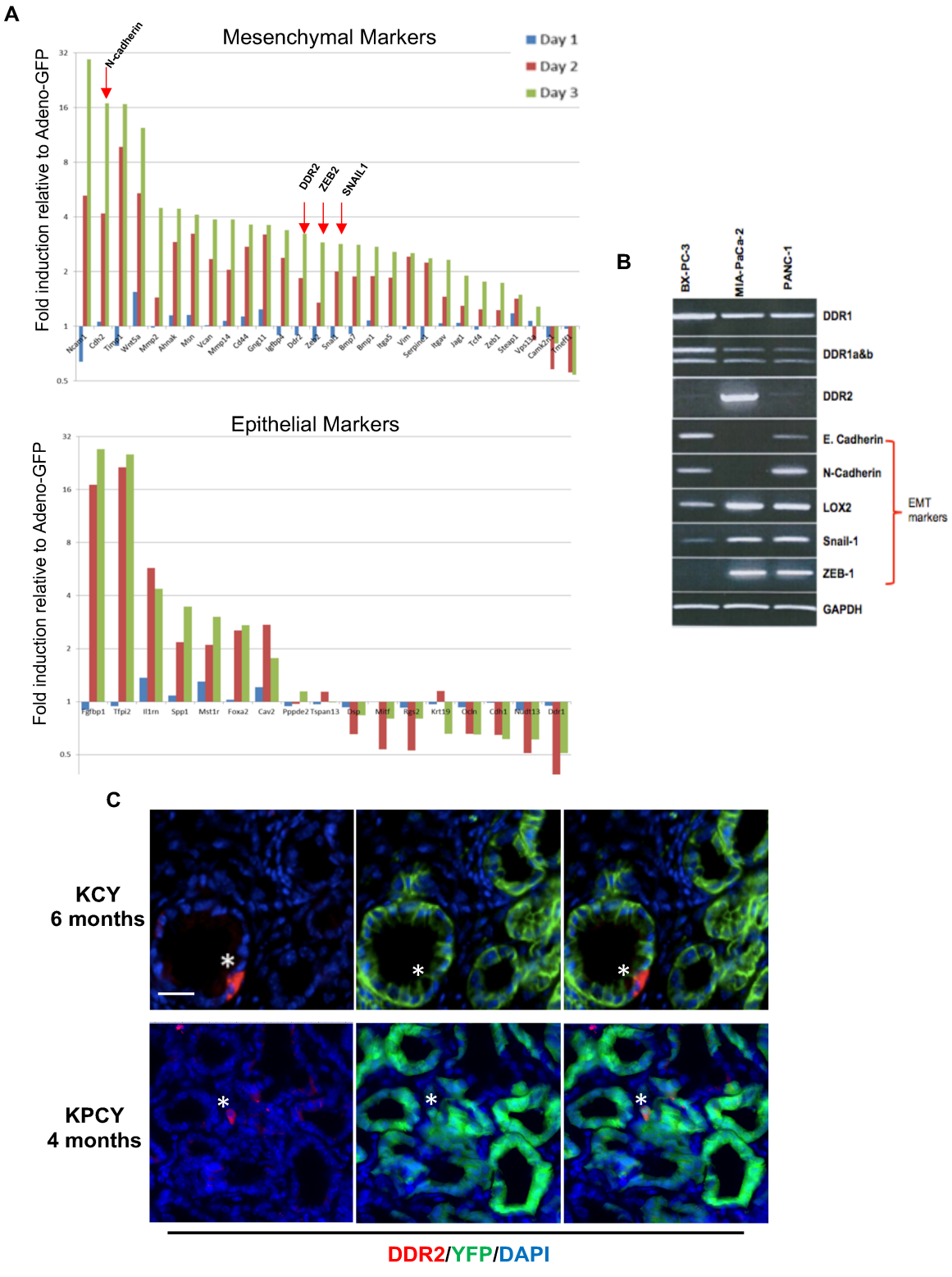
A
Mesenchymal Markers
Day 1
Day 2
Day 3
N-cadherin
DDR2
ZEB2
SNAIL1
Fold induction relative to Adeno-GFP
Epithelial Markers
Fold induction relative to Adeno-GFP
B
BX-PC-3
MIA-PaCa-2
PANC-1
DDR1
DDR1a&b
DDR2
E. Cadherin
N-Cadherin
LOX2
Snail-1
ZEB-1
GAPDH
EMT markers
C
KCY
6 months
KPCY
4 months
DDR2/YFP/DAPI

Figure 3.2. DDR2 is associated with ADM and EMT signatures of PDA. A.). DDR2 is upregulated in Kras-induced ADM in vitro. RNA-seq analyses was performed on acini harboring the inducible *Kras*$^{LSL\text{-}G12D/+}$ in its endogenous locus. Infecting cells with an adenovirus expressing Cre turned on KrasG12D results show ADM undergoes an EMT-like reprogramming signature. B.) RT-PCR from 3 PDA cell lines that express DDR2. DDR2 expression is associated with a partial EMT profile. C.) *KCY* mouse exhibits DDR2+ cells ADM lesion (red). DDR2+ cells (red) are found in more advanced neoplasia within the *KPCY* animal. DAPI (blue, nuclear stain) and YFP (green, lineage tracer). Scale bar =20μm

Figure 3.3

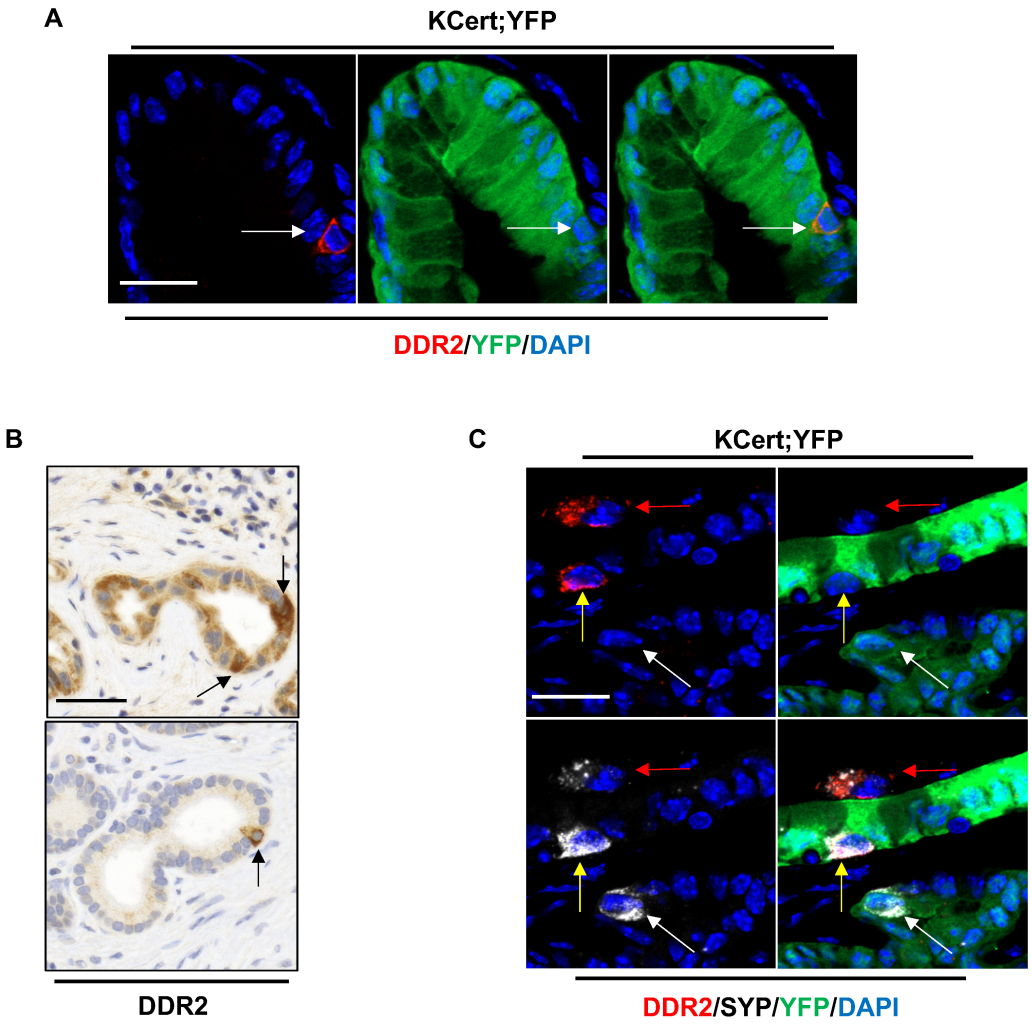

Figure 3.3. Metastatic potential of DDR2 positive cells. A.) *KCert; YFP* mouse presents with DDR2+ cell (red) with needle-nose phenotype in acinar-derived neoplastic lesion (white arrow) B.) Human TMA samples stained for DDR2. Arrow indicates DDR2+ cells that have needle-nose shape. C.) *KCert; YFP* mouse that shows triple positive cells for DDR2+; SYP+; YFP+ (yellow arrow), dual positive cells for DDR2+; SYP+ (red arrow), and SYP+; YFP+ cells (white arrow). Scale bars = 20μm (A), 50μm(B), 20μm (C).

Figure 3.4

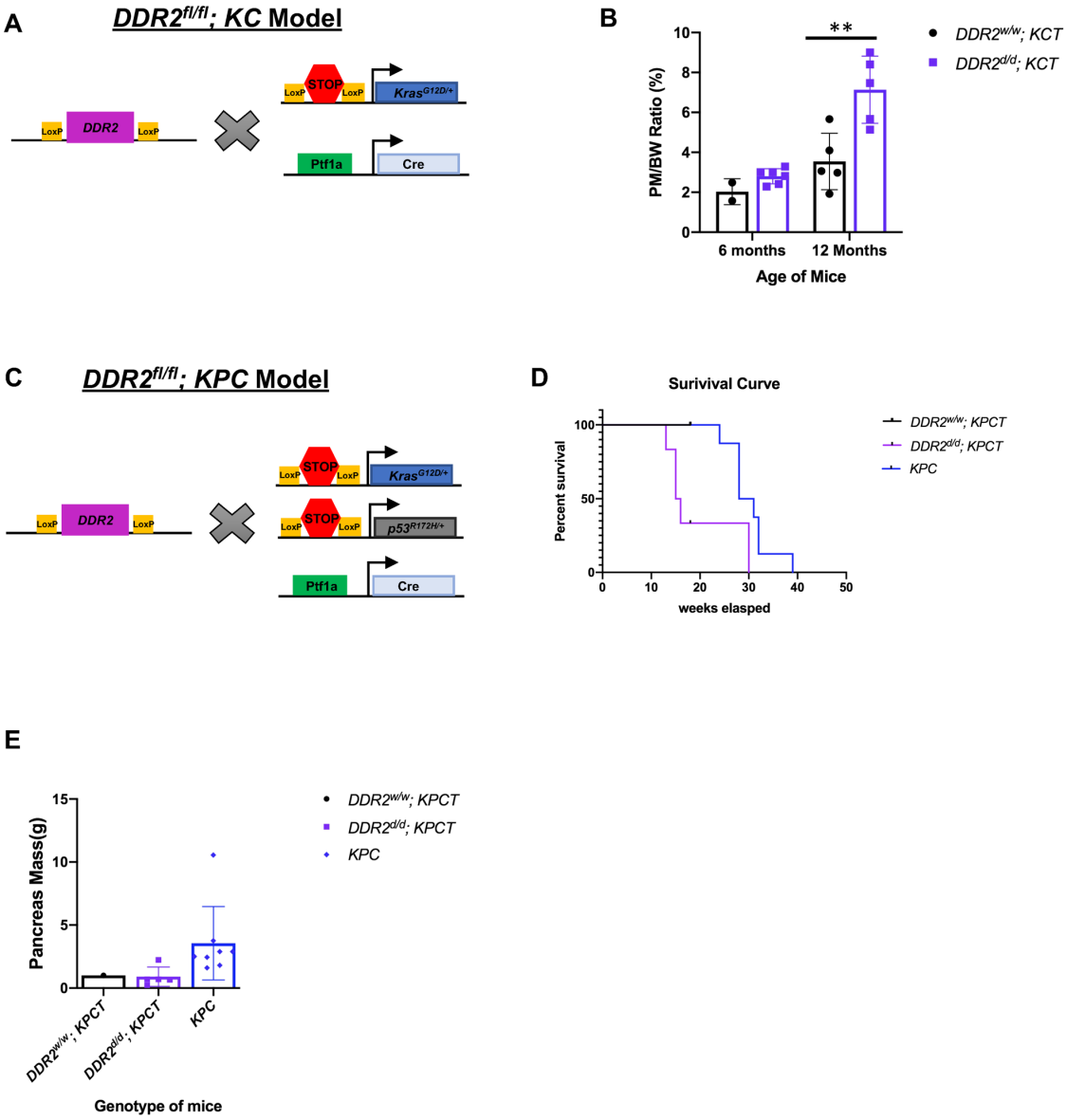

Figure 3.4.) Examining the role of DDR2 in neoplasia and PDA progression. A.) Schematic of DDR2 conditional knockout mouse crossed into the *KC* model B.) Pancreas mass to body weight (PM/BW) ratios of control and *DDR2$^{d/d}$; KC* animals at 6 and 12 months. C.) Schematic of DDR2 conditional knockout mouse crossed into the *KPC.* D.) Kaplan-Meier curve of controls and *DDR2$^{d/d}$; KPC* mice. *KPC* mice (blue) from DDR1 colony were used as a reference. E.) Pancreas mass to body weight (PM/BW) ratios of control and *DDR2$^{d/d}$; KPC* animals. *KPC* mice (blue) from DDR1 colony were used as a reference.

Figure 3.5

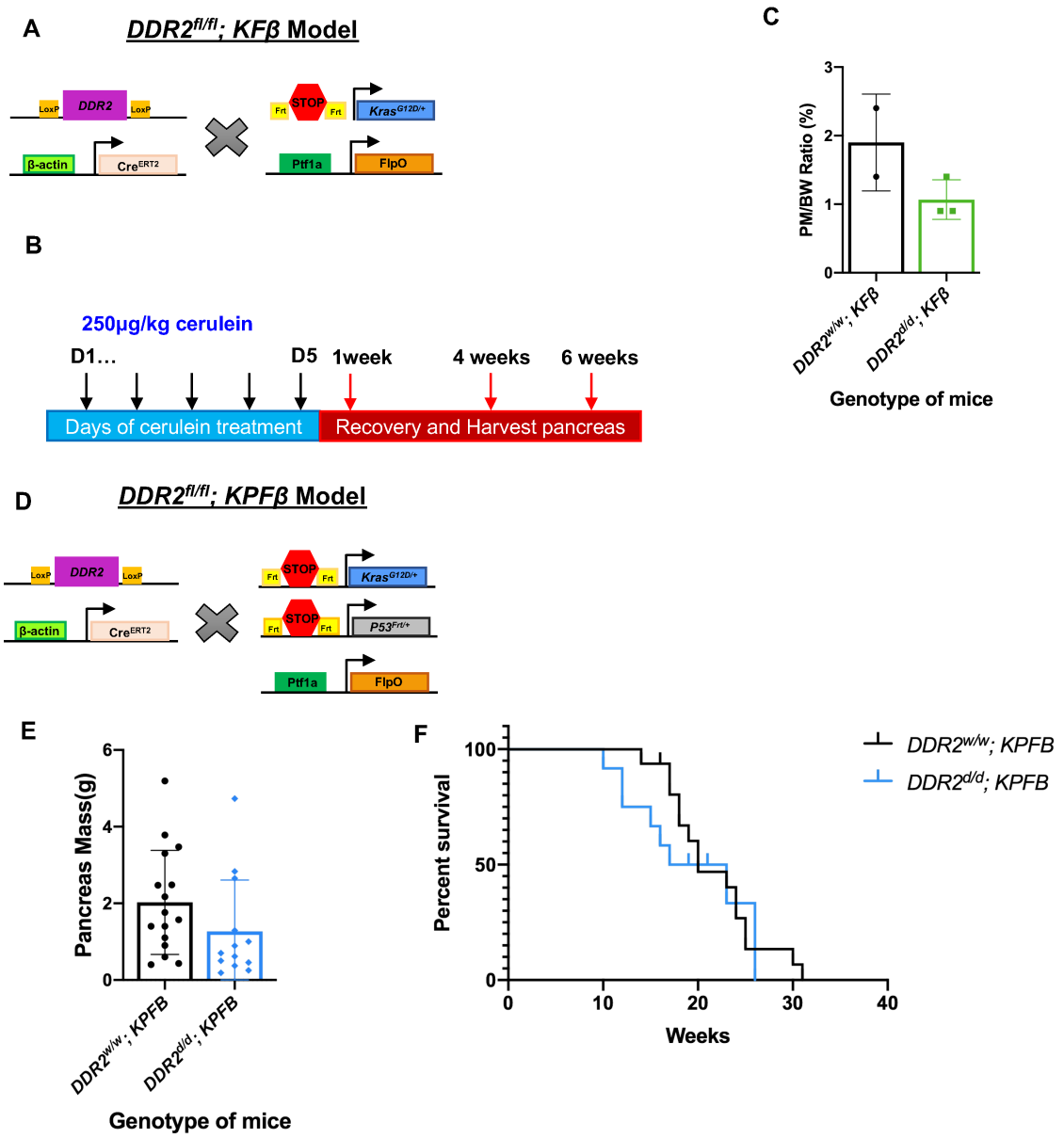

3.5 Determining the role of DDR2 in tumor cells and the stromal compartment of PDA. A.) Schematic of DDR2 conditional knockout mouse and *β-actinCre^{ERT2}* crossed into the *KF* model. B.) Schematic of cerulein-induced tumorigenesis. C.) PM/BW ratios of control and *DDR2$^{d/d}$; KFβ* mice after 5 days Tamoxifen, 5 days cerulein, the 4 weeks post-cerulein treatment. D.) Schematic of DDR2 conditional knockout mouse and *β-actin Cre^{ERT2}* crossed into the *KPF* model. E.) Pancreas mass in grams of control and *DDR2$^{d/d}$; KPFβ* mice. F.). Kaplan-Meier curve of controls and *DDR2$^{d/d}$; KPFβ* mice after 5 days of Tamoxifen and allowing to age until moribund. Vertical lines represent censored animals.

Figure 3.6

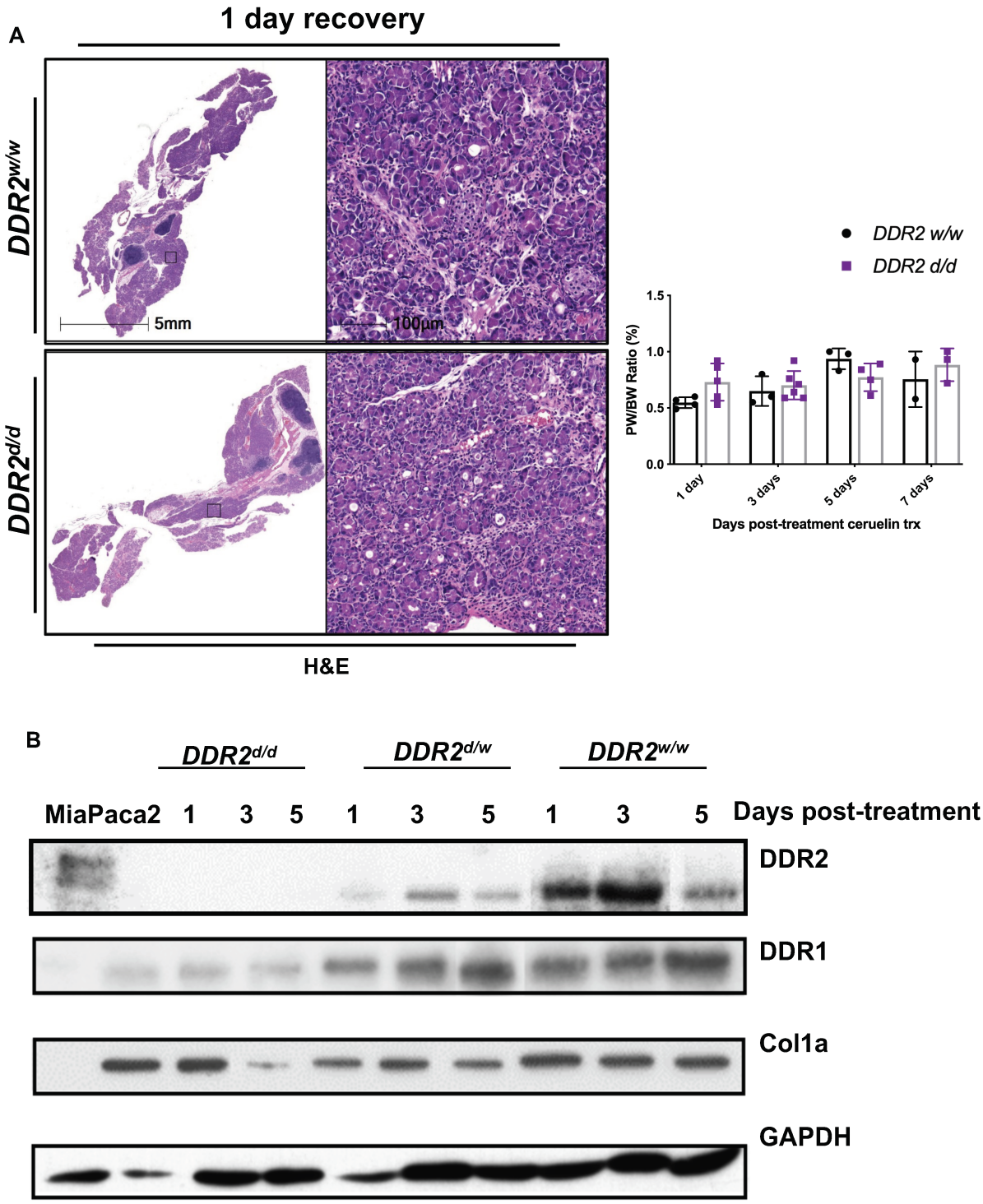
A
1 day recovery
DDR2w/w
DDR2d/d
5mm
100µm
H&E
DDR2 w/w
DDR2 d/d
PW/BW Ratio (%)
1.5
1.0
0.5
0.0
1 day
3 days
5 days
7 days
Days post-treatment ceruelin trx
B
DDR2d/d
DDR2d/w
DDR2w/w
MiaPaca2
1
3
5
1
3
5
1
3
5
Days post-treatment
DDR2
DDR1
Col1a
GAPDH

Figure 3.6. Testing the role of DDR2 in cerulein-induced pancreatitis. A.) H&E staining for cerulein treated, 1-day recovery *DDR2*$^{w/w}$ *and DDR2*$^{d/d}$ mice (left). PM/BW ratios of cerulein treated mice at 1,3,5,7 days cerulein (right). B.) Immunoblot analysis of cerulein treated mice for *DDR2*$^{w/w}$*, DDR2*$^{d.w}$*and DDR2*$^{d/d}$ whole tissue lysates. GAPDH was used as a loading control. MiaPaCa-2 was used a control for DDR2 expression.

Chapter 4: Discussion and Future Directions

4.1 Discussion

The first reported microscopic diagnosis of pancreatic ductal adenocarcinoma (PDA) was made in 1858 by Jacob Mende Da Costa[110]. Since then, we have made significant progress in the histological classification and awareness of pancreatic cancer, but have had minimal success in preventing and treating PDA. Currently, PDA stands as the third leading cause of cancer deaths and is projected to become the second leading cause by 2030[111]. This is largely due to a majority of patients diagnosed at metastatic stages when surgical and chemotherapeutic options are ineffective[104]. The lack of clinical presenting symptoms, early detection methods and targeted therapeutic options remain a challenge in preventing and treating PDA at earlier stages. However, recent advancements in genomic technologies, imaging techniques, and preclinical models have greatly expanded the repertoire of methods to study PDA in the field and exposed a multidisciplinary approach in combatting this deadly disease.

4.2 Emerging Concepts and Methods to Define Tumor Heterogeneity in PDA

Outlining and characterizing the genetic landscape of cancer is a critical component in precision medicine. In PDA, the roadmap of genes that drive the initiation and progression of tumors in a majority of patients are mutations found in *KRAS, p16(CDKN2A), TP53, and SMAD4(DPC4)*[112]. Almost 90% of PDA cases are driven by an acquired somatic *KRAS* mutation[20, 112]. Mutant *KRAS* is found at the onset of tumorigenesis and induces morphological changes to the epithelium resulting in acinar-ductal metaplasia (ADM)[83, 84]. Over an extended period of time, the tissue architecture changes as the pancreatic epithelium progresses from benign ADM lesions to pancreatic intraepithelial neoplasia (PanIN). These morphological changes are accompanied by sequential loss-of-function mutations in tumor suppressor genes *p16*, followed by *TP53*, and lastly *SMAD4* (Fig4.1A)[112].

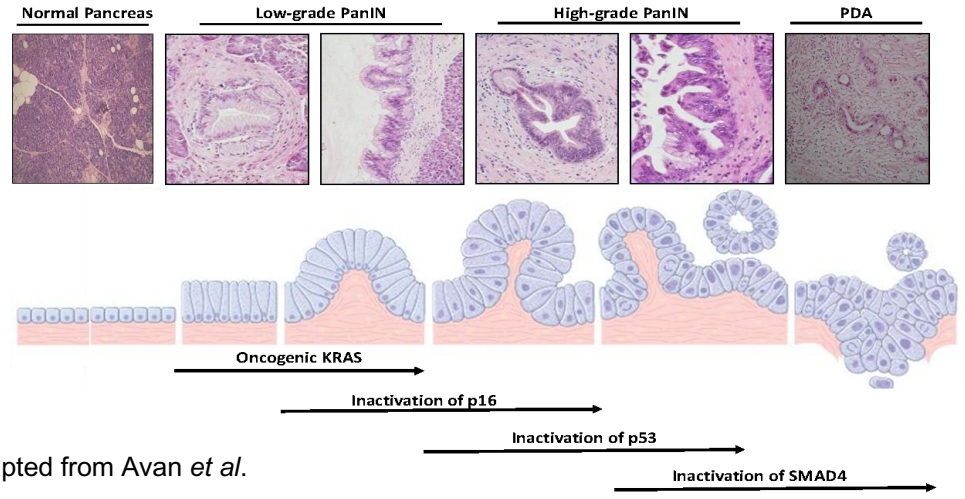

Adapted from Avan *et al*.

Figure 4.2 Progression of PDA. During the progression of PDA, the pancreas acquires a succession of somatic mutations. *KRAS* mutations are detected during the earliest stages in acinar cells and ADM. Mutations in *p16* are found in early stage PanINs. As PDA progresses, *TP53* mutants can be found in early to late stage PanIN lesion and *SMAD4* mutants are indicated at late stage to invasive PDA.

The discovery and verification of these driver genes in pancreatic cancer have served as a benefit for modeling PDA in preclinical models. With *KRAS* as the dominant driver mutation in PDA, most animal models are based on $Kras^{G12D}$. In 2003, the achievement of oncogenic *Kras* in mice recapitulated the early events of ADM and neoplasia with a gradual increase in stromal content[34]. These early transitional processes are often not observed in PDA patient samples due to the late presentation of disease and can help define the molecular events that contribute to the progression of PDA. For a more robust study of metastatic disease, mice were engineered to carry mutant $Trp53^{R172H/+}$ along with oncogenic *Kras*[89]. Generation of these models have advanced our understanding of the molecular and histological events of the tumor biology; however, preclinical models do not always translate to clinical applications and patient outcome remains at a dismal 10% 5-year survival [81]. Therefore, a multidisciplinary approach is necessary to define, classify, and “know thy enemy” to improve patient outcome.

The pathogenesis of PDA is more complex than a succession of acquired driver mutations. Further exploration into the integrated genomics, transcriptomics, and proteomics have revealed detailed epigenetic and genetic alterations within the tumor and stromal cells of patients. These extensive and elegant studies have been carried out by several groups to classify PDA into different subgroups to provide a guide in precision medicine based on the genomic landscape of a patient. Each group has built upon the previous in characterizing the subtypes of the tumor cells and stroma based on unbiased, gene transcript profiling from patient RNA of PDA tumors. In an attempt to unify the nomenclature and the overlapping classifications of PDA, Collison *et al*.

recently proposed 2 main categories based on the presence and loss of epigenetic marks that represent the status of pancreatic identity: Squamous and Classical-Pancreatic[22]. Branching out from these 2 main categories of PDA, patient tumors can be sub-divided based on the classifications from previous studies performed by Moffit *et al.,* Collison *et al*., Bailey *et al*., and Puleo *et al*[20, 23, 113, 114]. Unification of the different classifications of PDA specifies a starting point for clinical diagnosis and highlights the power of high-throughput studies that can be used to streamline results for clinical applications.

In addition to the classification methods provided by bulk sequencing analyses these studies also emphasize the heterogeneity of cells present within a tumor which adds to the difficulty in treating PDA. Histopathological studies suggest heterogenous populations of cancer cells, fibroblasts, and immune cells based on protein expression patterns. An example of tumor heterogeneity can be found from my own findings, in which there was heterogeneity among DDR2+ cells. A subset of DDR2+ cells co-localized with SYP+ cells, another subset was derived from the acinar-lineage, and others were found to be single stained for DDR2 in the stroma. Furthermore, DDR1 expression in the *KC* and *KPC* mouse models showed some, not all, ADM and neoplastic lesions expressed DDR1 adding to the concept of tumor heterogeneity throughout the development of PDA. A more comprehensive example in defining the tumor heterogeneity comes from Ölund *et al.* that used histological, bulk sequencing (GSEA and RNAseq), and functional methods to characterize the different fibroblast populations present from metastatic *KPC* animals. In this study, they reported 2 subpopulations of fibroblasts: myofibroblast cancer-associated fibroblasts (myCAFs,

express high levels of α-smooth muscle actin) and inflammatory cancer-associated fibroblasts (iCAFs, express high levels of IL-6). These findings add a possible explanation to the conflicting results reported in targeting cancer-associated fibroblasts [47, 50, 51]. These approaches may have targeted only one population of fibroblasts leaving the other populations to maintain or promote tumor growth. Additionally, this study verified the heterogeneity among fibroblasts populations that can be used for further identification of other fibroblasts subpopulations as well as a guide to the success of targeted therapies in the stroma.

In line with classification techniques, single-cell modalities have been used to define the tumor heterogeneity of PDA. Two relatively new techniques used to characterize tumor heterogeneity in both preclinical and human PDA samples are, mass cytometry by time of flight (CyTOF) and single-cell RNAseq. CyTOF combines the concepts of mass spectrometry and flow cytometry to perform a more accurate analysis in characterizing cell surface markers[115]. The main principle of CyTOF is to label single-cell suspension samples with antibodies conjugated to chelating groups that can bind to purified, stable heavy metal isotopes[115]. This allows for cells to be distinguished by distinct metal isotopes instead of broad-spectrum fluorophores for more cell specific parameters. Another advantage of CyTOF is the ability to incorporate up to 40 antibodies at a single-cell resolution[115]. With this technology, we can capture the identity and function of individual cells in a tumor and then group them according to the expression of cell surface markers to define a more personalized method of characterizing and treating PDA.

Single-cell RNA sequencing (scRNA-seq) is another single-cell modality to determine the complex gene expression patterns of rare, individual cells[30]. This allows for more detailed information of the intratumoral, heterogenous populations in a tumor for a better classification and understanding of the tumor biology. For example, Hosein *et al.* performed scRNA-seq on 3 different PDA metastatic mouse models, *KPC* (defined in chapter 2 and 3), *KPfC (Kras$^{LSL\text{-}G12D/+}$; Tpr53$^{fl/fl}$; Pdx1$^{Cre/+}$)* and KIC (*Kras$^{LSL\text{-}G12D/+}$; Ink4a$^{fl/fl}$; Ptf1a$^{Cre/+}$),* at both "early" and "late" stages[116]. Results from this study provides a comprehensive analysis of the tumor cell hierarchy in regard to the heterogeneity of gene expression profiles within tumor cells, fibroblasts and macrophages[116]. Comparison between early and late stage *KIC* samples revealed cancer cell populations do evolve as tumors progress to a more mesenchymal gene signature[116]. They also found that as *KIC* tumors progress, the population of cancer cells, macrophages, and fibroblast transcriptionally evolve from 3 distinct populations into only 2 at late stage that was also conserved in the *KPC* and *KPfC* models[116]. These findings not only report detailed characterization of the different cell types present among 3 different murine PDA models, but also highlight the potential avenues that can be used to direct targeted therapies based on the classification of cell types in tumors.

While CyTOF and scRNA-seq are in their infancy and require more studies to streamline the interpretation of the bioinformatic results they produce, it emphasizes the importance of studying and acknowledging the tumor heterogeneity that may contribute to therapeutic resistance. Utilization of these new advanced technologies in

combination with standard methods can be powerful tools in the diagnose and personalized treatment of PDA in the near future.

4.3 Improving Drug Delivery and Response

The innovation of sensitive and non-invasive diagnostic tools has been a challenge in the fight against PDA. Liquid biopsies and live imaging techniques have been proposed to detect biological markers of PDA at early stages, however, these methods need further optimization to increase sensitivity and reduce the number of false positive results[53]. Since a majority of patients are diagnosed at metastatic disease with a dense-fibrotic stromal response that makes up almost 90% of the tumor mass and is one of the biggest obstacles in drug delivery, most efforts have focused on targeting alterations in the stroma[103, 111]. Although the success of breaking down the "walls" of the stroma has been minimal, each attempt is a step closer at clarifying the complexity of the tumor biology and helps define the impact of the stroma on tumor growth and drug resistance.

The characteristic collagen-rich desmoplastic response was once thought to be an innocent, static bystander in PDA progression. The use of GEMMS and technological advancements in characterizing the components of the stroma debunks this idea and has shown the stroma plays a dynamic and active role in PDA tumor progression. Although the stroma is primarily composed of collagen, it consists of fibroblasts, which secrete collagen and ECM proteins, and immune cells, which create an immunosuppressive environment that help tumor cells evade immunosurveillance[53, 111]. The overproduction of collagen and tumor cell expansion form a stiff, fibrotic

response that compromises the blood supply to the tumor and reduces oxygen delivery, thus creating an avascular and hypoxic environment with high interstitial pressure[53, 55]. The tumor cells and stroma adapt to this environment through metabolic rewiring, reprogramming of factors that encourage metastasis and influence chemotherapeutic resistance[53].

The evolution of the tumor-stroma relationship during the development of PDA is another obstacle that hinders the success of a drug target. As outlined by Hosein *et al*., gene expression patterns from both the tumor cells and stromal changes as tumors progress in multiple mouse models[116]. The changes in gene expression over time may help explain chemotherapeutic resistance and the acknowledgement of these changes can aid in more efficient ways to manipulate the stroma for therapeutic success. As previously mentioned in Chapter 1 and 2, several studies have aimed at targeting components of the stroma in preclinical models with varying success. Predicting the success of a drug target is difficult due to the rapid evolution of the reprogramming and gene expression present in PDA tumors. Therefore, the duration and timing of a drug must be carefully considered in patients during clinical trials. We must also consider the adaptations the stromal and tumor cells overcome when a drug is introduced that assist in the resistance to therapeutic agents. With the advent of single-cell modalities such as scRNA-seq and CyTOF, we can potentially monitor the interactions and changes in the stroma before and after drug delivery to accurately predict the success of a drug target and develop more personalized methods in drug therapy. Other methods to help guide the success of targeting the tumor-stroma interactions were mentioned in Chapter 1, including patient-derived xenograft models and organoid

cultures. Collectively, these methods are powerful tools in predicting drug response and studying the ever-evolving tumor biology in PDA.

4.4 The Future of Discoidin Domain Receptors in Pancreatic Disease

Despite the technological advancements that have helped determine the multifaceted biology of PDA, the dynamics of the molecular events between the tumor-stroma relationship remain a challenge in diagnosing and treating patients. Numerous factors play into the tumor-stroma crosstalk which include activation or suppression of receptors by growth factors, cytokines, and ECM products that favor PDA progression[53, 111]. To narrow the scope of factors that contribute to PDA progression at the tumor-stroma interface, this dissertation has focused on a set of collagen-activated RTKs, named Discoidin domain receptors (DDR1 and DDR2). The unique aspect of transmembrane receptors to utilize collagen for the activation of downstream activities of cell proliferation, migration, and ECM remodeling makes DDRs an attractive target in pancreatic fibrotic disease and PDA[57, 59]. Both receptors have been implicated during the pathogenesis of various cancers, with an additional role of DDR1 in lung and kidney fibrosis[57, 59]. However, besides the study carried out by Aguilera *et al*. in which they used 7rh, a non-selective DDR1 inhibitor in PDA cell lines, GEMMS, and orthotopic models, there are no other studies to define the contribution of DDRs in pancreatic disease[64].

i. DDR1: Future Concepts and Ideas

In chapter 2, I showed germline DDR1-ablation impairs pancreatic recovery following an injury and shows DDR1 is necessary to maintain tissue homeostasis throughout PDA progression. Additionally, DDR1 ablation contributed to a smaller, less proliferative, fibrotic pancreas that reduces the number of metastases. While these experiments provided novel insights into the role of DDR1 in pancreatic disease a few questions and potential experiments still remain to define the functional aspects of DDR1. The following points are not limited to these ideas, but address personal interests and future directions for DDR1:

a.) Conditional DDR1-knockout Mice

A caveat of the experiments presented in Chapter 2 is the use of a germline DDR1 knockout. Germline ablation can define the developmental significance of a gene and provide information on how a protein contributes to a disease, however it does not always translate into clinical applications. In the case of DDR1, a germline deletion has made it difficult to pinpoint which signaling pathway is disrupted in disease states. It is possible that the subtle, rather than dramatic, changes of downstream targets such as p-Src, p-Akt, and p-Erk listed in Chapter 2 were not significant due to compensatory pathways that overcome embryonic, germline DDR1 depletion. These signaling targets and pathways are not exclusive to DDR1 and can be regulated by other receptors and cell activities. Using a time and pancreas specific conditional DDR1 knockout with the use of the Cre-LoxP technology (*DDR1*$^{fl/fl}$) may help elucidate the pathways that are disrupted in pancreatitis and pancreatic disease. To study pancreatitis, *DDR1*$^{fl/fl}$ would have to be crossed with *Ptf1a*$^{Cre/+}$ mice and then carry out

the same cerulein-induced pancreatitis protocol to both verify previous results and analyze for specific affected pathways in a pancreas specific manner. I would also cross *DDR1*$^{fl/fl}$ mice into the *KC* and *KPC* models to study pancreas specific deletion of DDR1 in tumorigenesis and progression. However, another more clinically relevant (and personally interesting) experiment would be to activate oncogenic *Kras* and knockout DDR1 after the pancreas has developed. In this case, I would use the *KCert; YFP* model from Chapter 3 and cross with the *DDR1*$^{fl/fl}$ model. When the mice reach 8 weeks, I can administer Tamoxifen once a day for 5 days to utilize *Ptf1a*^{CreERT} and activate oncogenic *Kras* in adult acinar cells while ablating DDR1 in the pancreas during neoplasia. This model can also be extended into studies in tumor progression and metastasis with the *KPCert; YFP* mouse. Using these models will help define the role of DDR1 in PDA after the pancreas has developed and is more akin to using a DDR1 specific inhibitor as opposed to a germline knockout.

Currently, a conditional DDR1-knockout mouse is under development at the University of Texas Southwestern and will help translate the contribution of DDR1 in preclinical models of various cancers. This model will be beneficial to encourage and support the results reported in Chapter 2. The closest experiment to defining the role of DDR1 in a pancreas/acinar specific manner was detailed in Chapter 2, Section iv in which acinar cells were isolated and left in culture to determine dysregulated pathways between *WT* and *DDR1*$^{-/-}$ mice. The limitation of this experiment is the lack of a microenvironment and presence of collagen, the primary ligand for DDR1. Crossing a conditional DDR1 knockout mouse into the *KC*, *KPC, KCert, and KPCert* models would help verify the role of DDR1 within the epithelia of PDA and not only support the

findings reported in Chapter 2, but may also help define a functional role for DDR1 in pancreatic disease.

b.) DDR1 and the Immune Response in Pancreatic Disease

The role of DDR1 on the immune response in pancreatic disease remains unknown. While there are no known reports of DDR1 expression or function in immune cells, it is possible it can play a role in the immune response. To help define DDR1 in the immune response following cerulein-induced pancreatitis, *KC* and *KPC* models I had stained tissues for immune markers such as CD45 (all immune cells), F4/80 (macrophages), CD3 (T-cell), Arginase (M2-like macrophage), and YM1 (M2-like macrophage) by IHC. Although this is not an exhaustive list of immune cell markers, I did not observe a difference in the number of immune cells present between controls and DDR1-ablated models. However, this does not mean there is not a difference in their function. Studying the mechanical differences such as migration and cytokine release using *in vitro* co-culture experiments between control and *DDR1*$^{-/-}$ animals would have strengthened my studies and helped elucidate a potential mechanism behind the smaller pancreata and more fibrotic tissue observed in all the DDR1-ablated models. This avenue is still an option to explore in the future and would be interesting to report any physical/mechanical differences in immune cells in the absence of DDR1.

ii. DDR2: Future Concepts and Ideas

In chapter 3, I interrogated the role of DDR2 during tumorigenesis and PDA metastasis. While additional studies are required to confirm the functional role of DDR2

in PDA progression, I established the expression of DDR2 in human and murine models during the onset and progression of PDA. A subset of DDR2+ cells were also found to be from the acinar-lineage implicating a role during EMT and have metastatic potential. This finding was unexpected due to the fact that DDR2 is primarily expressed in mesenchymal cells supporting tumor heterogeneity and fluidity of cells during PDA progression. Studies from the ubiquitous conditional DDR2 knockout mice in the neoplastic and metastatic models of PDA will help assess the functional role of DDR2 in PDA. Furthermore, the use of single-cell technologies can identify the parameters and characteristics of these DDR2+ cells in PDA that can be used to understand how DDR2 contributes to pancreatic disease.

While I was able to carry out some experiments to analyze DDR2 in pancreatic disease, there were additional experiments I had planned within the *KFβ* and *KPFβ* colonies. In both models, I administered Tamoxifen by oral gavage at 8 weeks to knockout DDR2 when some neoplasia has already been formed. Two other approaches I had in mind were to: 1.) Knockout DDR2 at a younger timepoint before neoplasia is present in $DDR2^{fl/fl}$*; KFβ* and $DDR2^{fl/fl}$*; KPFβ* mice by administering Tamoxifen chow at 3 weeks old. This would better define the requirement of DDR2 in the spontaneous progression of PDA. 2.) Knockout DDR2 after tumors had formed by oral gavage in the $DDR2^{fl/fl}$*; KPFβ* model to determine if DDR2 is a therapeutic option in PDA. This experiment would be more challenging due to the various times tumors may develop and sometimes rapid decline without any indication of cancer in mice, but was always a question I wanted to explore. Unfortunately, due to the unforeseen COVID-19 pandemic, the addition of more experiments and analysis from the various DDR2

mouse models cannot be completed, but the ideas and hope of getting back to lab still exist.

Concluding Remarks

Discovered in the late 90's, DDRs are considered fairly new RTKs and have limited information on their role in pancreatic disease. This dissertation aimed to focus on determining the contribution of DDRs in pancreatic disease through the use of pancreatic cancer cell lines and multiple GEMMS. Chapter 2 was dedicated to defining the significance of DDR1 in pancreatitis as well as the onset and progression of PDA. Results from these studies confirm that DDR1 is necessary for tissue homeostasis following an injury and that the use of a DDR1 inhibitor in pancreatic disease should be considered with caution. In chapter 3, the focus was shifted to the role of DDR2 in the progression and metastasis of PDA. Although the functional role of DDR2 was not confirmed, the novel expression of DDR2 and its potential role in regulating EMT and metastasis was established in several mouse models of PDA.

Targeting components of the collagen-dense stroma have been challenging to improve patient outcome in PDA. The data provided in this dissertation sheds light on the collagen receptors, DDR1 and DDR2, as potential liaisons at the tumor-stroma interface. Collectively, these data show a role for DDRs in the pathogenesis of PDA. The studies proposed in this defense help to fill the gap of knowledge of DDRs by studying their role in pancreatitis, tumorigenesis and metastatic PDA. The results I produced thus far encourage future studies of DDRs in disease and support further actions to consider using DDRs as promising therapeutic targets in the tumor-stroma crosstalk network.

Bibliography

[1] Pandol SJ: The Exocrine Pancreas. San Rafael (CA), 2010.
[2] Iacobuzio-Donahue CA: Genetic evolution of pancreatic cancer: lessons learnt from the pancreatic cancer genome sequencing project. Gut 2012, 61:1085-94.
[3] Innes JT, Carey LC: Normal pancreatic dimensions in the adult human. Am J Surg 1994, 167:261-3.
[4] Da Silva Xavier G: The Cells of the Islets of Langerhans. J Clin Med 2018, 7.
[5] Logsdon CD, Ji B: The role of protein synthesis and digestive enzymes in acinar cell injury. Nat Rev Gastroenterol Hepatol 2013, 10:362-70.
[6] Cleveland MH, Sawyer JM, Afelik S, Jensen J, Leach SD: Exocrine ontogenies: on the development of pancreatic acinar, ductal and centroacinar cells. Semin Cell Dev Biol 2012, 23:711-9.
[7] Yadav D, Lowenfels AB: The epidemiology of pancreatitis and pancreatic cancer. Gastroenterology 2013, 144:1252-61.
[8] Machicado JD, Yadav D: Epidemiology of Recurrent Acute and Chronic Pancreatitis: Similarities and Differences. Dig Dis Sci 2017, 62:1683-91.
[9] Witt H, Apte MV, Keim V, Wilson JS: Chronic pancreatitis: challenges and advances in pathogenesis, genetics, diagnosis, and therapy. Gastroenterology 2007, 132:1557-73.
[10] Strobel O, Dor Y, Alsina J, Stirman A, Lauwers G, Trainor A, Castillo CF, Warshaw AL, Thayer SP: In vivo lineage tracing defines the role of acinar-to-ductal transdifferentiation in inflammatory ductal metaplasia. Gastroenterology 2007, 133:1999-2009.
[11] Desai BM, Oliver-Krasinski J, De Leon DD, Farzad C, Hong N, Leach SD, Stoffers DA: Preexisting pancreatic acinar cells contribute to acinar cell, but not islet beta cell, regeneration. J Clin Invest 2007, 117:971-7.

[12] LaRusch J, Whitcomb DC: Genetics of pancreatitis. Curr Opin Gastroenterol 2011, 27:467-74.
[13] Søreide K, Primavesi, F., Labori, K.J. et al.: Molecular biology in pancreatic ductal adenocarcinoma: implications for future diagnostics and therapy. European Surgery 2019, 51:126-34.
[14] Ahn DH, Ramanathan RK, Bekaii-Saab T: Emerging Therapies and Future Directions in Targeting the Tumor Stroma and Immune System in the Treatment of Pancreatic Adenocarcinoma. Cancers (Basel) 2018, 10.
[15] Hezel AF, Kimmelman AC, Stanger BZ, Bardeesy N, Depinho RA: Genetics and biology of pancreatic ductal adenocarcinoma. Genes Dev 2006, 20:1218-49.
[16] Zhan W, Shelton CA, Greer PJ, Brand RE, Whitcomb DC: Germline Variants and Risk for Pancreatic Cancer: A Systematic Review and Emerging Concepts. Pancreas 2018, 47:924-36.
[17] Becker AE, Hernandez YG, Frucht H, Lucas AL: Pancreatic ductal adenocarcinoma: risk factors, screening, and early detection. World J Gastroenterol 2014, 20:11182-98.
[18] Klein AP: Genetic susceptibility to pancreatic cancer. Mol Carcinog 2012, 51:14-24.
[19] Kowalewski A, Szylberg L, Saganek M, Napiontek W, Antosik P, Grzanka D: Emerging strategies in BRCA-positive pancreatic cancer. J Cancer Res Clin Oncol 2018, 144:1503-7.
[20] Bailey P, Chang DK, Nones K, Johns AL, Patch AM, Gingras MC, Miller DK, Christ AN, Bruxner TJ, Quinn MC, Nourse C, Murtaugh LC, Harliwong I, Idrisoglu S, Manning S, Nourbakhsh E, Wani S, Fink L, Holmes O, Chin V, Anderson MJ, Kazakoff S, Leonard C, Newell F, Waddell N, Wood S, Xu Q, Wilson PJ, Cloonan N, Kassahn KS, Taylor D, Quek K, Robertson A, Pantano L, Mincarelli L, Sanchez LN, Evers L, Wu J, Pinese M, Cowley MJ, Jones MD, Colvin EK, Nagrial AM, Humphrey ES, Chantrill LA, Mawson A, Humphris J, Chou A, Pajic M, Scarlett CJ, Pinho AV, Giry-Laterriere M, Rooman I, Samra JS, Kench JG, Lovell JA, Merrett ND, Toon CW, Epari K, Nguyen NQ, Barbour A, Zeps N, Moran-Jones K, Jamieson NB, Graham JS, Duthie F, Oien K, Hair J, Grutzmann R, Maitra A, Iacobuzio-Donahue CA, Wolfgang CL, Morgan RA,

Lawlor RT, Corbo V, Bassi C, Rusev B, Capelli P, Salvia R, Tortora G, Mukhopadhyay D, Petersen GM, Australian Pancreatic Cancer Genome I, Munzy DM, Fisher WE, Karim SA, Eshleman JR, Hruban RH, Pilarsky C, Morton JP, Sansom OJ, Scarpa A, Musgrove EA, Bailey UM, Hofmann O, Sutherland RL, Wheeler DA, Gill AJ, Gibbs RA, Pearson JV, Waddell N, Biankin AV, Grimmond SM: Genomic analyses identify molecular subtypes of pancreatic cancer. Nature 2016, 531:47-52.
[21] Makohon-Moore A, Iacobuzio-Donahue CA: Pancreatic cancer biology and genetics from an evolutionary perspective. Nat Rev Cancer 2016, 16:553-65.
[22] Collisson EA, Bailey P, Chang DK, Biankin AV: Molecular subtypes of pancreatic cancer. Nat Rev Gastroenterol Hepatol 2019, 16:207-20.
[23] Puleo F, Nicolle R, Blum Y, Cros J, Marisa L, Demetter P, Quertinmont E, Svrcek M, Elarouci N, Iovanna J, Franchimont D, Verset L, Galdon MG, Deviere J, de Reynies A, Laurent-Puig P, Van Laethem JL, Bachet JB, Marechal R: Stratification of Pancreatic Ductal Adenocarcinomas Based on Tumor and Microenvironment Features. Gastroenterology 2018, 155:1999-2013 e3.
[24] Lerch MM, Gorelick FS: Models of acute and chronic pancreatitis. Gastroenterology 2013, 144:1180-93.
[25] Hyun JJ, Lee HS: Experimental models of pancreatitis. Clin Endosc 2014, 47:212-6.
[26] Niederau C, Ferrell LD, Grendell JH: Caerulein-induced acute necrotizing pancreatitis in mice: protective effects of proglumide, benzotript, and secretin. Gastroenterology 1985, 88:1192-204.
[27] Halbrook CJ, Wen HJ, Ruggeri JM, Takeuchi KK, Zhang Y, di Magliano MP, Crawford HC: Mitogen-activated Protein Kinase Kinase Activity Maintains Acinar-to-Ductal Metaplasia and Is Required for Organ Regeneration in Pancreatitis. Cell Mol Gastroenterol Hepatol 2017, 3:99-118.
[28] Wen HJ, Gao S, Wang Y, Ray M, Magnuson MA, Wright CVE, Di Magliano MP, Frankel TL, Crawford HC: Myeloid Cell-Derived HB-EGF Drives Tissue Recovery After Pancreatitis. Cell Mol Gastroenterol Hepatol 2019, 8:173-92.

[29] Deer EL, Gonzalez-Hernandez J, Coursen JD, Shea JE, Ngatia J, Scaife CL, Firpo MA, Mulvihill SJ: Phenotype and genotype of pancreatic cancer cell lines. Pancreas 2010, 39:425-35.
[30] Hwang CI, Boj SF, Clevers H, Tuveson DA: Preclinical models of pancreatic ductal adenocarcinoma. J Pathol 2016, 238:197-204.
[31] D'Agosto S, Andreani S, Scarpa A, Corbo V: Preclinical Modelling of PDA: Is Organoid the New Black? Int J Mol Sci 2019, 20.
[32] Herreros-Villanueva M, Hijona E, Cosme A, Bujanda L: Mouse models of pancreatic cancer. World J Gastroenterol 2012, 18:1286-94.
[33] Guerra C, Barbacid M: Genetically engineered mouse models of pancreatic adenocarcinoma. Mol Oncol 2013, 7:232-47.
[34] Hingorani SR, Petricoin EF, Maitra A, Rajapakse V, King C, Jacobetz MA, Ross S, Conrads TP, Veenstra TD, Hitt BA, Kawaguchi Y, Johann D, Liotta LA, Crawford HC, Putt ME, Jacks T, Wright CV, Hruban RH, Lowy AM, Tuveson DA: Preinvasive and invasive ductal pancreatic cancer and its early detection in the mouse. Cancer Cell 2003, 4:437-50.
[35] Tuveson DA, Hingorani SR: Ductal pancreatic cancer in humans and mice. Cold Spring Harb Symp Quant Biol 2005, 70:65-72.
[36] Schonhuber N, Seidler B, Schuck K, Veltkamp C, Schachtler C, Zukowska M, Eser S, Feyerabend TB, Paul MC, Eser P, Klein S, Lowy AM, Banerjee R, Yang F, Lee CL, Moding EJ, Kirsch DG, Scheideler A, Alessi DR, Varela I, Bradley A, Kind A, Schnieke AE, Rodewald HR, Rad R, Schmid RM, Schneider G, Saur D: A next-generation dual-recombinase system for time- and host-specific targeting of pancreatic cancer. Nat Med 2014, 20:1340-7.
[37] Moss RA, Lee C: Current and emerging therapies for the treatment of pancreatic cancer. Onco Targets Ther 2010, 3:111-27.
[38] Kota J, Hancock J, Kwon J, Korc M: Pancreatic cancer: Stroma and its current and emerging targeted therapies. Cancer Lett 2017, 391:38-49.
[39] Lee JC, Ahn S, Cho IK, Lee J, Kim J, Hwang JH: Management of recurrent pancreatic cancer after surgical resection: a protocol for systematic review, evidence mapping and meta-analysis. BMJ Open 2018, 8:e017249.

[40] Thomas D, Radhakrishnan P: Tumor-stromal crosstalk in pancreatic cancer and tissue fibrosis. Mol Cancer 2019, 18:14.
[41] Zeitouni D, Pylayeva-Gupta Y, Der CJ, Bryant KL: KRAS Mutant Pancreatic Cancer: No Lone Path to an Effective Treatment. Cancers (Basel) 2016, 8.
[42] Waters AM, Der CJ: KRAS: The Critical Driver and Therapeutic Target for Pancreatic Cancer. Cold Spring Harb Perspect Med 2018, 8.
[43] Samatar AA, Poulikakos PI: Targeting RAS-ERK signalling in cancer: promises and challenges. Nat Rev Drug Discov 2014, 13:928-42.
[44] Ostrem JM, Peters U, Sos ML, Wells JA, Shokat KM: K-Ras(G12C) inhibitors allosterically control GTP affinity and effector interactions. Nature 2013, 503:548-51.
[45] Ardito CM, Gruner BM, Takeuchi KK, Lubeseder-Martellato C, Teichmann N, Mazur PK, Delgiorno KE, Carpenter ES, Halbrook CJ, Hall JC, Pal D, Briel T, Herner A, Trajkovic-Arsic M, Sipos B, Liou GY, Storz P, Murray NR, Threadgill DW, Sibilia M, Washington MK, Wilson CL, Schmid RM, Raines EW, Crawford HC, Siveke JT: EGF receptor is required for KRAS-induced pancreatic tumorigenesis. Cancer Cell 2012, 22:304-17.
[46] Liu P, Cheng H, Roberts TM, Zhao JJ: Targeting the phosphoinositide 3-kinase pathway in cancer. Nat Rev Drug Discov 2009, 8:627-44.
[47] Olive KP, Jacobetz MA, Davidson CJ, Gopinathan A, McIntyre D, Honess D, Madhu B, Goldgraben MA, Caldwell ME, Allard D, Frese KK, Denicola G, Feig C, Combs C, Winter SP, Ireland-Zecchini H, Reichelt S, Howat WJ, Chang A, Dhara M, Wang L, Ruckert F, Grutzmann R, Pilarsky C, Izeradjene K, Hingorani SR, Huang P, Davies SE, Plunkett W, Egorin M, Hruban RH, Whitebread N, McGovern K, Adams J, Iacobuzio-Donahue C, Griffiths J, Tuveson DA: Inhibition of Hedgehog signaling enhances delivery of chemotherapy in a mouse model of pancreatic cancer. Science 2009, 324:1457-61.
[48] Gu D, Schlotman KE, Xie J: Deciphering the role of hedgehog signaling in pancreatic cancer. J Biomed Res 2016, 30:353-60.
[49] van Mackelenbergh MG, Stroes CI, Spijker R, van Eijck CHJ, Wilmink JW, Bijlsma MF, van Laarhoven HWM: Clinical Trials Targeting the Stroma in Pancreatic Cancer: A Systematic Review and Meta-Analysis. Cancers (Basel) 2019, 11.

[50] Rhim AD, Oberstein PE, Thomas DH, Mirek ET, Palermo CF, Sastra SA, Dekleva EN, Saunders T, Becerra CP, Tattersall IW, Westphalen CB, Kitajewski J, Fernandez-Barrena MG, Fernandez-Zapico ME, Iacobuzio-Donahue C, Olive KP, Stanger BZ: Stromal elements act to restrain, rather than support, pancreatic ductal adenocarcinoma. Cancer Cell 2014, 25:735-47.
[51] Ozdemir BC, Pentcheva-Hoang T, Carstens JL, Zheng X, Wu CC, Simpson TR, Laklai H, Sugimoto H, Kahlert C, Novitskiy SV, De Jesus-Acosta A, Sharma P, Heidari P, Mahmood U, Chin L, Moses HL, Weaver VM, Maitra A, Allison JP, LeBleu VS, Kalluri R: Depletion of carcinoma-associated fibroblasts and fibrosis induces immunosuppression and accelerates pancreas cancer with reduced survival. Cancer Cell 2014, 25:719-34.
[52] Sherman MH, Yu RT, Engle DD, Ding N, Atkins AR, Tiriac H, Collisson EA, Connor F, Van Dyke T, Kozlov S, Martin P, Tseng TW, Dawson DW, Donahue TR, Masamune A, Shimosegawa T, Apte MV, Wilson JS, Ng B, Lau SL, Gunton JE, Wahl GM, Hunter T, Drebin JA, O'Dwyer PJ, Liddle C, Tuveson DA, Downes M, Evans RM: Vitamin D receptor-mediated stromal reprogramming suppresses pancreatitis and enhances pancreatic cancer therapy. Cell 2014, 159:80-93.
[53] Vennin C, Murphy KJ, Morton JP, Cox TR, Pajic M, Timpson P: Reshaping the Tumor Stroma for Treatment of Pancreatic Cancer. Gastroenterology 2018, 154:820-38.
[54] Provenzano PP, Hingorani SR: Hyaluronan, fluid pressure, and stromal resistance in pancreas cancer. Br J Cancer 2013, 108:1-8.
[55] DuFort CC, DelGiorno KE, Carlson MA, Osgood RJ, Zhao C, Huang Z, Thompson CB, Connor RJ, Thanos CD, Scott Brockenbrough J, Provenzano PP, Frost GI, Michael Shepard H, Hingorani SR: Interstitial Pressure in Pancreatic Ductal Adenocarcinoma Is Dominated by a Gel-Fluid Phase. Biophys J 2016, 110:2106-19.
[56] Torphy RJ, Zhu Y, Schulick RD: Immunotherapy for pancreatic cancer: Barriers and breakthroughs. Ann Gastroenterol Surg 2018, 2:274-81.
[57] Valiathan RR, Marco M, Leitinger B, Kleer CG, Fridman R: Discoidin domain receptor tyrosine kinases: new players in cancer progression. Cancer Metastasis Rev 2012, 31:295-321.

[58] Weniger M, Honselmann KC, Liss AS: The Extracellular Matrix and Pancreatic Cancer: A Complex Relationship. Cancers (Basel) 2018, 10.
[59] Leitinger B: Discoidin domain receptor functions in physiological and pathological conditions. Int Rev Cell Mol Biol 2014, 310:39-87.
[60] Topalovski M, Brekken RA: Matrix control of pancreatic cancer: New insights into fibronectin signaling. Cancer Lett 2016, 381:252-8.
[61] Guerrot D, Kerroch M, Placier S, Vandermeersch S, Trivin C, Mael-Ainin M, Chatziantoniou C, Dussaule JC: Discoidin domain receptor 1 is a major mediator of inflammation and fibrosis in obstructive nephropathy. Am J Pathol 2011, 179:83-91.
[62] Avivi-Green C, Singal M, Vogel WF: Discoidin domain receptor 1-deficient mice are resistant to bleomycin-induced lung fibrosis. Am J Respir Crit Care Med 2006, 174:420-7.
[63] Takai K, Drain AP, Lawson DA, Littlepage LE, Karpuj M, Kessenbrock K, Le A, Inoue K, Weaver VM, Werb Z: Discoidin domain receptor 1 (DDR1) ablation promotes tissue fibrosis and hypoxia to induce aggressive basal-like breast cancers. Genes Dev 2018, 32:244-57.
[64] Aguilera KY, Huang H, Du W, Hagopian MM, Wang Z, Hinz S, Hwang TH, Wang H, Fleming JB, Castrillon DH, Ren X, Ding K, Brekken RA: Inhibition of Discoidin Domain Receptor 1 Reduces Collagen-mediated Tumorigenicity in Pancreatic Ductal Adenocarcinoma. Mol Cancer Ther 2017, 16:2473-85.
[65] Ambrogio C, Gomez-Lopez G, Falcone M, Vidal A, Nadal E, Crosetto N, Blasco RB, Fernandez-Marcos PJ, Sanchez-Cespedes M, Ren X, Wang Z, Ding K, Hidalgo M, Serrano M, Villanueva A, Santamaria D, Barbacid M: Combined inhibition of DDR1 and Notch signaling is a therapeutic strategy for KRAS-driven lung adenocarcinoma. Nat Med 2016, 22:270-7.
[66] Gonzalez ME, Martin EE, Anwar T, Arellano-Garcia C, Medhora N, Lama A, Chen YC, Tanager KS, Yoon E, Kidwell KM, Ge C, Franceschi RT, Kleer CG: Mesenchymal Stem Cell-Induced DDR2 Mediates Stromal-Breast Cancer Interactions and Metastasis Growth. Cell Rep 2017, 18:1215-28.
[67] Corsa CA, Brenot A, Grither WR, Van Hove S, Loza AJ, Zhang K, Ponik SM, Liu Y, DeNardo DG, Eliceiri KW, Keely PJ, Longmore GD: The Action of Discoidin Domain

Receptor 2 in Basal Tumor Cells and Stromal Cancer-Associated Fibroblasts Is Critical for Breast Cancer Metastasis. Cell Rep 2016, 15:2510-23.
[68] Zhang K, Corsa CA, Ponik SM, Prior JL, Piwnica-Worms D, Eliceiri KW, Keely PJ, Longmore GD: The collagen receptor discoidin domain receptor 2 stabilizes SNAIL1 to facilitate breast cancer metastasis. Nat Cell Biol 2013, 15:677-87.
[69] Borza CM, Pozzi A: Discoidin domain receptors in disease. Matrix Biol 2014, 34:185-92.
[70] Vogel WF, Aszodi A, Alves F, Pawson T: Discoidin domain receptor 1 tyrosine kinase has an essential role in mammary gland development. Mol Cell Biol 2001, 21:2906-17.
[71] Meyer zum Gottesberge AM, Gross O, Becker-Lendzian U, Massing T, Vogel WF: Inner ear defects and hearing loss in mice lacking the collagen receptor DDR1. Lab Invest 2008, 88:27-37.
[72] Kerroch M, Guerrot D, Vandermeersch S, Placier S, Mesnard L, Jouanneau C, Rondeau E, Ronco P, Boffa JJ, Chatziantoniou C, Dussaule JC: Genetic inhibition of discoidin domain receptor 1 protects mice against crescentic glomerulonephritis. FASEB J 2012, 26:4079-91.
[73] Borochowitz Z, Langer LO, Jr., Gruber HE, Lachman R, Katznelson MB, Rimoin DL: Spondylo-meta-epiphyseal dysplasia (SMED), short limb-hand type: a congenital familial skeletal dysplasia with distinctive features and histopathology. Am J Med Genet 1993, 45:320-6.
[74] Ali BR, Xu H, Akawi NA, John A, Karuvantevida NS, Langer R, Al-Gazali L, Leitinger B: Trafficking defects and loss of ligand binding are the underlying causes of all reported DDR2 missense mutations found in SMED-SL patients. Hum Mol Genet 2010, 19:2239-50.
[75] Kano K, Marin de Evsikova C, Young J, Wnek C, Maddatu TP, Nishina PM, Naggert JK: A novel dwarfism with gonadal dysfunction due to loss-of-function allele of the collagen receptor gene, Ddr2, in the mouse. Mol Endocrinol 2008, 22:1866-80.
[76] Yang SH, Baek HA, Lee HJ, Park HS, Jang KY, Kang MJ, Lee DG, Lee YC, Moon WS, Chung MJ: Discoidin domain receptor 1 is associated with poor prognosis of non-small cell lung carcinomas. Oncol Rep 2010, 24:311-9.

[77] Ford CE, Lau SK, Zhu CQ, Andersson T, Tsao MS, Vogel WF: Expression and mutation analysis of the discoidin domain receptors 1 and 2 in non-small cell lung carcinoma. Br J Cancer 2007, 96:808-14.
[78] Hammerman PS, Sos ML, Ramos AH, Xu C, Dutt A, Zhou W, Brace LE, Woods BA, Lin W, Zhang J, Deng X, Lim SM, Heynck S, Peifer M, Simard JR, Lawrence MS, Onofrio RC, Salvesen HB, Seidel D, Zander T, Heuckmann JM, Soltermann A, Moch H, Koker M, Leenders F, Gabler F, Querings S, Ansen S, Brambilla E, Brambilla C, Lorimier P, Brustugun OT, Helland A, Petersen I, Clement JH, Groen H, Timens W, Sietsma H, Stoelben E, Wolf J, Beer DG, Tsao MS, Hanna M, Hatton C, Eck MJ, Janne PA, Johnson BE, Winckler W, Greulich H, Bass AJ, Cho J, Rauh D, Gray NS, Wong KK, Haura EB, Thomas RK, Meyerson M: Mutations in the DDR2 kinase gene identify a novel therapeutic target in squamous cell lung cancer. Cancer Discov 2011, 1:78-89.
[79] Xu C, Buczkowski KA, Zhang Y, Asahina H, Beauchamp EM, Terai H, Li YY, Meyerson M, Wong KK, Hammerman PS: NSCLC Driven by DDR2 Mutation Is Sensitive to Dasatinib and JQ1 Combination Therapy. Mol Cancer Ther 2015, 14:2382-9.
[80] Ongusaha PP, Kim JI, Fang L, Wong TW, Yancopoulos GD, Aaronson SA, Lee SW: p53 induction and activation of DDR1 kinase counteract p53-mediated apoptosis and influence p53 regulation through a positive feedback loop. EMBO J 2003, 22:1289-301.
[81] Siegel RL, Miller KD, Jemal A: Cancer statistics, 2020. CA Cancer J Clin 2020, 70:7-30.
[82] Neoptolemos JP, Kleeff J, Michl P, Costello E, Greenhalf W, Palmer DH: Therapeutic developments in pancreatic cancer: current and future perspectives. Nat Rev Gastroenterol Hepatol 2018, 15:333-48.
[83] Hidalgo-Sastre A, Brodylo RL, Lubeseder-Martellato C, Sipos B, Steiger K, Lee M, von Figura G, Grunwald B, Zhong S, Trajkovic-Arsic M, Neff F, Schmid RM, Siveke JT: Hes1 Controls Exocrine Cell Plasticity and Restricts Development of Pancreatic Ductal Adenocarcinoma in a Mouse Model. Am J Pathol 2016, 186:2934-44.

[84] Kopp JL, von Figura G, Mayes E, Liu FF, Dubois CL, Morris JPt, Pan FC, Akiyama H, Wright CV, Jensen K, Hebrok M, Sander M: Identification of Sox9-dependent acinar-to-ductal reprogramming as the principal mechanism for initiation of pancreatic ductal adenocarcinoma. Cancer Cell 2012, 22:737-50.
[85] Guerra C, Schuhmacher AJ, Canamero M, Grippo PJ, Verdaguer L, Perez-Gallego L, Dubus P, Sandgren EP, Barbacid M: Chronic pancreatitis is essential for induction of pancreatic ductal adenocarcinoma by K-Ras oncogenes in adult mice. Cancer Cell 2007, 11:291-302.
[86] Halbrook CJ, Pasca di Magliano M, Lyssiotis CA: Tumor cross-talk networks promote growth and support immune evasion in pancreatic cancer. Am J Physiol Gastrointest Liver Physiol 2018, 315:G27-G35.
[87] Provenzano PP, Cuevas C, Chang AE, Goel VK, Von Hoff DD, Hingorani SR: Enzymatic targeting of the stroma ablates physical barriers to treatment of pancreatic ductal adenocarcinoma. Cancer Cell 2012, 21:418-29.
[88] Hou G, Vogel W, Bendeck MP: The discoidin domain receptor tyrosine kinase DDR1 in arterial wound repair. J Clin Invest 2001, 107:727-35.
[89] Hingorani SR, Wang L, Multani AS, Combs C, Deramaudt TB, Hruban RH, Rustgi AK, Chang S, Tuveson DA: Trp53R172H and KrasG12D cooperate to promote chromosomal instability and widely metastatic pancreatic ductal adenocarcinoma in mice. Cancer Cell 2005, 7:469-83.
[90] Wu CY, Carpenter ES, Takeuchi KK, Halbrook CJ, Peverley LV, Bien H, Hall JC, DelGiorno KE, Pal D, Song Y, Shi C, Lin RZ, Crawford HC: PI3K regulation of RAC1 is required for KRAS-induced pancreatic tumorigenesis in mice. Gastroenterology 2014, 147:1405-16 e7.
[91] Flamant M, Placier S, Rodenas A, Curat CA, Vogel WF, Chatziantoniou C, Dussaule JC: Discoidin domain receptor 1 null mice are protected against hypertension-induced renal disease. J Am Soc Nephrol 2006, 17:3374-81.
[92] Wollny D, Zhao S, Everlien I, Lun X, Brunken J, Brune D, Ziebell F, Tabansky I, Weichert W, Marciniak-Czochra A, Martin-Villalba A: Single-Cell Analysis Uncovers Clonal Acinar Cell Heterogeneity in the Adult Pancreas. Dev Cell 2016, 39:289-301.

[93] Astarita JL, Acton SE, Turley SJ: Podoplanin: emerging functions in development, the immune system, and cancer. Front Immunol 2012, 3:283.
[94] Elyada E, Bolisetty M, Laise P, Flynn WF, Courtois ET, Burkhart RA, Teinor JA, Belleau P, Biffi G, Lucito MS, Sivajothi S, Armstrong TD, Engle DD, Yu KH, Hao Y, Wolfgang CL, Park Y, Preall J, Jaffee EM, Califano A, Robson P, Tuveson DA: Cross-Species Single-Cell Analysis of Pancreatic Ductal Adenocarcinoma Reveals Antigen-Presenting Cancer-Associated Fibroblasts. Cancer Discov 2019, 9:1102-23.
[95] Chronopoulos A, Robinson B, Sarper M, Cortes E, Auernheimer V, Lachowski D, Attwood S, Garcia R, Ghassemi S, Fabry B, Del Rio Hernandez A: ATRA mechanically reprograms pancreatic stellate cells to suppress matrix remodelling and inhibit cancer cell invasion. Nat Commun 2016, 7:12630.
[96] Hingorani SR, Harris WP, Beck JT, Berdov BA, Wagner SA, Pshevlotsky EM, Tjulandin SA, Gladkov OA, Holcombe RF, Korn R, Raghunand N, Dychter S, Jiang P, Shepard HM, Devoe CE: Phase Ib Study of PEGylated Recombinant Human Hyaluronidase and Gemcitabine in Patients with Advanced Pancreatic Cancer. Clin Cancer Res 2016, 22:2848-54.
[97] Hakim N, Patel R, Devoe C, Saif MW: Why HALO 301 Failed and Implications for Treatment of Pancreatic Cancer. Pancreas (Fairfax) 2019, 3:e1-e4.
[98] Jiang H, Hegde S, Knolhoff BL, Zhu Y, Herndon JM, Meyer MA, Nywening TM, Hawkins WG, Shapiro IM, Weaver DT, Pachter JA, Wang-Gillam A, DeNardo DG: Targeting focal adhesion kinase renders pancreatic cancers responsive to checkpoint immunotherapy. Nat Med 2016, 22:851-60.
[99] Sasson AR, Wetherington RW, Hoffman JP, Ross EA, Cooper H, Meropol NJ, Freedman G, Pingpank JF, Eisenberg BL: Neoadjuvant chemoradiotherapy for adenocarcinoma of the pancreas: analysis of histopathology and outcome. Int J Gastrointest Cancer 2003, 34:121-8.
[100] Erkan M, Michalski CW, Rieder S, Reiser-Erkan C, Abiatari I, Kolb A, Giese NA, Esposito I, Friess H, Kleeff J: The activated stroma index is a novel and independent prognostic marker in pancreatic ductal adenocarcinoma. Clin Gastroenterol Hepatol 2008, 6:1155-61.

[101] Franco-Barraza J, Francescone R, Luong T, Shah N, Madhani R, Cukierman G, Dulaimi E, Devarajan K, Egleston BL, Nicolas E, Katherine Alpaugh R, Malik R, Uzzo RG, Hoffman JP, Golemis EA, Cukierman E: Matrix-regulated integrin alphavbeta5 maintains alpha5beta1-dependent desmoplastic traits prognostic of neoplastic recurrence. Elife 2017, 6.
[102] Meng Z, Moroishi T, Guan KL: Mechanisms of Hippo pathway regulation. Genes Dev 2016, 30:1-17.
[103] Gupta GP, Massague J: Cancer metastasis: building a framework. Cell 2006, 127:679-95.
[104] Stromnes IM, Greenberg PD: Pancreatic Cancer: Planning Ahead for Metastatic Spread. Cancer Cell 2016, 29:774-6.
[105] Rhim AD, Mirek ET, Aiello NM, Maitra A, Bailey JM, McAllister F, Reichert M, Beatty GL, Rustgi AK, Vonderheide RH, Leach SD, Stanger BZ: EMT and dissemination precede pancreatic tumor formation. Cell 2012, 148:349-61.
[106] Whittle MC, Hingorani SR: Disconnect between EMT and metastasis in pancreas cancer. Oncotarget 2015, 6:30445-6.
[107] Kobayashi-Watanabe N, Sato A, Watanabe T, Abe T, Nakashima C, Sueoka E, Kimura S, Sueoka-Aragane N: Functional analysis of Discoidin domain receptor 2 mutation and expression in squamous cell lung cancer. Lung Cancer 2017, 110:35-41.
[108] Farrell AS, Joly MM, Allen-Petersen BL, Worth PJ, Lanciault C, Sauer D, Link J, Pelz C, Heiser LM, Morton JP, Muthalagu N, Hoffman MT, Manning SL, Pratt ED, Kendsersky ND, Egbukichi N, Amery TS, Thoma MC, Jenny ZP, Rhim AD, Murphy DJ, Sansom OJ, Crawford HC, Sheppard BC, Sears RC: MYC regulates ductal-neuroendocrine lineage plasticity in pancreatic ductal adenocarcinoma associated with poor outcome and chemoresistance. Nat Commun 2017, 8:1728.
[109] Bayer SV, Grither WR, Brenot A, Hwang PY, Barcus CE, Ernst M, Pence P, Walter C, Pathak A, Longmore GD: DDR2 controls breast tumor stiffness and metastasis by regulating integrin mediated mechanotransduction in CAFs. Elife 2019, 8.

[110] Ansari D, Tingstedt B, Andersson B, Holmquist F, Sturesson C, Williamsson C, Sasor A, Borg D, Bauden M, Andersson R: Pancreatic cancer: yesterday, today and tomorrow. Future Oncol 2016, 12:1929-46.
[111] Lafaro KJ, Melstrom LG: The Paradoxical Web of Pancreatic Cancer Tumor Microenvironment. Am J Pathol 2019, 189:44-57.
[112] Yachida S, White CM, Naito Y, Zhong Y, Brosnan JA, Macgregor-Das AM, Morgan RA, Saunders T, Laheru DA, Herman JM, Hruban RH, Klein AP, Jones S, Velculescu V, Wolfgang CL, Iacobuzio-Donahue CA: Clinical significance of the genetic landscape of pancreatic cancer and implications for identification of potential long-term survivors. Clin Cancer Res 2012, 18:6339-47.
[113] Moffitt RA, Marayati R, Flate EL, Volmar KE, Loeza SG, Hoadley KA, Rashid NU, Williams LA, Eaton SC, Chung AH, Smyla JK, Anderson JM, Kim HJ, Bentrem DJ, Talamonti MS, Iacobuzio-Donahue CA, Hollingsworth MA, Yeh JJ: Virtual microdissection identifies distinct tumor- and stroma-specific subtypes of pancreatic ductal adenocarcinoma. Nat Genet 2015, 47:1168-78.
[114] Collisson EA, Sadanandam A, Olson P, Gibb WJ, Truitt M, Gu S, Cooc J, Weinkle J, Kim GE, Jakkula L, Feiler HS, Ko AH, Olshen AB, Danenberg KL, Tempero MA, Spellman PT, Hanahan D, Gray JW: Subtypes of pancreatic ductal adenocarcinoma and their differing responses to therapy. Nat Med 2011, 17:500-3.
[115] Spitzer MH, Nolan GP: Mass Cytometry: Single Cells, Many Features. Cell 2016, 165:780-91.
[116] Hosein AN, Huang H, Wang Z, Parmar K, Du W, Huang J, Maitra A, Olson E, Verma U, Brekken RA: Cellular heterogeneity during mouse pancreatic ductal adenocarcinoma progression at single-cell resolution. JCI Insight 2019, 5.